UNIVERSITY OF CALIFORNIA

Los Angeles

Conformal Junctions, Entanglement Entropy, and Holography

A dissertation submitted in partial satisfaction

of the requirements for the degree

Doctor of Philosophy in Physics

by

John David Miller

2019

ABSTRACT OF THE DISSERTATION

Conformal Junctions, Entanglement Entropy, and Holography

by

John David Miller

Doctor of Philosophy in Physics

University of California, Los Angeles, 2019

Professor Michael Gutperle, Chair

We explore interfaces and junctions joining multiple two-dimensional conformal field theories, with the goal of calculating entanglement entropies in their presence and exploring their holographic duals. In chapter 1 we start with an overview of the three subjects, collecting various well-known results and reviewing some foundational works.

In chapter 2 we calculate the holographic entanglement entropy in the presence of a conformal interface for a geometric configuration in which the entangling region $\mathcal{A}$ lies on one side of the interface. For the supersymmetric Janus solution we find exact agreement between the holographic and conformal field theory calculation of the entanglement entropy.

In chapter 3 we calculate the entanglement entropy for topological interfaces in rational conformal field theories for the case where the interface lies at the boundary of the entangling interval and for the case where it is located in the center of the entangling interval. We compare the results to each other and also to the left/right entropy of a related boundary conformal field theory. We also comment on the entanglement entropies for topological interfaces in Liouville theory.

In chapter 4 we consider entanglement through permeable junctions of N free boson and free fermion conformal field theories. We constrain the form of the general boundary state and calculate the replicated partition functions with interface operators inserted, from which

the entanglement entropy is calculated. We find the functional form of the universal and constant terms to be similar to the $N = 2$ case, depending only of the total transmission of the junction and the unit volume of the zero mode lattice. For $N > 2$ we see a subleading divergent term which does not depend on the parameters of the junction. For $N = 3$ we consider some specific geometries and discuss various limits.

In chapter 5 we investigate topological interfaces between three-dimensional Abelian Chern-Simons theories in the context of the AdS_3/CFT_2 correspondence. We show that it is possible to connect the topological interfaces in the bulk Chern-Simons theory to topological interfaces in the dual conformal field theory on the boundary. In addition to the $[U(1)]^{2N}$ Chern-Simons theory on AdS_3, we show that it is possible to find boundary counter terms which lead to the N conserved currents in the dual two-dimensional conformal field theory.

The dissertation of John David Miller is approved.

Eric D'Hoker

Ciprian Manolescu

Michael Gutperle, Committee Chair

University of California, Los Angeles

2019

To Chrystin Green, for everything.

Contents

1 Introduction **1**

1.1 Conformal interfaces 3

1.2 Entanglement entropy 9

1.2.1 Asymmetric intervals in free field theories 13

1.3 Holography 18

1.3.1 Janus solutions 21

1.3.2 Chern-Simons theories 25

2 Entanglement Entropy at Holographic Interfaces **29**

2.1 Non-supersymmetric Janus solution 30

2.2 Supersymmetric Janus solution 34

2.3 Discussion 37

3 Entanglement Entropy at RCFT Topological Interfaces **40**

3.1 Topological interfaces in RCFT 41

3.2 Entanglement entropy at a topological interface 43

3.3 Symmetric and left/right entanglement entropy 44

3.4 Examples of entanglement entropies 48

3.5 Remarks on entanglement entropies for Liouville theory 50

3.6 Discussion 53

4 Entanglement Entropy at CFT Junctions **54**

4.1 CFT construction of junctions 55

4.1.1 Reflection and transmission for junctions 59

4.2 Entanglement entropy at N-junctions 61

4.2.1 Bosonic junction 62

4.2.2 Fermionic NS junction 67

4.2.3 BPS junction 72

4.3 Specific 3-junction geometries 73

4.3.1 Boundary state construction 73

4.3.2 Transmission and entanglement entropy 81

4.4 Discussion 83

4.A Special functions 85

4.A.1 Theta functions and S-transformations 85

4.A.2 Dedekind eta and related functions 89

4.A.3 Bernoulli polynomials and dilogarithms 90

4.B Intermediate Gaussian integrals 94

4.B.1 Bosonic integrals 94

4.B.2 Fermionic integrals 96

4.C Calculation of determinants 98

4.C.1 Bosonic determinant 99

4.C.2 Fermionic determinant 102

5 Holographic Topological Interfaces **104**

5.1 Background 105

5.2 Topological interfaces in the AdS bulk 108

5.2.1 AdS_2 slicing 108

5.2.2 Simple holomorphic example 109

5.2.3 Pure CS counter terms and conserved currents 111

5.2.4 Interfaces with conserved currents 115
5.3 Higher-dimensional generalizations 117
5.4 Discussion 118

A CFT conventions **119**

A.1 Free scalar field 119
A.2 Free spin-$\frac{1}{2}$ field 121

List of Figures

1.1 Folding and unfolding an interface 4

1.2 D1-branes in the bosonic 2-torus 7

1.3 Mapping to the replicated geometry 15

1.4 Universal prefactors for 2D free conformal fields 19

1.5 AdS_2 slicing of AdS_3 in Poincaré coordinates 23

2.1 Minimal surfaces for symmetric and asymmetric regions 31

2.2 Extremal surface phase spaces for the non-supersymmetric Janus solution . . 32

2.3 Comparison of non-supersymmetric entanglement entropy factors 34

3.1 Mapping of a non-central interface to the replica torus 46

4.1 Folding and partially unfolding a junction 56

4.2 Constructing D2-branes in the bosonic 3-torus 74

4.3 An angled D2-brane wrapping the bosonic 3-torus 75

List of Tables

3.1 Entanglement entropies for the Ising model. 49

3.2 Entanglement entropies for the tri-critical Ising model. 50

Acknowledgements

It is my pleasure to thank Michael Gutperle for his mentorship and collaboration; it has been an honor and a privilege to learn from and work with such a brilliant physicist and supportive advisor. I would like to thank Per Kraus and Eric D'Hoker, who along with Michael Gutperle provided me with a unique and valuable education, and whose efforts to challenge and encourage me have greatly enriched my development at UCLA. I would also like to thank Ciprian Manolescu for his support.

I would like to thank my peers in the group, especially David Corbino, Justin Kaidi, Julio Martinez, Stathis Megas, Allic Sivaramakrishnan, and River Snively. I thank Mert Besken, Ashwin Hegde, and Andrea Trivella for the many years of camaraderie and conversation, productive or otherwise. Outside of particle theory I thank Liz Mills and Agnieszka Wergieluk for their help over the years. I would like to particularly thank Daniel Hill for his close friendship and stimulating rivalry, without which my time at UCLA would have been less full. I would also like to thank Josh Samani and Shanna Shaked for their guidance and timely support.

I would like to thank my parents for staying as concerned about my education during my doctoral studies as they were during my primary education, and for showing me I could do well in anything I put my mind to. I would like to thank my brothers for helping keep me silly and sane. I thank Amy and Sharon Côté for being just down the street, no matter where I go. I thank Jeannette and Nicole Green for taking me in and making me family from the start. Finally, I thank Chrystin Green, my wife, for more than I can put into words.

Without these people, all their time and support over the years, myself and this work would have been much lesser.

Contribution of authors

Chapters 2, 3, 4, and 5 are based on [1–4] in collaboration with Michael Gutperle.

Vita

2013	B.S. (Physics, Mathematics), Cal Poly Pomona
2014	M.S. (Physics), UCLA
2013 – 2019	Teaching Assistant, Department of Physics and Astronomy, UCLA

Publications

"Topological interfaces in Chern-Simons theory and the AdS_3/CFT_2 correspondence,"
Gutperle, M., Miller, J. D., Phys. Rev. D99 no. 2 (2019) 026014
DOI: 10.1103/PhysRevD.99.026014, arXiv:1810.08713 [hep-th]

"Entanglement entropy at CFT junctions,"
Gutperle, M., Miller, J. D., Phys. Rev. D95 no. 10 (2017) 106008
DOI: 10.1103/PhysRevD.95.106008, arXiv:1701.08856 [hep-th]

"A note on entanglement entropy for topological interfaces in RCFTs,"
Gutperle, M., Miller, J. D., JHEP 04 (2016) 176
DOI: 10.1007/JHEP04(2016)176, arXiv:1512.07241 [hep-th]

"Entanglement entropy at holographic interfaces,"
Gutperle, M., Miller, J. D., Phys. Rev. D93 no. 2 (2016) 026006
DOI: 10.1103/PhysRevD.93.026006, arXiv:1511.08955 [hep-th]

Chapter 1

Introduction

In this work we study the joining together of systems that respect conformal symmetry, a large spacetime symmetry group which only leaves angles invariant. At criticality, conformal symmetry is an almost generic feature of a quantum field theory[1], and thus the study of general conformal field theories (CFTs) uncovers universal features of a large variety of physical systems. In particular, we almost exclusively consider two-dimensional systems. Unlike higher dimensions, conformal symmetry in two dimensions is realized by two copies of the Virasoro algebra and hence is infinite-dimensional, resulting in a high degree of integrability in two-dimensional CFTs [6]. As such these systems are often exactly solvable, making it possible to pursue interesting and highly nontrivial questions. In Euclidean settings there are many two-dimensional condensed matter systems whose underlying critical CFTs have been identified (e.g. the Ising model [6], the 3-state Potts model [7], and the $O(N)$ model [8] to name a few), and in Lorentzian settings the dynamic variables of the two-dimensional worldsheets of string theory are described by CFTs.

More so than fully conformally invariant theories, we are interested in interfaces joining two CFTs and junctions joining three or more CFTs together, which introduce nontrivial extensions away from full conformal symmetry. In addition to describing defects in critical quantum systems, such interfaces also describe domain wall scenarios that arise from sponta-

[1]For one of the few examples in which only the additional scaling symmetry is introduced, see [5]

neously broken symmetry. Furthermore, CFT junctions describe physical interfaces between critical quantum wires [9] and the joining together of open strings [10]. Interfaces can also reveal interesting features of the homogeneous theory, e.g. certain classes of interfaces have been shown to generate symmetries of the undeformed theory [11].

A natural quantity to consider in an interface or junction theory is the entanglement entropy, a standard measure of the entanglement of quantum states in a given region with quantum states outside that region. Entanglement entropy has become a key quantity of interest in diverse areas of physics: from modern condensed matter treatments where quantum phases of matter are characterized by their ground state entanglement (e.g. [12]), to quantum gravity where the entanglement entropy whose associated region is the space outside a black hole horizon represents the entropy seen by observers in that region [13, 14]. With the presence of a permeable division between two theories, the choice of entangling region gains significance and the associated entropy contains more information than in the homogeneous theory.

Calculations of entanglement entropy invite comparison with dual results via the holographic principle, which states that the information in certain bulk theories is contained in dual theories living on the boundary of the bulk region. For CFTs we can make use of the AdS/CFT correspondence, which relates quantities in gravitational theories in (asymptotically) Anti-de Sitter spacetimes of dimension d with those of $(d-1)$-dimensional CFTs located on the asymptotic boundaries of those spacetimes. In AdS holography there exists a standard procedure by which the entanglement entropy of a boundary region can be computed from the bulk metric [15], and the focus of much recent work has been to show that information about the bulk geometry can likewise be extracted from the boundary entanglement entropy [16–18]. Interface theories are particularly interesting within the holographic context not only due to the significant deformation away from well-studied dual systems they produce, but also due to the unclear bulk interpretation of such interfaces.

The structure of this introduction is as follows: in section 1.1 we review the construction

of conformal interfaces, mostly following [19, 20]. In section 1.2 we outline methods to compute the entanglement entropy within a CFT and summarize the entropy calculations of [21, 22] which we will reference and extend in later chapters. In section 1.3 we review two gravitational theories known to be dual to interface conformal field theories – which we will use in chapter 2 – as well as review holographic aspects of a well-known gauge field theory in AdS_3 that we explore further in chapter 5.

1.1 Conformal interfaces

Here we review the general properties and construction of conformally invariant interfaces in two-dimensional CFTs, and give explicit constructions for interfaces in free boson and free fermion theories. As inserting a line division in the plane is sure to break the full Virasoro $\otimes$ Virasoro conformal algebra in most cases, by a conformally invariant interface we mean one which preserves at least one Virasoro algebra. If one considers the interface to be located at $y = 0$ in $\mathbb{R}^2$, then the condition

$$[T^1_{zz}(x) - T^1_{\bar{z}\bar{z}}(x)]_{y=0} = [T^2_{zz}(x) - T^2_{\bar{z}\bar{z}}(x)]_{y=0}, \quad x \in \mathbb{R} \tag{1.1.1}$$

will ensure this property, where in the above the left- and right-hand sides contain the stress tensor components of the two theories CFT_1 and CFT_2 the interface lies between, respectively. This is due to the fact that transformations which leave the line $y = 0$ invariant are generated by this combination of stress tensor components.

Our starting point is then an operator $I_{1,2}$ located at the interface that satisfies

$$\left(L^1_n - \bar{L}^1_{-n}\right) I_{1,2} = I_{1,2} \left(L^2_n - \bar{L}^2_{-n}\right) \tag{1.1.2}$$

for $n \geq 0$, where L^i_n and $\bar{L}^i_n$ with $i = 1, 2$ are the Virasoro generators of CFT_1 and CFT_2. Finding operators that satisfy (1.1.2) can be mapped to finding conformal boundary states

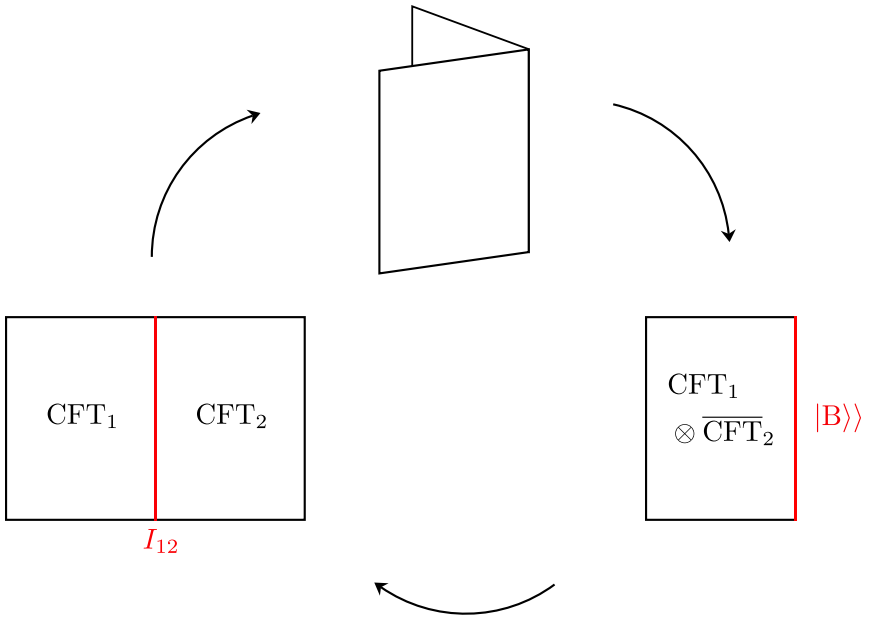

Figure 1.1: Illustration of the parity transformation relating the interface between CFT_1 and CFT_2 to the tensor product $\text{CFT}_1 \otimes \overline{\text{CFT}_2}$ with boundary.

satisfying

$$\left(L_n^{\text{total}} - \bar{L}_{-n}^{\text{total}}\right)|\text{B}\rangle\rangle = 0 \tag{1.1.3}$$

by use of a parity transformation. This is the content of the folding trick [19], which is illustrated in figure 1.1. The folded picture is useful for characterizing classes of interfaces and some simple calculations; as a relevant example, in [23] it was shown that the reflection and transmission coefficients for interfaces between CFTs with the same central charge c are found from

$$\mathcal{R} = \frac{\langle 0|L_2^1\bar{L}_2^1 + L_2^2\bar{L}_2^2|\text{B}\rangle\rangle}{c\,\langle 0|\text{B}\rangle\rangle} \quad \text{and} \quad \mathcal{T} = \frac{\langle 0|L_2^1\bar{L}_2^2 + L_2^2\bar{L}_2^1|\text{B}\rangle\rangle}{c\,\langle 0|\text{B}\rangle\rangle} \tag{1.1.4}$$

For calculations such as that of the entanglement entropy the boundary states need to be unfolded once they are found.

For general CFTs, the boundary states satisfying (1.1.3) are often difficult to find. If boundary states of the individual CFTs are known, we could take

$$|\text{B}\rangle\rangle = |\text{B}_1\rangle\rangle \otimes |\text{B}_2\rangle\rangle \tag{1.1.5}$$

where $|\mathrm{B}_1\rangle\rangle$ is a boundary state of CFT_1 and $|\mathrm{B}_2\rangle\rangle$ is a boundary state of CFT_2. For such a boundary state the corresponding interface has both sides of (1.1.2) vanish, and thus the two CFTs decouple. When $c_{\mathrm{total}} < 1$ the folded CFT is rational, and for a finite number of primary fields all solutions to (1.1.3) have been found [24] and organized into modular invariant boundary states via the Cardy construction [25]. However, since we are considering a tensor product CFT in the folded picture, the resulting folded CFT almost always has $c > 1$ and hence is not rational. If one imposes additional conditions such as preservation of a current algebra or permutation symmetry, more general constructions of boundary states and interfaces are possible [26–28]. Another possibility is given by strengthening the conditions (1.1.3) to boundary states satisfying

$$\left(L^1_n - \bar{L}^2_{-n}\right)|\mathrm{B}\rangle\rangle = 0 \quad \text{and} \quad \left(L^2_n - \bar{L}^1_{-n}\right)|\mathrm{B}\rangle\rangle = 0 \tag{1.1.6}$$

separately; i.e.

$$[T^1_{zz}(x) - T^2_{zz}(x)]_{y=0} = 0, \quad [T^1_{\bar{z}\bar{z}}(x) - T^2_{\bar{z}\bar{z}}(x)]_{y=0} = 0, \quad x \in \mathbb{R} \tag{1.1.7}$$

This leads to so-called topological defects or interfaces [20, 29, 30]. The conditions (1.1.6) allow for solutions to be constructed in wider classes of CFTs; in chapter 3 we will work with such interfaces and explain their properties in more detail. When considering free fields, as in the next section and chapter 4, the conditions can be written in terms of the creation and annihilation operators and can be solved by a coherent state anzatz.

We will now show how this works for free bosonic interfaces (see appendix A for our CFT conventions). Under the replacement $a^i_n \to S_{ij}\,\bar{a}^j_{-n}$ for a 2×2 matrix S, the operator combinations in the generators L^i_n are altered as

$$:a^i_{n-m}a^i_m: \longrightarrow \; S_{ij}\,S_{ik} :\bar{a}^j_{m-n}\bar{a}^k_{-m}: \tag{1.1.8}$$

Considering summation over the index i in the above and the form of the generators (A.1.8), it is seen that $L_n^{\text{total}} \to \bar{L}_{-n}^{\text{total}}$ if S is an orthogonal matrix. Thus, the conformal condition (1.1.3) simplifies to

$$\left(a_n^i - S_{ij}\,\bar{a}_{-n}^j\right)|\mathrm{B}\rangle\rangle = 0 \tag{1.1.9}$$

for S an element of $O(2)$. This condition can also be constructed explicitly for free fields by requiring continuity of the stress tensor at the location of the interface [19]. These new conditions (1.1.9) can be solved by a coherent state anzatz

$$|S\rangle\rangle = g\prod_{n=1}^{\infty}\exp\left(\frac{1}{n}\,S_{ij}\,a_{-n}^i\bar{a}_{-n}^j\right)|\Omega\rangle \tag{1.1.10}$$

The form of (1.1.9) describes a D-brane in the boundary state formalism (see [31, 32] for review), and this correspondence is used to find and classify all the possible boundary states for the two scalar model. The D-brane interpretation also gives us physical meaning for the normalization, the so-called g-factor, and the ground state $|\Omega\rangle$ in (1.1.10).

The one-dimensional special case of (1.1.9) emits the unit scalar choices $S = \pm 1$, which correspond to the two possible D-brane states for a single compact scalar

$$|\mathrm{D0}\rangle\rangle = \sqrt{\frac{R}{\sqrt{2\alpha'}}}\prod_{n=1}^{\infty}\exp\left(\frac{1}{n}\,a_{-n}\bar{a}_{-n}\right)\sum_{N=-\infty}^{\infty}e^{-iN\varphi_0/R}\,|N,0\rangle \tag{1.1.11}$$

$$|\mathrm{D1}\rangle\rangle = \sqrt{\frac{1}{R}\sqrt{\frac{\alpha'}{2}}}\prod_{n=1}^{\infty}\exp\left(-\frac{1}{n}\,a_{-n}\bar{a}_{-n}\right)\sum_{M=-\infty}^{\infty}e^{iM\tilde{\varphi}_0}\,|0,M\rangle \tag{1.1.12}$$

respectively, where the D0-brane enforces a Dirichlet condition at the boundary and the D1-brane enforces a Neumann condition at the boundary. The constants φ_0 and $\tilde{\varphi}_0$ are the position and dual Wilson line moduli of the D-brane. For an interface between two $c = 1$ CFTs the D-brane states of the two scalar model are needed. These were constructed in [20] using rotations and T-duality transformations on the tensor products of (1.1.11) and

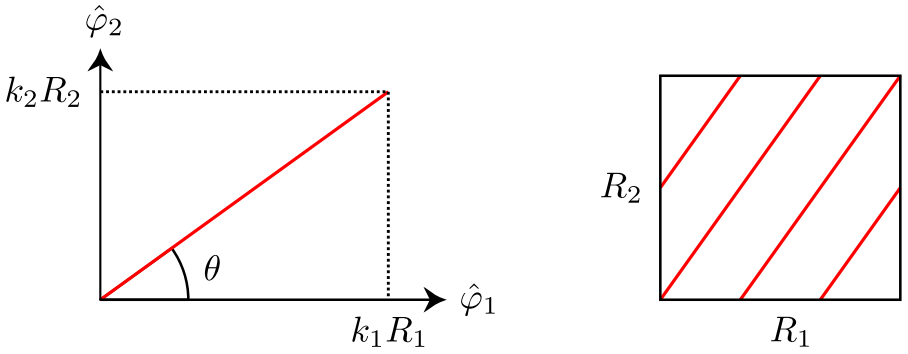

Figure 1.2: On the right: A D1-brane wrapping the bosonic 2-torus continued into the compactification lattice so as to show the lattice intercept at $(k_1 R_1, k_2 R_2)$. On the left: A D1-brane wrapping the bosonic 2-torus (corresponding to the parameters $k_1 = 2$ and $k_2 = 3$) shown in the unit cell of the compactification lattice.

(1.1.12). The first class of states are the rotations of

$$|\mathrm{D1}, 0\rangle\rangle = |\mathrm{D1}\rangle\rangle \otimes |\mathrm{D0}\rangle\rangle \tag{1.1.13}$$

by an arbitrary angle in the compactification lattice parametrized by two integers k_1 and k_2

$$\tan\theta = \frac{k_2 R_2}{k_1 R_1} \tag{1.1.14}$$

as shown in figure 1.2. The explicit boundary state is given by

$$|\mathrm{D1}, \theta(k_1, k_2)\rangle\rangle = \sqrt{\frac{k_1^2 R_1^2 + k_2^2 R_2^2}{2 R_1 R_2}} \prod_{n=1}^{\infty} \exp\left(\frac{1}{n} S_{ij}(\theta)\, a^i_{-n} \bar{a}^j_{-n}\right) |\Omega\rangle \tag{1.1.15}$$

where

$$S(\theta) = \begin{pmatrix} \cos\theta & \sin\theta \\ -\sin\theta & \cos\theta \end{pmatrix} \begin{pmatrix} -1 & 0 \\ 0 & 1 \end{pmatrix} \begin{pmatrix} \cos\theta & -\sin\theta \\ \sin\theta & \cos\theta \end{pmatrix} = \begin{pmatrix} -\cos 2\theta & -\sin 2\theta \\ -\sin 2\theta & \cos 2\theta \end{pmatrix} \tag{1.1.16}$$

and

$$|\Omega\rangle = \sum_{N,M=-\infty}^{\infty} e^{iN\alpha - iM\beta} |k_2 N, k_1 M\rangle \otimes |-k_1 N, k_2 M\rangle \tag{1.1.17}$$

The other class of states, corresponding to bound states between k_2 D2-branes and k_1 D0-branes, is obtained from (1.1.15) through a T-duality transformation (A.1.12) of φ_1. Explicitly, the state is given by

$$|k_2\mathrm{D2}/k_1\mathrm{D0}\rangle\rangle = \sqrt{\frac{k_1^2\alpha'^2 + k_2^2R_1^2R_2^2}{2\alpha' R_1R_2}} \prod_{n=1}^{\infty} \exp\left(\frac{1}{n}\, S'_{ij}(\theta')\, a^i_{-n}\bar{a}^j_{-n}\right)|\Omega'\rangle \tag{1.1.18}$$

where

$$S'(\theta') = S(\theta')\begin{pmatrix} -1 & 0 \\ 0 & 1 \end{pmatrix} = \begin{pmatrix} \cos 2\theta' & -\sin 2\theta' \\ \sin 2\theta' & \cos 2\theta' \end{pmatrix} \tag{1.1.19}$$

with "angle"

$$\tan\theta' = \frac{k_2R_1R_2}{k_1\alpha'} \tag{1.1.20}$$

obtained from the replacement $R_1 \to \alpha'/R_1$ in (1.1.14), and

$$|\Omega'\rangle = \sum_{N,M=-\infty}^{\infty} e^{iN\alpha' - iM\beta'}|k_1M, k_2N\rangle \otimes |-k_1N, k_2M\rangle \tag{1.1.21}$$

obtained from the replacement $n_1 \leftrightarrow w_1$ in (1.1.17). As it will be of interest later, we note that from (1.1.4) the transmission coefficient for the interface corresponding to the D1-brane boundary state is

$$\mathcal{T} = \sin^2 2\theta \tag{1.1.22}$$

with $\theta \to \theta'$ for the D2/D0-brane boundary state. The normalization factors appearing in the boundary states are determined by Cardy's condition, which we will explain for a general bosonic D-brane state in chapter 4.

Owing to their much less complicated zero mode structure, the boundary states corresponding to interfaces between free fermion CFTs have a simpler construction and can be expressed entirely in terms of arbitrary $O(2)$ elements. The fermionic analog to (1.1.9) is

$$\left(\psi^i_n + iS_{ij}\bar{\psi}^j_{-n}\right)|\mathrm{B}\rangle\rangle = 0 \tag{1.1.23}$$

In contrast to (1.1.11) and (1.1.12) the single fermion has the four possible boundary states

$$|\epsilon\rangle\rangle_{\rm NS} = \prod_{n\in\mathbb{N}-\frac{1}{2}} \exp\left(i\epsilon\psi_{-n}\bar{\psi}_{-n}\right)|0\rangle \tag{1.1.24}$$

$$|\epsilon\rangle\rangle_{\rm R} = 2^{\frac{1}{4}}\prod_{n=1}^{\infty} \exp\left(i\epsilon\psi_{-n}\bar{\psi}_{-n}\right)|\epsilon\rangle \tag{1.1.25}$$

corresponding to $\epsilon = \pm 1$ and the different modings in the Neveu-Schwarz (NS) and Ramond sectors. Each of these boundary states are normalized via Cardy's condition as in the bosonic case. In [26] the various fermionic boundary states were found; for the Neveu-Schwarz sector we have

$$|S\rangle\rangle_{\rm NS} = \prod_{n\in\mathbb{N}-\frac{1}{2}} \exp\left(iS_{ij}\psi^i_{-n}\bar{\psi}^j_{-n}\right)|0\rangle|0\rangle \tag{1.1.26}$$

and for the Ramond sector

$$|S\rangle\rangle_{\rm R} = \sqrt{2}\prod_{n=1}^{\infty} \exp\left(iS_{ij}\psi^i_{-n}\bar{\psi}^j_{-n}\right)\left(\cos\frac{\phi}{2}|+\rangle|+\rangle + \sin\frac{\phi}{2}|-\rangle|-\rangle\right) \tag{1.1.27}$$

where ϕ is the angle of rotation for the pure rotation part of S; i.e. after writing S as a rotation composed with an elementary reflection. If S is taken to be of the form (1.1.16) or (1.1.19) then this angle is θ or θ', respectively. As the construction generalizes straightforwardly to larger tensor product fermion theories we will not review their explicit construction.

1.2 Entanglement entropy

The entanglement entropy of a region $\mathcal{A}$ is defined to be the von Neumann entropy

$$\mathcal{S}_{\mathcal{A}} = {\rm Tr}_{\mathcal{A}}\left[\rho_{\mathcal{A}}\log\rho_{\mathcal{A}}\right] \tag{1.2.1}$$

associated with the reduced density matrix $\rho_{\mathcal{A}}$ of that region. This reduced density matrix is a mixed state density matrix obtained by integrating out the degrees of freedom in the

complement $\mathcal{A}^c$ from the total system in a pure state

$$\rho_{\mathcal{A}} = \mathrm{Tr}_{\mathcal{A}^c}\big[|\Psi\rangle\langle\Psi|\big] \tag{1.2.2}$$

and thus encodes the entangling of the degrees of freedom outside $\mathcal{A}$ with those inside $\mathcal{A}$. In this work we will only consider the entanglement entropy of the vacuum state $|\Psi\rangle = |0\rangle$. It is generally difficult to calculate (1.2.1) directly; often it is easier to compute the Renyi entropies

$$\mathcal{S}_{\mathcal{A}}^K \propto \mathrm{Tr}_{\mathcal{A}}\big[\rho_{\mathcal{A}}^K\big] \tag{1.2.3}$$

and evaluate the entanglement entropy as a specific limit

$$\mathcal{S}_{\mathcal{A}} = -\frac{\partial}{\partial K}\,\mathrm{Tr}_{\mathcal{A}}\big[\rho_{\mathcal{A}}^K\big]\Big|_{K=1} \tag{1.2.4}$$

A particularly attractive feature of the power form of (1.2.3) is that it can be interpreted as a partition function $Z(K)$ of a K-times copy of the original theory

$$\mathcal{S} = (1-\partial_K)\log Z(K)\,\big|_{K=1} \tag{1.2.5}$$

This method is known as the replica trick, has been used to calculate entanglement entropy in a wide variety of theories (see e.g. the seminal work of Calabrese and Cardy [33]).

In higher dimensions and with less symmetry, replica calculations can be quite complicated; however, in two-dimensional CFTs the power of conformal transformations in the plane allow for a geometric version of the replica trick, which was first formulated in [34]. The method involves mapping the theory on a K-sheeted Riemann surface to a torus, so that (1.2.5) becomes

$$Z(K) = \mathrm{Tr}\big[(e^{-\delta H})^K\big] = q^{-\frac{c}{12}}\,\mathrm{Tr}\big[q^{L_0+\bar{L}_0}\big] \tag{1.2.6}$$

where $\tau = \frac{i\delta K}{2\pi}$ and $\frac{1}{\delta} = \log\frac{L}{\epsilon}$, with L the length of the entangling region and ϵ a geometric

cutoff at the edges of the entangling region to regulate the short-distance entanglement. After a modular transformation $\tau \to -\frac{1}{\tau}$, we now have that $\tau \propto \frac{1}{K}$ which allows us to write (1.2.5) directly in terms of the original partition function

$$\mathcal{S}_L = \left(1 + \log q \, \frac{\partial}{\partial \log q}\right) \log Z(1) \tag{1.2.7}$$

If the vacuum of the CFT is non-degenerate, then the trace in the partition function has the expansion

$$\mathrm{Tr}\left[q^{L_0+\bar{L}_0}\right] = 1 + \cdots \tag{1.2.8}$$

where the dots indicate higher (positive) powers of q. Keeping only the terms which are non-vanishing as the cutoff is removed, we obtain

$$\mathcal{S}_L = \frac{c}{3} \log \frac{L}{\epsilon} \tag{1.2.9}$$

The prefactor of logarithmically divergence is universal and only depends on the central charge of the CFT. When the vacuum is degenerate the normalization in the expansion (1.2.8) is changed by introducing factors which have K-dependence other than δK, introducing additional subleading terms

$$\mathcal{S}_L = \frac{c}{3} \log \frac{L}{\epsilon} + C \tag{1.2.10}$$

where the prefactors in C are in general dependent on the UV cutoff and thus are not physical.

For a CFT with a boundary or interface, however, the subleading term C becomes physically meaningful [33, 35]. To see why, consider the entropy for an entangling region which is chosen to be an interval lying symmetrically across the interface. Since the removal of the UV cutoff is equivalent to the limit of infinite interval length, the universal term should be the same as (1.2.10) as the endpoints of the interval where entanglement is strongest are symmetrically positioned far away from the location of the interface. Thus the entanglement

entropy has the same form as (1.2.10)

$$\mathcal{S}_{\text{symm}} = \frac{c}{3} \log \frac{L}{\epsilon} + C'(\mathcal{I}) \tag{1.2.11}$$

where now the subleading term C' is a function of the parameters of the interface $\mathcal{I}$. By considering the relative entropy between a given CFT with an interface and without, one can extract physical information about the ground state degeneracy of the interface theory. This difference turns out to be a constant and is called the boundary entropy, which was first introduced in [36]. Often this symmetric entanglement entropy is written to only include physical terms, the precise form being

$$\mathcal{S}_{\text{symm}} = \frac{c}{3} \log \frac{L}{\epsilon} + \log g_B \tag{1.2.12}$$

where the so-called g-factor is the vacuum overlap with the boundary state describing the interface in the folded picture [37, 38]

$$g_B = \langle 0|\mathrm{B}\rangle\rangle \tag{1.2.13}$$

There is another choice of entangling region that we can distinguish from the symmetric interval. We can instead locate the interface at the boundary of the region $\mathcal{A}$ and enlarge $\mathcal{A}$ to cover the whole of one of the two CFTs in the limit as L becomes very large, so that the end-point of the interval is fixed to the location of the interface. As the short distance entanglement occurs precisely at the location of the interface, the universal term should now depend on the parameters of the interface

$$\mathcal{S}_{\text{asymm}} = \frac{c}{3} f(\mathcal{I}) \log \frac{L}{\epsilon} + \tilde{C}(\mathcal{I}) \tag{1.2.14}$$

We call this the asymmetric entanglement entropy, though sometimes in the literature this

is simply referred to as the entanglement entropy *at* the interface. The function $f(\mathcal{I})$ varies depending on the CFT; however, in general $f(\mathcal{I})$ must obey some limits. For an interface that completely decouples the two CFTs it must be the case that $f(\mathcal{I}) = 0$, while for an interface that is completely transmissive (i.e. topological interfaces) it must be the case that $f(\mathcal{I}) = 1/2$. The reason that $f(\mathcal{I}) = 1/2$ instead of 1 has to do with the fact that we are now considering an semi-infinite entangling interval with only one end-point, and thus should have half the entropy of the two end-point case in (1.2.10). The subleading term $\tilde{C}(\mathcal{I})$ is in general different from the one in (1.2.11).

As the asymmetric entanglement entropy depends strongly on the details of the interface, it is generally more difficult to calculate than the symmetric entanglement entropy and therefore is only known in a few cases. Much of this work is focused on calculations of this type of entanglement entropy, and thus we'll now devote some attention to the early work in this area.

1.2.1 Asymmetric intervals in free field theories

Here we review the asymmetric entanglement entropy calculations of [21] and [22] for interfaces between free boson and free fermion CFTs. We choose to first highlight the bosonic calculation as it will be the one most readily generalizable to the junction calculations of chapter 4. In section 1.1 the starting point for characterizing an interface was to consider the corresponding boundary state in the folded picture. Once the boundary state is obtained the folded CFT must then be unfolded to produce the interface operator satisfying (1.1.2) that is needed for the calculation.

The bosonic boundary states in (1.1.15) and (1.1.18) are unfolded into operators via what is essentially a parity transformation on the quantities of one of the CFTs [20]

$$|n, w\rangle \longrightarrow \langle -n, w| \,, \quad a_{-n} \longrightarrow -\bar{a}_n \,, \quad \bar{a}_{-n} \longrightarrow -a_n \tag{1.2.15}$$

Choosing to unfold φ_2 for the state (1.1.15) produces the interface operator

$$I_{1,2} = G_{1,2} \prod_{n=1}^{\infty} \exp\left\{ \frac{1}{n} \left[S_{11}(\theta)\, a^1_{-n} \bar{a}^1_{-n} - S_{12}(\theta)\, a^1_{-n} a^2_n - S_{21}(\theta)\, \bar{a}^2_n \bar{a}^1_{-n} + S_{22}(\theta)\, \bar{a}^2_n a^2_n \right] \right\} \tag{1.2.16}$$

where the ground state operator is given by

$$G_{1,2} = \sqrt{\frac{k_1^2 R_1^2 + k_2^2 R_2^2}{2 R_1 R_2}} \sum_{N,M=-\infty}^{\infty} e^{iN\alpha - iM\beta} |k_2 N, k_1 M\rangle\langle k_1 N, k_2 M| \tag{1.2.17}$$

The expression for the interface operator in (1.2.16) is a formal one, as the negatively-moded oscillators must be placed on the left side of the ground state operator after the full expansion of the exponential. An explicit expression for the interface operator can be obtained by a linearization of the exponential as in (4.1.4), one such choice being

$$\begin{aligned} I_{1,2} = \prod_{n=1}^{\infty} \int \frac{d^2\mathbf{z}_n\, d^2\bar{\mathbf{z}}_n}{\pi^2}\; e^{-\mathbf{z}_n \cdot \bar{\mathbf{z}}_n} e^{-\frac{1}{n} z_{n1} a^1_{-n} - (S_{11}\bar{z}_{n1} - S_{21}\bar{z}_{n2})\, \bar{a}^1_{-n}} \\ \times G_{1,2} \prod_{n=1}^{\infty} e^{-\frac{1}{n} z_{n2} \bar{a}^2_n - (S_{22}\bar{z}_{n2} - S_{12}\bar{z}_{n1})\, a^2_n} \end{aligned} \tag{1.2.18}$$

With expressions for the interface operator like the above the entanglement entropy can be calculated through the geometric replica trick of [34], which is illustrated in figure 1.3. The entanglement entropy is calculated as the usual limit of Renyi entropies of the reduced density matrix

$$\mathcal{S} = -\frac{\partial}{\partial K} \operatorname{Tr}_1[\rho_1^K]\Big|_{K=1} \tag{1.2.19}$$

The trace of the K-th power of the reduced density matrix is re-written as a partition function on a K-sheeted Riemann surface $\mathcal{R}_K$ whose branch cut runs along a time-slice of CFT_1. Cutting off the w-plane outside the annulus $\epsilon < |w| < L$, the mapping $z = \log w$ maps this K-sheeted region into a rectangular region in the z-plane with $\operatorname{Im} z = 0$ and $\operatorname{Im} z = 2\pi K$ identified. For ease of calculation we further identify $\operatorname{Re} z = \log \epsilon$ and $\operatorname{Re} z = \log L$ so that the replicated partition function becomes the torus partition function with $2K$ interfaces

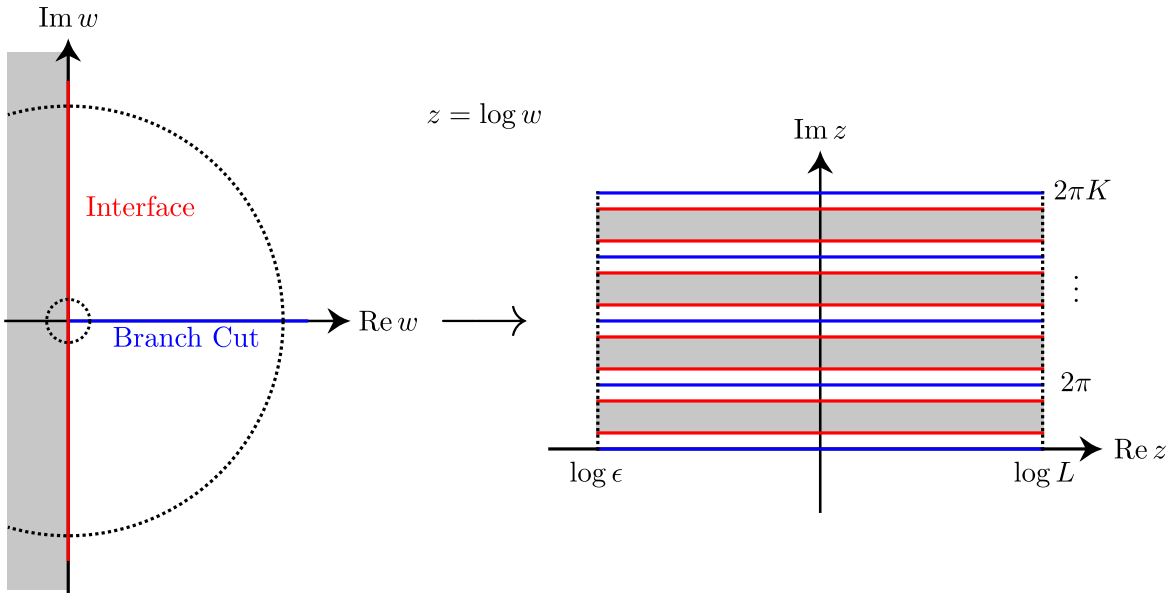

Figure 1.3: The logarithmic map $z = \log w$ maps the K-sheeted Riemann surface – a single branch of which is shown on the left – to the geometry on the right. The circles on the left part of the figure correspond to an UV cutoff located at $|w| = \epsilon$ and an IR cutoff located at $|w| = L$, with their image under the mapping forming the negative and positive real boundaries of the geometry on the right. This figure was adapted from [22].

inserted

$$Z(K) = \mathrm{Tr}_1 \left[\left(I_{1,2}\, q^{H_2} I_{1,2}^{\dagger}\, q^{H_1} \right)^K \right] \tag{1.2.20}$$

for $q = e^{-2\pi t}$ with $t = \pi/\log(L/\epsilon)$ after a rescaling of the z-plane (see [21] for more details). Combined with explicit interface operator expressions like (1.2.18), the operator expression in (1.2.20) can be used to calculate the exact form of the replicated partition function.

Calculating the commutation of the various operators between the ground state operators of successive interfaces, the partition function (1.2.20) is written as a $2K$-(complex) dimensional Gaussian integral. Thus the final evaluation of $Z(K)$ is performed through calculation of a determinant and re-expressed in terms of modular functions

$$Z(K) = g^{2K} K |\sin 2\theta|^{K-1} \theta_3 \left(\frac{itKk_2^2\alpha'}{R_1^2 \sin^2\theta} \right) \theta_3 \left(\frac{itKk_1^2 R_1^2}{\alpha' \cos^2\theta} \right) [\eta(2it)]^{K-3} \prod_{k=1}^{K-1} \theta_1^{-1}(\nu_k | 2it) \tag{1.2.21}$$

where

$$\sin \pi\nu_k = |\sin 2\theta| \sin \frac{\pi k}{K} \tag{1.2.22}$$

The remaining product in the partition function is analytically continued in K, which is reviewed in appendix 4.A.3, so that from (1.2.5) the entanglement entropy is

$$\mathcal{S} = \frac{1}{2}\,\sigma\big(|\sin 2\theta|\big)\log\frac{L}{\epsilon} - \log|k_1 k_2| \tag{1.2.23}$$

with the function $\sigma(s)$ in (4.A.49). The function $\sigma(s)$ increases monotonically from $\sigma(0) = 0$ to $\sigma(1) = 1/3$, matching the behavior of the universal term expected of the entanglement entropy of a semi-infinite interval in a $c = 1$ CFT as discussed at the beginning of this section.

The entanglement entropy of the fermionic interface follows the same general procedure as the bosonic interface calculation, i.e. inserting the unfolded interface operators into (1.2.20) in order to calculate (1.2.5). The fermionic boundary states of (1.1.26) and (1.1.27) are unfolded into operators via the transformation [20]

$$|0\rangle \;\longrightarrow\; \langle 0|\,, \quad |\epsilon\rangle \;\longrightarrow\; \langle\epsilon|\,, \quad \psi_n \;\longrightarrow\; -i\bar{\psi}_{-n}\,, \quad \bar{\psi}_n \;\longrightarrow\; i\psi_{-n} \tag{1.2.24}$$

For the fermionic interfaces the explicit expansion of the quadratic operator exponential is considerably simpler than in the bosonic interfaces due to the fact that for each fixed mode n the Hilbert space $\mathcal{H}_n$ of the corresponding fermionic oscillator is 4-dimensional (as opposed to the infinite-dimensional situation for the bosonic oscillators). As such, the matrix representation on the ordered basis $\{\psi_{-n}|0\rangle, \bar{\psi}_{-n}|0\rangle, \psi_{-n}\bar{\psi}_{-n}|0\rangle, |0\rangle\}$ is

$$I_{1,2} = \left\{\prod_{n>0} I^n_{1,2}\right\} I^0_{1,2} \tag{1.2.25}$$

where

$$I^n_{1,2} = \begin{pmatrix} S_{12} & 0 & 0 & 0 \\ 0 & S_{21} & 0 & 0 \\ 0 & 0 & -\det S & -iS_{11} \\ 0 & 0 & -iS_{22} & 1 \end{pmatrix} \tag{1.2.26}$$

The partition function is then calculated in terms of the four eigenvalues $\lambda_{j,n}$ of the block matrix

$$I^n_{1,2} P^n_2 \left(I^n_{1,2}\right)^\dagger P^n_1 \tag{1.2.27}$$

where matrix representations of the propagators are

$$P^n_i = \begin{pmatrix} q^n & 0 & 0 & 0 \\ 0 & q^n & 0 & 0 \\ 0 & 0 & q^{2n} & 0 \\ 0 & 0 & 0 & 1 \end{pmatrix} \tag{1.2.28}$$

Explicitly for the NS interface, the partition function in terms of the eigenvalues can be re-expressed in terms of modular functions

$$Z(K) = \prod_{n \in \mathbb{N} - \frac{1}{2}} \left(\lambda^K_{1,n} + \lambda^K_{2,n} + \lambda^K_{3,n} + \lambda^K_{4,n}\right) = \frac{\theta_3(2it)}{[\eta(2it)]^K} \prod_{k=1}^{K-1} \theta_3(\nu_k | 2it) \tag{1.2.29}$$

by utilizing the algebraic identity[2]

$$\prod_{k=1}^{K-1} \left[x^2 - 2xy \cos\left(\theta + \frac{2\pi k}{K}\right) + y^2\right] = x^{2K} - 2x^K y^K \cos\left(K\theta\right) + y^{2K} \tag{1.2.30}$$

The analytic continuation in K is similar to the bosonic case, and the entanglement entropy

[2]From the form of (1.2.30) it appears that the final equality in (1.2.29) is only valid for odd values of K. In [22] it was shown that this suffices for calculating the entanglement entropy. Interestingly enough, we will later show in section 4.2.2 that the expression is valid for even K as well.

for both the NS and Ramond interfaces is

$$\mathcal{S} = \frac{1}{2}\left[\frac{1}{2}\sqrt{1-S_{11}^2} - \sigma\big(\sqrt{1-S_{11}^2}\big)\right]\log\frac{L}{\epsilon} \tag{1.2.31}$$

with the universal term satisfying the same limiting behavior as (1.2.23) for a $c = 1/2$ CFT.

For reasons that will be discussed more generally in section 4.2.3, the entanglement entropy of a supersymmetry-preserving conformal interface between two free field theories can be calculated from the boundary state

$$|S\rangle\rangle_{\text{super}} = |S\rangle\rangle_{\text{bos}} \otimes |S\rangle\rangle_{\text{ferm}} \tag{1.2.32}$$

where $|S\rangle\rangle_{\text{bos}}$ is one of the boundary states (1.1.15) or (1.1.18), and $|S\rangle\rangle_{\text{ferm}}$ is either of the boundary states (1.1.26) or (1.1.27) with the same matrix S as $|S\rangle\rangle_{\text{bos}}$. Using this boundary state, the prefactor in the entanglement entropy becomes

$$\mathcal{S}_{\text{super}} = \frac{1}{4}\, s \log\frac{L}{\epsilon} - \log|k_1 k_2| \tag{1.2.33}$$

where s is either $\sin 2\theta$ or $\sin 2\theta'$. Note the simplified form of the universal prefactor in the above, which is a result of the high degree of cancellation between the bosonic and fermionic oscillator contributions to the entropy. All three prefactors discussed in this section are plotted in figure 1.4.

1.3 Holography

Here we discuss the AdS/CFT correspondence and review some well-known bulk theories that will be of later interest. The foundational example of the AdS/CFT correspondence is the duality between type IIB string theory on $AdS_5 \times S^5$ and $\mathcal{N} = 4$ $SU(N)$ Super-Yang-Mills theory in four dimensions [39–41]. The large N, large 't Hooft coupling limit of the field theory is dual to type IIB supergravity, the low energy limit of the string theory.

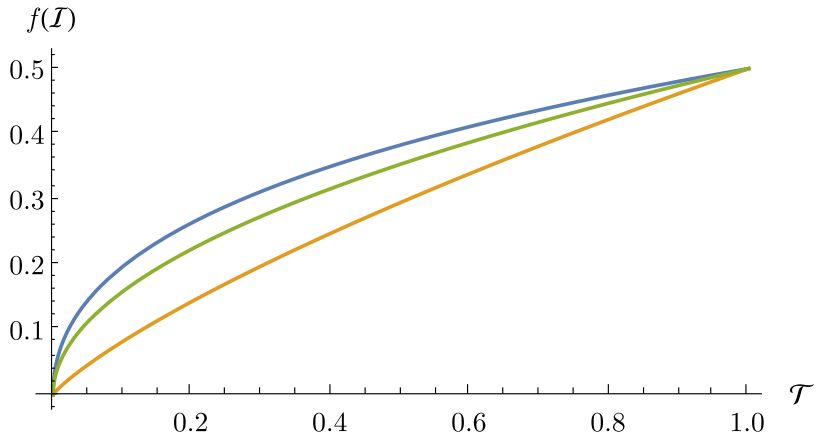

Figure 1.4: Universal prefactors of the entanglement entropy at interfaces between two-dimensional conformal free field theories. The blue curve is the prefactor for bosonic interfaces (1.2.23), the yellow curve is the prefactor for fermionic interfaces (1.2.31), and the green curve is the prefactor for supersymmetric interfaces (1.2.33). Each has been normalized according to (1.2.14) and plotted as a function of the transmission of the interface (1.1.22).

More generally, the AdS/CFT correspondence involves an inversion of the coupling constants between the boundary and bulk theories, with the strongest dualities in the large coupling regimes of the CFT, resulting in the dual gravity description being weakly coupled with small curvatures. In this work we will stay within this classical gravity limit.

We now set out to make a rough statement of the AdS/CFT correspondence (see e.g. [42–44] for more detailed presentations). This is usually given as an equivalence between partition functions

$$Z_{\text{grav}}[\phi] = Z_{\text{CFT}}[\mathcal{O}] \tag{1.3.1}$$

For simplicity we'll consider for the moment a single field ϕ in the bulk and its dual operator $\mathcal{O}$ on the boundary. The connection between ϕ and $\mathcal{O}$ is seen by examining the asymptotic behavior of ϕ. If the action governing ϕ is quadratic and non-degenerate, then ϕ has two independent solutions on the boundary determined by its equation of motion in AdS and two boundary functions

$$\phi(\eta, x) = \frac{j(x)}{\eta^{\Delta_-}} + \cdots + \frac{\mathcal{O}(x)}{\eta^{\Delta_+}} + \cdots \tag{1.3.2}$$

where η is a radial coordinate such that $\eta \to \infty$ approaches the spacetime boundary and

x are the $d-1$ coordinates of the boundary (we have set the AdS radius to 1). The dots represent the subleading terms of each solution, whose x-dependence is governed by $j(x)$ and $\mathcal{O}(x)$, respectively. The values of the constants Δ_- and Δ_+ satisfy[3] $\Delta_- \leq \Delta_+$, with the particular values depending on the mass/spin of ϕ as well as the spacetime dimension. Thus in order for a well-defined variational principle we must either set $j(x) = 0$ or else consider it fixed; i.e. we take as a boundary condition

$$\lim_{\eta\to\infty} \eta^{\Delta_-}\phi(\eta, x) = j(x) \tag{1.3.3}$$

for some fixed $j(x)$, so that $\mathcal{O}(x)$ is the dynamic part of $\phi(\eta, x)$ which is sourced by $j(x)$. We can then re-write (1.3.1) in a more descriptive form

$$e^{iS_{\text{grav}}[\phi_{\text{cl}}(\eta,x)\,;\,j(x)]} = \left\langle e^{i\int_{\partial AdS} d^{d-1}x\, j(x)\,\mathcal{O}(x)} \right\rangle \tag{1.3.4}$$

where $S_{\text{grav}}[\phi_{\text{cl}}(\eta, x)\,;\, j(x)]$ is the classical action for the classical field solution $\phi_{\text{cl}}(\eta, x)$ subject to the boundary condition (1.3.3). From the above we see that the one-point function of the dual boundary operator can be determined as a variation of bulk boundary conditions

$$\langle \mathcal{O}(x)\rangle = \frac{1}{i}\,\frac{\delta Z_{\text{CFT}}}{\delta j}\,\Big|_{j=0} = \frac{\delta S_{\text{grav}}}{\delta j}\,\Big|_{j=0} \tag{1.3.5}$$

which is a useful way to identify dual operators without needing to examine solutions to bulk equations of motion.

Here we have only considered a single field governed by a second-order wave equation. When we incorporate more fields it is possible for the boundary conditions of one field to source the dynamic parts of other fields, a fact we will make explicit use of in chapter 5. Additionally, one can consider fields governed by first-order equations, in which case we still have the basic feature that half of all independent classical solutions must be fixed for a good

[3] If $\Delta_- = \Delta_+$ the $j(x)$ solution picks up a $\log\eta$ dependence.

variational principle to exist. We will defer more discussion of this to section 1.3.2.

Besides linking bulk fields to their dual boundary operators, there exist other entries in the holographic dictionary mapping observable quantities in the boundary to those in the bulk. In particular, we will make use of the Ryu-Takayanagi prescription [15], which states that the entanglement entropy in a CFT can computed holographically via

$$\mathcal{S}_{\mathcal{A}} = \frac{A[\Gamma]}{4G_N} \tag{1.3.6}$$

where $A[\Gamma]$ is the area of the static co-dimension 2 minimal surface in the bulk whose boundary coincides with the edge of the boundary entangling region, i.e. $\partial\Gamma = \partial\mathcal{A}$. The motivation behind this prescription comes from noting that when the information in a region of the boundary becomes inaccessible there must be some horizon in the bulk hiding a part of the spacetime from bulk observers. The entropy associated with integrating out the degrees of freedom behind the horizon should then be proportional to the area of the horizon as given by the Beckenstein-Hawking formula. Selecting the minimal surface as the horizon then corresponds to assigning the lowest entropy possible for the lost information.

1.3.1 Janus solutions

Janus solutions [45–48] are holographic realizations of conformal interfaces[4]. In particular, we are interested in solutions which are asymptotically $AdS_3 \times X_7$ – where X_7 is a 7-dimensional compact manifold – in order to connect with two-dimensional CFT interfaces. Here we review the basic features of both a non-supersymmetric and a supersymmetric solution, and leave calculations of entanglement entropy in these solutions to chapter 2.

The Janus solutions we'll describe are both constructed as fibrations of $AdS_2 \times Y_{8-d}$ over a base manifold Σ_d (here Y_{8-d} is compact and Σ_d contains a single non-compact dimension), thus to better understand the nature of the solutions we'll first review the AdS_2-slicing

[4]See [49–51] for other approaches to describe interfaces in AdS.

coordinates of AdS_3. As a starting point, consider the standard Poincaré AdS_3 metric

$$ds^2 = \frac{1}{\eta^2}\left(d\eta^2 + dx^2 - dt^2\right) \tag{1.3.7}$$

where the boundary is reached by $\eta \to 0$. If we make the coordinate transformation

$$\mu = \tanh^{-1}\left(\frac{x}{\sqrt{\eta^2 + x^2}}\right), \quad z = \sqrt{\eta^2 + x^2} \tag{1.3.8}$$

the metric (1.3.7) becomes

$$ds^2 = d\mu^2 + \cosh^2\mu\,\frac{dz^2 - dt^2}{z^2} \tag{1.3.9}$$

from which we see that constant μ slices of the bulk are AdS_2 geometries. In these coordinates, the boundary of AdS_3 consists of three components: two half-spaces reached by taking $\mu \to \pm\infty$ and the common boundary of the AdS_2 slices reached by taking $z \to 0$. While it may seem that the three conformal boundary components are disconnected this is an artifact of the coordinate system which can be seen by examining the mapping (1.3.8) (see figure 1.5), which shows that the boundary half-spaces $\mu \to \pm\infty$ are glued together at the interface $z = 0$.

The non-supersymmetric Janus solution was constructed in [52]. Through dimensional reduction we can take three-dimensional Einstein gravity with a negative cosmological constant coupled to a massless scalar (e.g. the dilaton field) as a starting point

$$S[g,\phi] = \frac{1}{16\pi G_N}\int d^3x\sqrt{g}\left(R - \partial_\mu\phi\,\partial^\mu\phi + \frac{2}{\ell^2}\right) \tag{1.3.10}$$

The Janus solution solves the equations of motion coming from this action and is given by

$$ds^2 = \ell^2\Big(d\mu^2 + f(\mu)\,\frac{dz^2 - dt^2}{z^2}\Big) \tag{1.3.11}$$

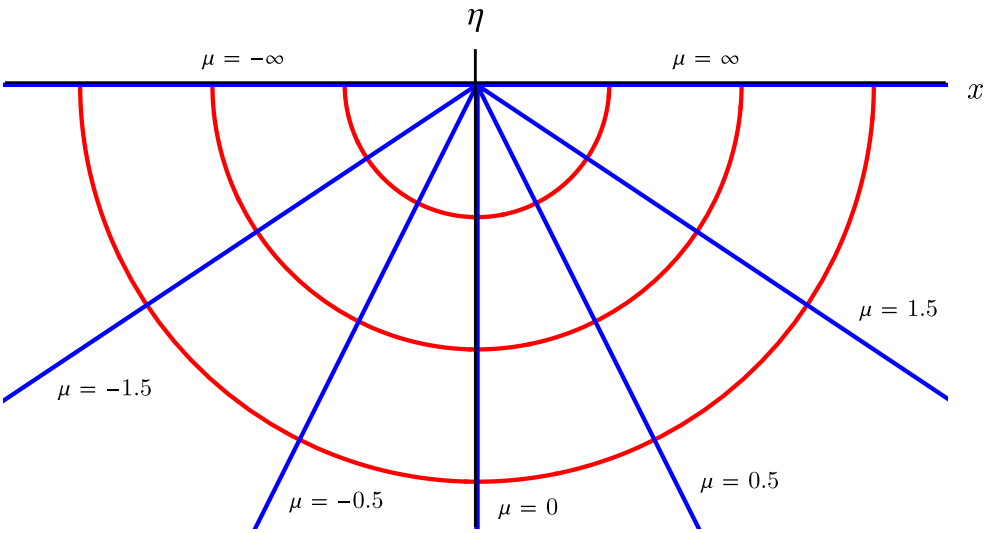

Figure 1.5: AdS_2 slicing in Poincaré coordinates. Curves of constant μ (blue) and z (red) illustrate how the spatial boundary coordinate on one side of the boundary interface extends through the bulk to the opposite side of the boundary interface.

where

$$f(\mu) = \frac{1}{2}\Big(1 + \sqrt{1-2\gamma^2}\,\cosh(2\mu)\Big) \tag{1.3.12}$$

and

$$\phi(\mu) = \phi_0 - \sqrt{2}\,\tanh^{-1}\left(\frac{-1+\sqrt{1-2\gamma^2}}{\sqrt{2}\gamma}\tanh\mu\right) \tag{1.3.13}$$

The solution depends on one parameter γ, and from (1.3.12) and (1.3.9) we see that $\gamma = 0$ corresponds to pure AdS_3. The holographic solution corresponds to an interface connecting two half-spaces which are reached on the boundary of the spacetime by taking $\mu \to \pm\infty$. The massless scalar ϕ takes two asymptotic values in this limit and as shown in [53] the jump in ϕ can be identified with the jump in the radius of the free boson

$$\frac{R_2}{R_1} = \frac{\lim_{\mu\to+\infty} e^{-\phi/2}}{\lim_{\mu\to-\infty} e^{-\phi/2}} = \exp\left\{\sqrt{2}\,\tanh^{-1}\left(\frac{-1+\sqrt{1-2\gamma^2}}{\sqrt{2}\gamma}\right)\right\} \tag{1.3.14}$$

or

$$\gamma = \frac{1}{\sqrt{2}} \tanh\left(\sqrt{2} \log \frac{R_1}{R_2}\right) \tag{1.3.15}$$

where R_2 is taken to be the smaller of the two radii.

The supersymmetric Janus solution of type IIB which is locally asymptotic to $AdS_3 \times S^3 \times M_4$, where M_4 is either T_4 or K_3, was constructed in [54] (see [55, 56] for some earlier work in this direction and [57, 58] for generalizations). The ten-dimensional Janus metric is constructed as a fibration of $AdS_2 \times S^2 \times M_4$ over a two-dimensional Riemann surface Σ

$$ds^2 = f_1^2 ds^2_{AdS_2} + f_2^2 ds^2_{S^2} + f_3^2 ds^2_{M_4} + \rho^2 dw d\bar{w} \tag{1.3.16}$$

All fields depend on the coordinates $w, \bar{w}$ of the surface Σ. For the supersymmetric Janus solution we choose Σ as an infinite strip as follows

$$w = x + iy, \qquad x \in [-\infty, +\infty], \;\; y \in [0, \pi] \tag{1.3.17}$$

The boundaries of the strip are located at $y = 0, \pi$. Asymptotically the real coordinate on the strip joins the coordinates of the AdS_2 factor to form an AdS_3 factor (and hence is the analog of the fibered coordinate μ in the non-supersymmetric solution), while the imaginary coordinate on the strip asymptotically becomes the polar angle of an S^3 factor containing the S^2 factor. The supersymmetric Janus solution depends on four parameters k, ℓ, θ and ψ. The dilaton and axion are given, respectively, by

$$e^{-2\phi} = k^4 \, \frac{\cosh^2(x+\psi)\,\mathrm{sech}^2\psi + \left(\cosh^2\theta - \mathrm{sech}^2\psi\right)\sin^2 y}{\left(\cosh x - \cos y \tanh\theta\right)^2} \tag{1.3.18}$$

$$\chi = -\frac{k^2}{2} \, \frac{\sinh 2\theta \sinh x - 2\tanh\psi \cos y}{\cosh x \cosh\theta - \cos y \sinh\theta} \tag{1.3.19}$$

The metric factors on Σ and M_4 are

$$\begin{aligned}\rho^4 &= e^{-\phi}\,\frac{\ell^2}{k^2}\,\frac{\cosh^2 x\cosh^2\theta-\cos^2 y\sinh^2\theta}{\cosh^2(x+\psi)}\cosh^4\psi\\ f_3^4 &= e^{-\phi}\,\frac{4}{k^2}\,\frac{\cosh x\cosh\theta-\cos y\sinh\theta}{\cosh x\cosh\theta+\cos y\sinh\theta}\end{aligned}\tag{1.3.20}$$

The following expressions for the AdS_2 and S^2 metric factors will be useful

$$\begin{aligned}\frac{f_1^2}{\rho^2} &= \frac{\cosh^2(x+\psi)}{\cosh^2\theta\cosh^2\psi}\\ \frac{\rho^2}{f_2^2} &= \frac{1}{\sin^2 y}+\frac{\cosh^2\theta\cosh^2\psi-1}{\cosh^2\big(x+\psi\big)}\end{aligned}\tag{1.3.21}$$

While the form of the anti-symmetric tensor fields is not essential, we quote from [54] the expressions for the D1 and D5 brane charges

$$\begin{aligned}Q_{D5} &= 4\pi^2 k\ell\,\mathrm{Vol}(M_4)\cosh\psi\cosh\theta\\ Q_{D1} &= \frac{16\pi^2\ell}{k}\cosh\psi\cosh\theta\end{aligned}\tag{1.3.22}$$

The dual CFT is a $\mathcal{N}=(4,4)$ SCFT which, at a particular point of its moduli space, is a $(M_4)^{Q_{D1}Q_{D5}}/S_{Q_{D1}Q_{D5}}$ orbifold. The central charge c of this CFT takes the following form

$$c=\frac{6}{4\pi\kappa_{10}^2}\,Q_{D1}Q_{D5}=\frac{3\times 32\,\pi^3\,\mathrm{Vol}(M_4)\,\ell^2}{\kappa_{10}^2}\,\cosh^2\psi\cosh^2\theta\tag{1.3.23}$$

1.3.2 Chern-Simons theories

Topological field theories have a wide use in condensed matter, high energy and mathematical physics, with one of the best-studied examples being three-dimensional Chern-Simons (CS) theory [59]. In the context of the AdS_3/CFT_2 correspondence, Abelian CS theory is entirely responsible for the introduction of objects in the CFT which are charged under global $U(1)$ currents. Additionally, CS fields have a natural origin from compactifications of type II

string theory or M-theory (see e.g. [60]). In the presence of Maxwell kinetic terms the gauge fields decompose into massive gauge fields and a flat topological sector [61], and since our interest with CS theory in this work is to answer topological questions we do not take the Maxwell terms into account. For discussion of Maxwell-Chern-Simons theories in the context of AdS/CFT see e.g. [62–64].

Consider a theory of N Abelian gauge fields $A^I, I = 1, 2, \ldots, N$ on a 3-manifold $\mathcal{M}$, all with period 2π and with action given by

$$S_{\text{CS}} = \frac{K_{IJ}}{4\pi} \int_{\mathcal{M}} A^I \wedge dA^J \tag{1.3.24}$$

where K_{IJ} is a symmetric matrix called the level matrix. Following [65], we note that the level matrix K has to be integer-valued and even for the theory to be well-defined on topologically nontrivial surfaces under large gauge transformations. The CS theory is a topological field theory as the action is independent of a metric on $\mathcal{M}$. The equations of motion following from (1.3.24) force the connections A^I to be flat

$$K_{IJ}\, dA^J = 0, \quad I = 1, 2, \ldots, N \tag{1.3.25}$$

and hence there are no local propagating degrees of freedom. The only global gauge invariant observables are Wilson lines; however, for three-dimensional manifolds with boundary there can be nontrivial dynamical fields on the boundary relating three-dimensional CS theory to two-dimensional CFTs [59].

There are several uses for three-dimensional CS theory in AdS_3/CFT_2. First, there is the reformulation of three-dimensional gravity in AdS_3 in terms of an $SL(2,\mathbb{R}) \times SL(2,\mathbb{R})$ CS theory [66, 67] and the subsequent formulation of higher spin gravity as a CS theory (see e.g. [68, 69]). Here we will consider a different setup, namely the addition of Abelian CS matter to Einstein gravity.

Consider an asymptotically AdS_3 spacetime in Fefferman-Graham form, with the AdS_3

boundary located at $\eta = +\infty$

$$ds^2 = d\eta^2 + e^{\frac{2\eta}{\ell}} g^{(0)}_{\alpha\beta}\, dx^\alpha dx^\beta + g^{(2)}_{\alpha\beta}\, dx^\alpha dx^\beta + O[e^{-\frac{2\eta}{\ell}}] \tag{1.3.26}$$

In the gauge $A^I_\eta = 0$ the asymptotic form of a gauge field for a general action, including Maxwell or higher derivative terms, is given by

$$A^I_\alpha = A^I_{(0),\alpha} + e^{-\frac{2\eta}{\ell}} A^I_{(2),\alpha} + O[e^{-\frac{3\eta}{\ell}}] \tag{1.3.27}$$

where $A^I_{(0)}$ is flat and only determined through the CS part of the action. As the equation of motion (1.3.25) is first-order, a good variational principle allows us to hold fixed only one boundary component of $A^I_{(0),\alpha}$. However, the CS action is then not stationary due to the appearance of a boundary term in the variation. The standard resolution (see e.g. [60]) is to add a counter term to the action (1.3.24)

$$S_{\rm CT} = \frac{1}{8\pi} K_{IJ} \int d^2z \sqrt{-g^{(0)}}\; g^{(0),\alpha\beta} A^I_{(0),\alpha} A^J_{(0),\beta} \tag{1.3.28}$$

With the addition of this counter term and a flat boundary metric $g^{(0)}_{\alpha\beta} = \eta_{\alpha\beta}$, the variation of the action becomes

$$\delta S_{\rm total} = \delta(S_{\rm CS} + S_{\rm CT}) = \frac{1}{2\pi} K_{IJ} \int d^2z\, A^I_z \delta A^J_{\bar z} \tag{1.3.29}$$

Hence we can identify $A_{\bar z}$ with the source and the dual current is purely holomorphic

$$J_{I,z} = \frac{\delta S_{\rm total}}{\delta A^I_{\bar z}} = \frac{1}{2\pi} K_{IJ} A^J_z \tag{1.3.30}$$

The holomorphic stress tensor can be obtained from (1.3.28) and takes the following form

$$T_{zz} = \frac{\pi}{2} K^{IJ} J_{I,z} J_{J,z} \tag{1.3.31}$$

where K^{IJ} is the inverse of the matrix K_{IJ}. If we instead wish to source anti-holomorphic currents, we then subtract the counter term (1.3.28). In this case we can identify A_z with the source, so that the dual current is purely anti-holomorphic

$$J_{I,\bar{z}} = \frac{\delta S_{\text{total}}}{\delta A_z^I} = -\frac{1}{2\pi} K_{IJ} A_{\bar{z}}^J \tag{1.3.32}$$

and the anti-holomorphic stress tensor takes the form

$$T_{\bar{z}\bar{z}} = -\frac{\pi}{2} K^{IJ} J_{I,\bar{z}} J_{J,\bar{z}} \tag{1.3.33}$$

Chapter 2

Entanglement Entropy at Holographic Interfaces

As the Janus solutions reviewed in section 1.3.1 are dual to conformal interfaces, it is natural to use the Ryu-Takayanagi prescription (1.3.6) to calculate entanglement entropy for these solutions and compare the results to CFT calculations. For the symmetric entangling surface this was done in [35] using the non-supersymmetric Janus solution in three dimensions and in [53] using the supersymmetric Janus solution in six dimensions. In both cases the minimal surfaces were found to wrap all dimensions other than the spatial coordinate of the AdS_2 factor; i.e. the surfaces were described by $z = L/2$ (red curves in figure 1.5), as they would be in undeformed AdS_3. After suitable regularization, the boundary entropy was calculated from the minimal surface area to be

$$\mathcal{S}_{\text{bndy}} = \frac{c}{6} \log \frac{1}{\sqrt{1-2\gamma^2}} \tag{2.0.1}$$

for the non-supersymmetric Janus solution, and

$$\mathcal{S}_{\text{bndy}} = \frac{c}{3} \log \left(\cosh \psi \cosh \theta\right) \tag{2.0.2}$$

for the supersymmetric Janus solution, where in each we have written the result in terms of the central charge of the dual CFT for the sake of comparison.

Our aim in this chapter is to calculate the asymmetric entanglement entropies in these solutions and compare them with the symmetric results and CFT calculations. In section 2.1 we consider the non-supersymmetric Janus solution where we identify the asymmetric minimal surface, compute the entanglement entropy, and compare the results with (1.2.23) and (2.0.1). In section 2.2 we go through the same calculations with the supersymmetric Janus solutions and compare the results with (1.2.33) and (2.0.2). In section 2.3 we provide some discussion of the results and provide some concluding remarks.

2.1 Non-supersymmetric Janus solution

According to the Ryu-Takayanagi prescription the holographic entanglement entropy is determined by finding the area of a minimal surface (at constant time) which at the boundary of the bulk spacetime coincides with the boundary $\partial\mathcal{A}$ of the entangling region $\mathcal{A}$. In this note we calculate the entanglement entropy for the entangling region on one side of the interface. We give a sketch of this geometry (b) in figure 2.1 and contrast it with the symmetric case depicted in (a).

In three dimensions the minimal surface Γ at fixed t is a curve and we have to choose an embedding. As we want the curve to be anchored on the boundary at the location of the interface the appropriate choice for the embedding is $\mu = \mu(z)$ so that we can directly investigate solutions which are regular as $z \to 0$. For this choice the induced line element leads to the following action

$$A[\Gamma] = \int dz \sqrt{\frac{f(\mu)}{z^2} + \left(\frac{\partial \mu}{\partial z}\right)^2} \tag{2.1.1}$$

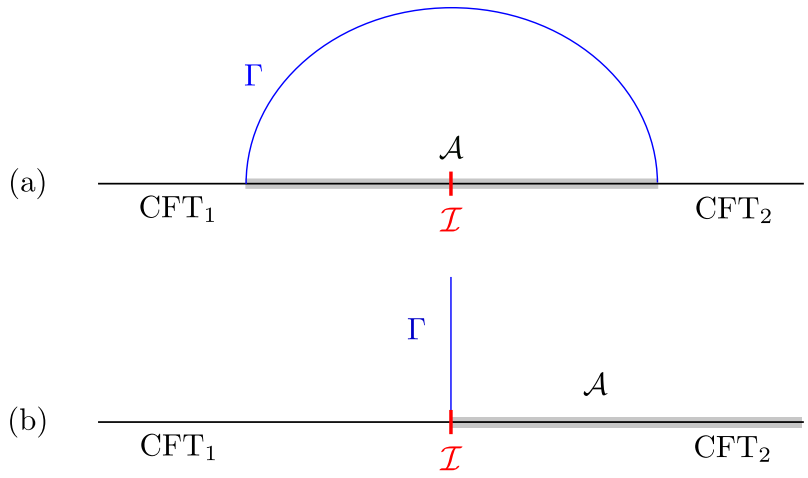

Figure 2.1: Two different geometries for the entangling region $\mathcal{A}$ and interface $\mathcal{I}$: (a) the entangling region is placed symmetrically about the interface, (b) the entangling surface is on one side of the interface. Γ is a sketch of the respective minimal surfaces in the bulk.

The minimal area is found by solving the Euler-Lagrange equation which follows from (2.1.1)

$$f'(\mu)\left(\frac{1}{z^2}+\frac{(\partial_z\mu)^2}{f(\mu)+z^2(\partial_z\mu)^2}\right)-\frac{2}{z}\frac{f(\mu)\,(\partial_z\mu+z\partial_z^2\mu)}{f(\mu)+z^2(\partial_z\mu)^2}=0 \tag{2.1.2}$$

Solutions to the Euler-Lagrange equation can explored through the Hamiltonian flow corresponding to the area functional (2.1.1); i.e. for the canonical conjugate

$$\pi_\mu=\frac{\partial_z\mu}{\sqrt{\frac{f(\mu)}{z^2}+(\partial_z\mu)^2}} \tag{2.1.3}$$

the corresponding Hamilton equations are

$$\partial_z\pi_\mu=\frac{f'(\mu)}{2z}\sqrt{\frac{1-\pi_\mu^2}{f(\mu)}} \tag{2.1.4}$$

$$\partial_z\mu=\frac{\pi_\mu}{z}\sqrt{\frac{f(\mu)}{1-\pi_\mu^2}} \tag{2.1.5}$$

Due to the common explicit dependence on z in the above, we can directly plot the streams of the vector field $\partial_\mu\pi_\mu$ in phase space; see figure 2.2. There is just one fixed point in the

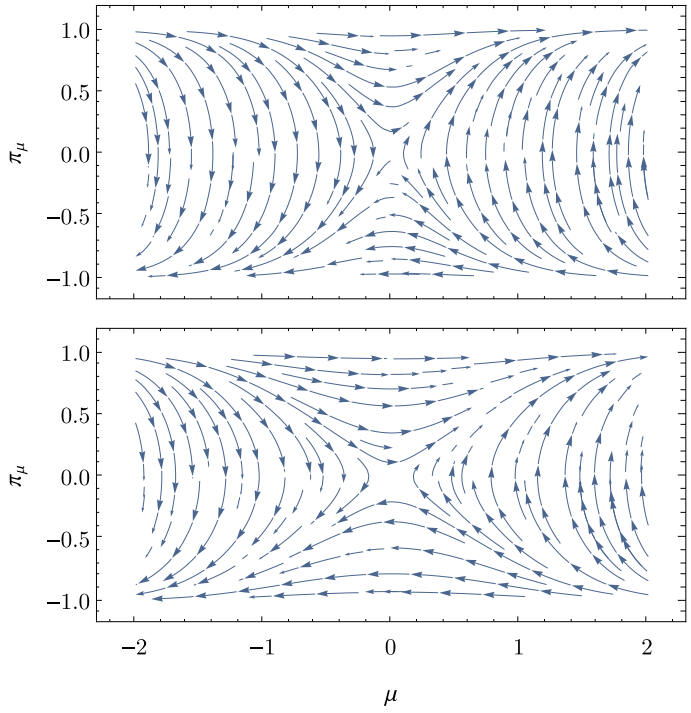

Figure 2.2: Extremal surface phase spaces for the non-supersymmetric Janus solution. The top is purely AdS_3 ($\gamma = 0$) and the bottom is near the maximum deformation ($\gamma \sim 1/\sqrt{2}$).

phase plane, an unstable saddle at the origin with opening angle

$$\cos^{-1}\left(\frac{-1+3\sqrt{1-2\gamma^2}}{1+5\sqrt{1-2\gamma^2}}\right) \tag{2.1.6}$$

which monotonically increases from $\cos^{-1}(1/3)$ when $\gamma = 0$ to π as $\gamma \to 1/\sqrt{2}$. Thus we see that the only solution for which $\partial_z \mu$ remains bounded for all z (a necessary condition for solutions which reach arbitrarily far into the bulk) is $\mu(z) = 0$. It is easy to see that this solution is indeed an absolute minimum for the length, as $\mu = 0$ minimizes the first term and $\partial_z \mu = 0$ minimizes the second term under the square root in the functional (2.1.1).

The holographic entanglement entropy is then given by

$$\begin{aligned}\mathcal{S}_{\text{hol}} &= \frac{\ell}{4G_N}\sqrt{f(0)}\int\frac{dz}{z} \\ &= \frac{c}{6\sqrt{2}}\sqrt{1+\sqrt{1-2\gamma^2}}\,\log\frac{L}{\epsilon}\end{aligned} \tag{2.1.7}$$

where we have regulated the divergent integral over z and used the Brown-Henneaux relation $c = \frac{3\ell}{2G_N}$. In order to compare the functional dependence it is useful to expand the result as a power series in terms of small γ, for the holographic entanglement entropy one finds

$$\mathcal{S}_{\text{hol}} = \left(1 - \frac{1}{4}\,\gamma^2 - \frac{5}{32}\,\gamma^4 + O[\gamma^6]\right)\,\frac{c}{6}\log\frac{L}{\epsilon} \tag{2.1.8}$$

We can compare this to the CFT result for the entanglement entropy (1.2.23). We set $k_1 = k_2 = 1$ which makes the constant term vanish, and expanding (4.A.49) around $s = 1$ gives

$$\begin{aligned}\frac{1}{2}\,\sigma(s) &= \frac{1}{6} - \frac{1}{8}\,(1-s) - \frac{1}{4\pi^2}\,(1-s)^2 + O[(1-s)^3] \\ &= \frac{1}{6} - \frac{1}{16}\,\gamma^2 - \left(\frac{11}{192} + \frac{1}{16\pi^2}\right)\gamma^4 + O[\gamma^6]\end{aligned} \tag{2.1.9}$$

where we have used the expansion

$$s = 1 - \frac{\gamma^2}{2} - \frac{11}{24}\,\gamma^4 + O[\gamma^6] \tag{2.1.10}$$

which follows from (1.1.14) and (1.3.14). Using this expansion in the CFT entanglement entropy (1.2.23) and restoring a general value for the central charge (i.e. by considering c copies of the single boson) gives

$$\mathcal{S}_{\text{CFT}} = \left(1 - \frac{3}{8}\,\gamma^2 - \left(\frac{11}{32} + \frac{3}{8\pi^2}\right)\gamma^4 + O[\gamma^6]\right)\,\frac{c}{6}\log\frac{L}{\epsilon} \tag{2.1.11}$$

Comparing (2.1.9) and (2.1.11) shows that the two expressions only agree for $\gamma = 0$ which corresponds to the case where no interface is present. This result is to be contrasted with the result (2.0.1) of [35], where agreement to order γ^2 was found between the holographic

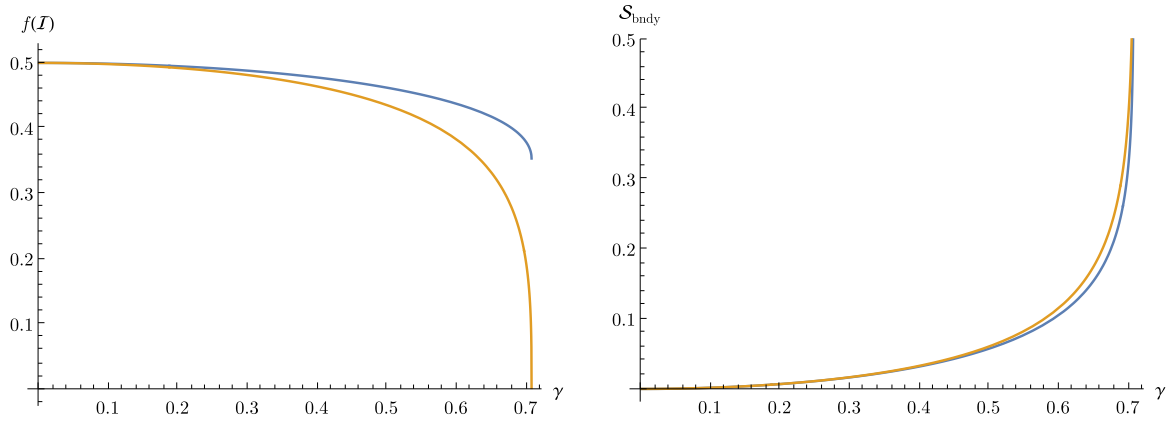

Figure 2.3: Comparison of non-supersymmetric entanglement entropy factors arising in holographic calculations (blue curves) and CFT calculations (yellow curves). On the left the universal prefactors of the asymmetric entanglement entropy are plotted and on the right the constant term of the symmetric entanglement entropy are plotted, all against the Janus deformation parameter γ.

entanglement entropy

$$\mathcal{S}_{\text{hol}} = \frac{c}{6} \log \frac{1}{\sqrt{1-2\gamma^2}} = \frac{c}{6} \left(\gamma^2 + \gamma^4 + O[\gamma^6]\right) \tag{2.1.12}$$

and the ($2c/3$ times copied) CFT entanglement entropy

$$\mathcal{S}_{\text{CFT}} = -\frac{c}{3} \log s = \frac{c}{6} \left(\gamma^2 + \frac{7}{6}\gamma^4 + O[\gamma^6]\right) \tag{2.1.13}$$

given by (1.2.11) and (1.1.15). The results of the holographic and CFT calculations are plotted in figure 2.3 for both the symmetric and asymmetric entanglement entropies.

2.2 Supersymmetric Janus solution

In the supersymmetric solution the non-compact coordinate x of Σ is the along of the coordinate μ of the non-supersymmetric solution, thus we will embed this coordinate. We parametrize the minimal surface for the entanglement entropy by $t = t_0$ and $x = x(z, y)$, i.e. the eight-dimensional surface is spanned by $\xi^a = \{z, y, \phi_1, \phi_2\}$ and the four coordinates of

M_4. The induced metric is then given by

$$\gamma_{ab} = \frac{\partial x^\mu}{\partial \xi^a}\frac{\partial x^\nu}{\partial \xi^b} g_{\mu\nu} \tag{2.2.1}$$

and the action for the minimal surface is

$$A[\Gamma] = \int d^8\xi \sqrt{\det \gamma} \tag{2.2.2}$$

$$= \int_{M_4} dV \int d\phi_1 \, d\phi_2 \, \sin\phi_1 \int dz \, dy \, \frac{1}{z} f_2^2 f_3^4 \rho \sqrt{f_1^2\left(1 + (\partial_y x)^2\right) + z^2\rho^2(\partial_z x)^2} \tag{2.2.3}$$

The Euler-Lagrange equation following from (2.2.2) is given by

$$\begin{aligned} 0 \, = & \frac{1}{z}\,\partial_x\left(f_2^2 f_3^4 \rho \sqrt{f_1^2\left(1 + (\partial_y x)^2\right) + z^2\rho^2(\partial_z x)^2}\right) \\ & - \partial_z\left(\frac{z f_2^2 f_3^4 \rho^3\, \partial_z x}{\sqrt{f_1^2\left(1 + (\partial_y x)^2\right) + z^2\rho^2(\partial_z x)^2}}\right) - \partial_y\left(\frac{f_1^2 f_2^2 f_3^4 \rho\, \partial_y x}{z\sqrt{f_1^2\left(1 + (\partial_y x)^2\right) + z^2\rho^2(\partial_z x)^2}}\right) \end{aligned} \tag{2.2.4}$$

While it seems formidable to find a solution to (2.2.4), a simple solution can be found by specializing to surfaces which wrap the y coordinate. Using the expression for the dual central charge (1.3.23), we note that the action can be written as

$$A[\Gamma] = \frac{c\kappa_{10}^2}{6\pi} \int dz\, dy \, \sin^2 y \sqrt{\frac{f(x)}{z^2}\big(1 + (\partial_y x)^2\big) + (\partial_z x)^2} \tag{2.2.5}$$

with

$$f(x) = \frac{\cosh^2(x+\psi)}{\cosh^2\psi \cosh^2\theta} \tag{2.2.6}$$

owing to (1.3.21) and

$$f_1 f_2^2 f_3^4 \rho = 4\ell^2 \cosh\psi \cosh\theta \cosh(x+\psi) \sin^2 y \tag{2.2.7}$$

This is nearly the same form as (2.1.1), the major difference being the $\partial_y x$ term. Taking this to be zero to minimize its term under the square root, the action becomes

$$A[\Gamma] = \frac{c\kappa_{10}^2}{12} \int dz \sqrt{\frac{f(x)}{z^2} + (\partial_z x)^2} \tag{2.2.8}$$

Interestingly, this is proportional to the action of a minimal surface in a time-slice of empty AdS_3, which can be seen from the coordinate transformation

$$\mu \to x + \psi \quad \text{and} \quad z \to z^{\operatorname{sech}\psi \operatorname{sech}\theta} \tag{2.2.9}$$

applied to the metric (1.3.9). Thus, from the arguments of the previous section, the constant solution $x = -\psi$ is the appropriate minimal surface. Since the expression under the square root in the action functional (2.2.5) is the sum of positive terms which are all minimized by the solution, we have indeed an absolute minimum as demanded by the Ryu-Takayanagi prescription.

For this solution the area is given by

$$A = \frac{c\kappa_{10}^2}{12} \sqrt{f(-\psi)} \int \frac{dz}{z} = \frac{c\kappa_{10}^2}{12 \cosh\psi \cosh\theta} \log\frac{L}{\epsilon} \tag{2.2.10}$$

and the holographic entanglement entropy can then be expressed as

$$\mathcal{S}_{\text{hol}} = \frac{A}{4G_N^{(10)}} = \frac{1}{\cosh\theta \cosh\psi} \frac{c}{6} \log\frac{L}{\epsilon} \tag{2.2.11}$$

where we used the identification $1/16G_N^{(10)} = 1/2\kappa_{10}^2$. In order to compare the holographic result (2.2.11) to the CFT (1.2.33) we have to set $\theta = 0$, which on the CFT side corresponds to an interface where only the radius of M_4 jumps and there is no jump of the RR modulus [53]. The jump of the radius can be identified with the parameter ψ of the supergravity solution

as follows [53]

$$\frac{R_2}{R_1} = e^{\psi} \tag{2.2.12}$$

and hence

$$2\cosh\psi = \frac{R_1}{R_2} + \frac{R_2}{R_1} \tag{2.2.13}$$

The identification of s is then given by

$$s = \sin 2\theta = \frac{2R_1R_2}{R_1^2 + R_2^2} = \frac{1}{\cosh\psi} \tag{2.2.14}$$

Hence in this special case the holographic entanglement entropy (2.2.11) becomes

$$\mathcal{S}_{\rm hol} = \frac{c}{6}\, s \log\frac{L}{\epsilon} \tag{2.2.15}$$

which is in exact agreement with the CFT result (1.2.33) if we replace the value $c = 3/2$ for a real boson and a real fermion with the general value of the central charge, again setting $k_1 = k_2 = 1$. As far as this identification is concerned in our case the symmetric orbifold CFT which is dual to supergravity on $AdS_3 \times S^3 \times M_4$ can simply be viewed as $4N = 4Q_5Q_1$ copies of the $c = 3/2$ system. This is precisely the same exact agreement found in [53], which can be seen from the equality between (2.1.13) and (2.0.2) with $\theta = 0$ and ψ given by (2.2.14).

2.3 Discussion

In this chapter the holographic entanglement entropy was calculated for a surface $\mathcal{A}$ which lies on one side of a conformal interface. It is interesting to contrast the result (2.1.7) with the result for the entanglement entropy for a surface which is lying symmetrically across the

interface

$$S_{\mathcal{A}}^{\text{symm}} = \frac{c}{6}\log\frac{L}{\epsilon} + \frac{c}{6}\log\frac{1}{\sqrt{1-2\gamma^2}} \tag{2.3.1}$$

Note that for the geometric setup discussed in this note the logarithmically divergent term does not have a universal prefactor $c/6$ but depends on the parameters of the interface via the function $\sqrt{f(0)}$. This difference makes sense as the interface is located at the boundary between $\mathcal{A}$ and its complement, where the entanglement between the two regions is strongest.

It is also interesting to compare the holographic calculations of the entanglement entropy for the two cases. In [35] the non-supersymmetric Janus solution was used to calculate (2.3.1) and in particular the holographic boundary entropy $\log g_B$ was calculated. A comparison with the CFT calculation led to an agreement of $\log g_B$ to first nontrivial order in the deformation parameter γ. In section 2.1 we found that in our case the result disagrees even to the lowest nontrivial order in γ.

This state is to be contrasted with the supersymmetric Janus solution where both for the symmetric entangling region [53] and the asymmetric case calculated in section 2.2 the CFT and the holographic entanglement entropy agree. Note that the CFT and the gravity calculations are performed at very different points in the moduli space of the dual CFT. It is likely that the high degree of supersymmetry allows the extrapolation of the results from one point to the other[1].

The supersymmetric Janus solution depends on two parameters θ and ψ and we set $\theta = 0$ for the comparison. The parameter θ corresponds to an RR modulus and consequently to a twist field in the symmetric orbifold CFT. It would be interesting to see whether the CFT calculation can be performed for a general interface operator $I_{1,2}$ which includes a jump in the twist field.

Recently the CFT at the symmetric orbifold point has been conjectured to be dual to a

[1] In a recent paper [70] the entanglement entropy in a (nonsupersymmetric) holographic model of the Kondo model was calculated and agreement with field theory results was found.

higher spin theory [71, 72]. The region in moduli space where supergravity is valid is far removed from this point. Supersymmetry seems to make the result of the entanglement entropy independent of where on its moduli space the theory is. It would be interesting to investigate whether it is possible to construct the relevant interface theories in the Chern-Simons formulation following [73] and calculate the entanglement entropy following the proposals relating the entanglement entropy and the Wilson loop in higher spin theory [74–76].

Chapter 3

Entanglement Entropy at RCFT Topological Interfaces

As discussed in section 1.1, the stronger topological interface condition (1.1.6) allows for interface operators to be found in larger classes of theories. In particular, through the work of Petkova and Zuber [77, 78] interface operators were found for topological interfaces in a general (diagonally embedded) rational CFT (RCFT). RCFTs encompass a large number of interesting theories, including the minimal models, the free compactified boson at certain radii, and Liouville theory. While it is interesting to explore the entanglement entropy for interfaces in larger classes of theories, topological interfaces have special properties not present in a general conformal interface. One can define a fusion product of topological interfaces by bringing two of them close together [20]. It has also been argued in [11, 79, 80] that topological interfaces can furnish spectrum generating symmetries. Topological interfaces have been constructed for a single free boson in [19, 29] and for N free bosons compactified on an N-dimensional torus in [26]. Topological interfaces in orbifold theories have been studied in [30].

The focus of this chapter is to calculate the entanglement entropy for both symmetric and asymmetric intervals around topological interfaces in RCFTs. The structure of the

chapter is as follows: in section 3.1 we review the construction of topological interfaces in rational CFTs which goes back to the work of Petkova and Zuber [77, 78]. In section 3.2 we adapt the calculation of [21, 22] (reviewed in section 1.2.1) to calculate the asymmetric entanglement entropy[1]. In section 3.3 we again adapt the calculation of [21, 22] to re-derive the symmetric entanglement entropy (1.2.12) and also give an argument that the location of the interface does not change the result as long as it is a finite distance away from the boundaries of the entangling interval. In section 3.4 we compare the entanglement entropies for various specific cases. We also include the recently computed left/right entropy [82, 83] for reference. In section 3.5 we use the construction of topological interfaces in Liouville theory given in [84, 85] to attempt a calculation of the entanglement entropy for this system. We close with a discussion of our results in section 3.6.

3.1 Topological interfaces in RCFT

In this section we consider the construction of topological interfaces in rational CFTs. A rational CFT (RCFT) [86] contains a finite number of primary states and hence a finite number of representations of the Virasoro algebra, labeled by i, with characters $\chi_i(q)$. The partition function on the torus is given by

$$Z = \sum_{i,\bar{j}} Z_{i\bar{j}}\ \chi_i(q)\chi_{\bar{j}}(\bar{q}) \tag{3.1.1}$$

where $Z_{i\bar{j}}$ are positive integers which denote how many times a representation appears in the spectrum of the theory. We mostly limit ourselves the the case where $Z_{i\bar{j}} = \delta_{i\bar{j}}$ and the theory has a diagonal spectrum.

The canonical examples for rational CFTs[2] are the unitary minimal models which have

[1] While the paper [2] this chapter is based on was finalized a paper [81] appeared, which has significant overlap with the material presented in section 3.2.

[2] We limit ourselves to minimal models with respect to the Virasoro algebra here, generalizing the discussion to rational CFTs with respect to extended conformal algebras would be very interesting.

central charge

$$c = 1 - \frac{6}{m(m+1)}\,, \qquad m = 3, 4, \cdots \tag{3.1.2}$$

and the primaries are labeled by two integers $r = 1, 2, \ldots, m-1$ and $s = 1, 2, \ldots r$ and have conformal dimension

$$h_{r,s} = \frac{\big((m+1)r - ms\big)^2 - 1}{4m(m+1)} \tag{3.1.3}$$

The simplest minimal model is the Ising model which has $m = 3$ and hence we have $c = \frac{1}{2}$ and there are three primaries with $h = 0$, $h = \frac{1}{2}$ and $h = \frac{1}{16}$.

In [77, 78] twisted partition functions for rational CFTs were studied. They are characterized by the insertion of an operator I into the partition function, where I satisfies

$$[L_n, I] = [\bar{L}_n, I] = 0 \tag{3.1.4}$$

In [77] a classification of such operators was given analogous to the construction of Cardy states [25]. For the diagonal theories one finds

$$I_a = \sum_i \frac{S_{ai}}{S_{0i}}\, P^{i\bar{i}} \tag{3.1.5}$$

Here $P^{i\bar{i}}$ is a projector on the space spanned by the i-th primary and its descendants

$$P^{i\bar{i}} = \sum_{n\bar{n}} |i, n\rangle \otimes |i, \bar{n}\rangle\langle i, n| \otimes \langle i, \bar{n}| \tag{3.1.6}$$

This means that in the simple diagonal case there are as many topological interfaces as there are primaries, where for simplicity we assume that each primary only appears once in the theory; a degeneracy can be easily included in the construction.[3] The matrix S is the modular

[3] See [87] for a discussion of more general projectors including non-diagonal theories.

S matrix which denotes how the characters transform under modular transformation

$$\chi\big(-\tfrac{1}{\tau}\big) = \sum_j S_{ij}\chi_j(\tau) \tag{3.1.7}$$

where τ is defined by $q = e^{2\pi i\tau}$. The conjugate interface operator is given by

$$I_a^\dagger = \sum_i \left(\frac{S_{ai}}{S_{0i}}\right)^* P^{i\bar{i}} \tag{3.1.8}$$

In summary it is notable that the classification of [77, 78] of twisted partition functions also provides us with a classification of topological interfaces in RCFTs.

3.2 Entanglement entropy at a topological interface

The K-th partition function with a topological interface (3.1.5) labeled by a primary a inserted is

$$\begin{aligned} Z_a(K) &= \mathrm{Tr}\Big[\Big(I_a q^{L_0-\frac{c}{24}}\bar{q}^{\bar{L}_0-\frac{c}{24}} I_a^\dagger q^{L_0-\frac{c}{24}}\bar{q}^{\bar{L}_0-\frac{c}{24}}\Big)^K\Big] \\ &= \mathrm{Tr}\Big[(I_a I_a^\dagger)^K q^{2K(L_0-\frac{c}{24})}\bar{q}^{2K(\bar{L}_0-\frac{c}{24})}\Big] \\ &= \sum_i \left|\frac{S_{ai}}{S_{0i}}\right|^{2K} \chi_i(q^{2K})\chi_{\bar{i}}(\bar{q}^{2K}) \end{aligned} \tag{3.2.1}$$

where we have introduced $q = \bar{q} = e^{-t}$. In the second line we have used (3.1.4) to commute I_a through the Hamiltonian and in the third line we used the fact that the P^{ii} in (3.1.5) are projectors to the i-th representation so that the trace produces the associated character χ_i.

Since we are interested in taking the UV cutoff $\epsilon \to 0$ (and equivalently taking $L \to \infty$), we have to evaluate (3.2.1) in the limit $q \to 1$. With the identification of a new modular parameter τ' by

$$q^{2K} = e^{-2Kt} = e^{2\pi i\tau'} \tag{3.2.2}$$

with $t = 2\pi^2/\log(L/\epsilon)$, the limit can taken by performing a modular transformation on the characters

$$\begin{aligned}\lim_{q\to 1}\chi_i(q^{2K})\chi_{\bar{i}}(\bar{q}^{2K}) &= \lim_{\tau'\to 0}\chi_i(\tau')\chi_i(\bar{\tau}') \\ &= \lim_{\tau'\to 0}\sum_{j,k} S_{ij}S^*_{ik}\,\chi_j(-1/\tau')\,\chi_k(-1/\bar{\tau}') \\ &= \sum_{j,k} S_{ij}S^*_{ik} e^{\frac{\pi^2 c}{6Kt}} e^{-\frac{2\pi^2 h_j}{Kt}} e^{-\frac{2\pi^2 h_k}{Kt}} \left(1 + O[e^{-2\pi^2/Kt}]\right) \end{aligned} \tag{3.2.3}$$

In the limit $t \to 0$ the leading contribution in (3.2.3) will come from the vacuum characters which have $h_j = h_k = 0$. In that case the partition function (3.2.1) becomes

$$Z_a(K) \approx \exp\left(\frac{c}{12K}\log\frac{L}{\epsilon}\right)\sum_i |S_{ai}|^{2K}|S_{0i}|^{2-2K} + \cdots \tag{3.2.4}$$

where the dots indicate terms which vanish as the cutoff is taken to zero. Further calculating

$$\begin{aligned}\left(1-\partial_K\right)\log\left(\sum_i |S_{ai}|^{2K}|S_{0i}|^{2-2K}\right)\Big|_{K=1} &= -2\,\frac{\sum_i |S_{ai}|^{2K}|S_{0i}|^{2-2K}\left(\log|S_{ai}| - \log|S_{0i}|\right)}{\sum_j |S_{aj}|^{2K}|S_{0j}|^{2-2K}}\Big|_{K=1} \\ &= -2\sum_i |S_{ai}|^2 \log\left|\frac{S_{ai}}{S_{0i}}\right| \end{aligned} \tag{3.2.5}$$

where we have repeatedly used the fact that S is symmetric, unitary, and in particular the relation $\sum_j |S_{aj}|^2 = 1$. Putting everything together we arrive at the following expression for the entanglement entropy at a topological interface

$$\mathcal{S}_a = \frac{c}{6}\log\frac{L}{\epsilon} - 2\sum_i |S_{ai}|^2 \log\left|\frac{S_{ai}}{S_{0i}}\right| \tag{3.2.6}$$

3.3 Symmetric and left/right entanglement entropy

For an interface which is located symmetrically on the entangling interval $\mathcal{A}$ the entanglement entropy is given by (1.2.12), with the subleading constant term related to the boundary g-

factor which is determined by the overlap of the boundary state corresponding to the doubled interface with the vacuum state. For the topological interface (3.1.5) the boundary state becomes

$$|\mathrm{B}_a\rangle\rangle = \sum_i \frac{S_{ai}}{S_{0i}} \sum_{n,\bar{n}} |i,n\rangle \otimes |i,\bar{n}\rangle |i,\bar{n}\rangle \otimes |i,n\rangle \tag{3.3.1}$$

Consequently the g-factor is given by

$$g_B = \frac{S_{a0}}{S_{00}} \tag{3.3.2}$$

and the symmetric entanglement entropy becomes

$$\mathcal{S}_a^{\mathrm{symm}} = \frac{c}{3} \log \frac{L}{\epsilon} + \log \frac{S_{a0}}{S_{00}} \tag{3.3.3}$$

Up to now we have considered the symmetric case where the interface is located at the center of the entangling interval $\mathcal{A}$. There is however a simple argument showing that for topological interfaces the location of the interface does not change the result as long as it is a finite distance away from the boundary of the entangling interval. We illustrate the argument in figure 3.1. We start in the ζ plane with a finite interval $\mathcal{A}$ with boundary at $\zeta = 0$ and $\zeta = l$, where the interface is located along $\zeta = y + i\xi$, $\xi \in \mathbb{R}$. We map the ζ plane into the w plane by the map

$$z = \frac{\zeta}{l - \zeta} \tag{3.3.4}$$

This maps the finite interval to the positive real axis and the interface gets mapped to an off-center circle. Finally we perform the replica map to the z coordinate via $z = \log w$ and impose periodic boundary conditions as before at the cutoff $z = \log \epsilon$ and $z = \log L$. This produces again a torus. Unlike the case of the interface at the boundary here the interface

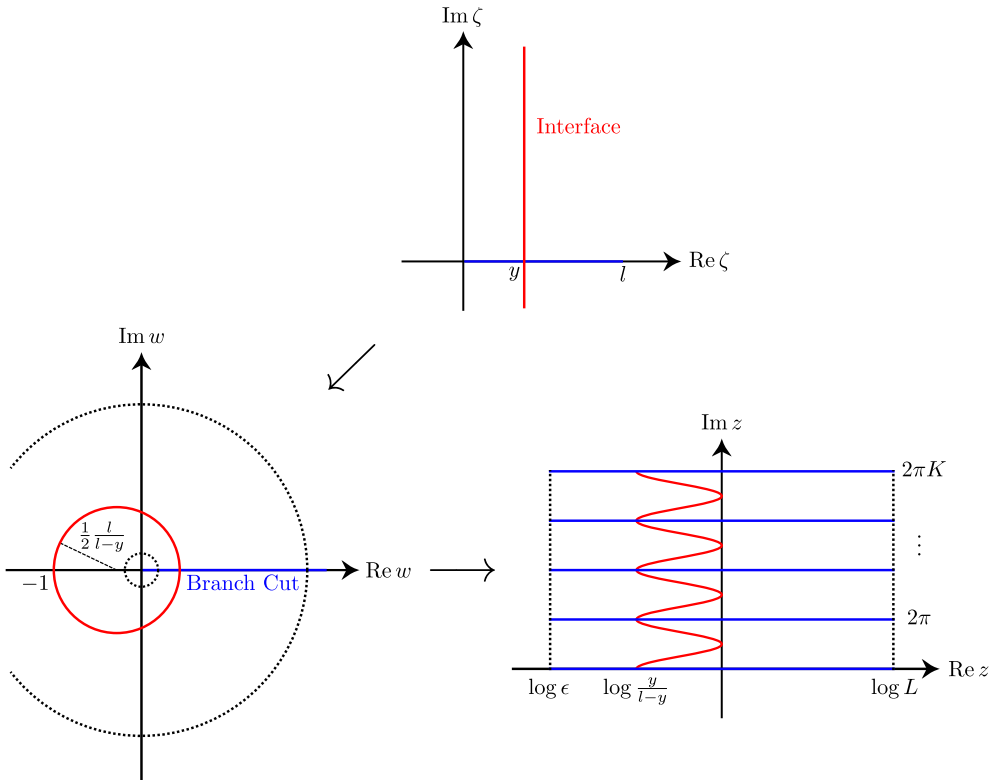

Figure 3.1: Mapping of a non-central interface to the replica torus.

is mapped into a vertical curve on the torus. For a topological interface it is clear that the shape can be changed and changing the location along the real part of z corresponds to changing the original location y of the interface. This shows that partition function on the K-th sheeted Riemann surface is independent of y as long as the interface is a finite distance away form the cutoffs. We can be more specific and evaluate the partition function

$$\begin{aligned} Z_a(K) &= \mathrm{Tr}[I_a e^{-tH}] \\ &= \sum_i \frac{S_{ai}}{S_{0i}} \chi_i(q)\chi_i(\bar{q}) \end{aligned} \tag{3.3.5}$$

where $q = \bar{q} = e^{-\frac{\pi^2}{Kt}}$ where again $t = 2\pi^2/\log(L/\epsilon)$, hence in the limit of vanishing cutoff the sum over representations in the partition function gets projected on the vacuum character

and one has

$$Z_a(K) \sim \frac{S_{a0}}{S_{00}} \exp\left(\frac{c}{12K} \log \frac{L}{\epsilon}\right) + \cdots \tag{3.3.6}$$

Applying the replica formula (1.2.5) one obtains

$$\mathcal{S}_a^{\text{symm}} = \frac{c}{6} \log \frac{L}{\epsilon} + \log \frac{S_{a0}}{S_{00}} \tag{3.3.7}$$

Comparing (3.3.7) with (3.3.3) one notices an extra factor of 1/2 in (3.3.7) in the $\log(L/\epsilon)$ term. This seeming discrepancy comes from the fact that the replica calculation leading to (3.3.7) calculates the entanglement entropy for a semi-infinite entangling surface (as we take L to be very large) with only one end point, whereas the result of Cardy and Calabrese (3.3.3) is for an interval with two end points, which doubles the logarithmically divergent contribution according to the area law for entanglement entropy. The same remark applies when one compares (1.2.12) and (3.2.6).

Additionally it is clear that for a topological interface moving the interface along the real axis in the z coordinates does not change (3.3.5) as the interface operator commutes with the generator of these translations, which is the Hamiltonian. It is clear from Figure 3.1 that the independence of the symmetric entanglement entropy from the location of the interface breaks down if the interface approaches the UV cutoff ϵ, as part of the interface would be removed by the cutoff. This explains why the entanglement entropies (3.2.6) and (3.3.3) can be different.

A third type of entanglement entropy which takes a similar form is the so-called left/right entanglement entropy [82, 83, 88]. This is defined for a boundary CFT, where the entanglement entropy is calculated with a reduced density matrix obtained by tracing over left-moving modes. Interestingly for a boundary CFT defined by a Cardy state [25] (for a single copy of

the CFT, not the doubled one we are considering in the previous sections)

$$|\mathrm{B}_a^{\mathrm{Cardy}}\rangle\rangle = \sum_j \frac{S_a^j}{\sqrt{S_0^j}} |j\rangle\rangle \tag{3.3.8}$$

where $|j\rangle\rangle$ are the Ishibashi states [24] enforcing conformal boundary conditions. We quote the result of the calculation of the left/right entanglement entropy which is also labeled by a primary a in a RCFT, obtained in [83]

$$\mathcal{S}_a^{\mathrm{l/r}} = \frac{\pi c l}{24\epsilon} - \sum_j S_{aj}^2 \log \frac{S_{aj}^2}{S_{0j}} \tag{3.3.9}$$

The physical interpretation of the left/right entanglement entropy (as it is non-geometrical) is not clear at this point as well as its relation to the other two entropies is not clear at the moment. The similarities of the resulting entropies might still suggest that such a relation exists. A better understanding of the relation of the cutoffs utilized may be necessary to accomplish this.

3.4 Examples of entanglement entropies

For the m-th unitary minimal models the modular S matrix is given by (see e.g. [89])

$$S_{rs;\rho\sigma} = 2\sqrt{\frac{2}{m(m+1)}}\,(-1)^{1+s\rho+r\sigma} \sin\left(\pi \frac{m+1}{m} r\rho\right) \sin\left(\pi \frac{m}{m+1} s\sigma\right) \tag{3.4.1}$$

Using this formula it is in principle straightforward to evaluate the three entanglement entropies: $\mathcal{S}_a$ given in (3.2.6), $\mathcal{S}_a^{\mathrm{symm}}$ given in (3.3.3) and $\mathcal{S}_a^{\mathrm{l/r}}$ given in (3.3.9). Here we give tables for the two simplest cases, namely the Ising model with $m = 3$ and the tri-critical Ising model with $m = 4$.

The Ising model has 3 primaries which we can label by their conformal dimension $h =$

$0, \frac{1}{16}, \frac{1}{2}$ and has the modular S matrix

$$S = \frac{1}{2}\begin{pmatrix} 1 & 1 & \sqrt{2} \\ 1 & 1 & -\sqrt{2} \\ \sqrt{2} & -\sqrt{2} & 0 \end{pmatrix} \tag{3.4.2}$$

The entanglement entropies then take the following values

	$\mathcal{S}_a$	$\mathcal{S}_a^{\text{symm}}$	$\mathcal{S}_a^{\text{l/r}}$
$h = 0$	0	0	$\frac{3}{4}\ln 2$
$h = \frac{1}{2}$	0	0	$\frac{3}{4}\ln 2$
$h = \frac{1}{16}$	$-\ln 2$	$\frac{\ln 2}{2}$	0

Table 3.1: Entanglement entropies for the Ising model.

The next simplest minimal model is the tri-critical Ising model which has $m = 4$ and has six primary states which are labelled by their conformal dimension

$$h = 0, \frac{1}{10}, \frac{3}{5}, \frac{3}{2}, \frac{3}{80}, \frac{7}{16} \tag{3.4.3}$$

The modular S matrix is given by

$$S = \begin{pmatrix} s_2 & s_1 & s_1 & s_2 & \sqrt{2}s_1 & \sqrt{2}s_2 \\ s_1 & -s_2 & -s_2 & s_1 & \sqrt{2}s_2 & -\sqrt{2}s_1 \\ s_1 & -s_2 & -s_2 & s_1 & -\sqrt{2}s_2 & \sqrt{2}s_1 \\ s_2 & s_1 & s_1 & s_2 & -\sqrt{2}s_1 & -\sqrt{2}s_2 \\ \sqrt{2}s_1 & \sqrt{2}s_2 & -\sqrt{2}s_2 & -\sqrt{2}s_1 & 0 & 0 \\ \sqrt{2}s_2 & -\sqrt{2}s_1 & \sqrt{2}s_1 & -\sqrt{2}s_2 & 0 & 0 \end{pmatrix} \tag{3.4.4}$$

where s_1 and s_2 are given by

$$s_1 = \sin\left(\frac{2\pi}{5}\right), \qquad s_2 = \sin\left(\frac{4\pi}{5}\right) \tag{3.4.5}$$

The entanglement entropies then take the following values

a	$\mathcal{S}_a$	$\mathcal{S}_a^{\text{symm}}$	$\mathcal{S}_a^{\text{l/r}}$
$h=0$	0	0	$\frac{-2\sqrt{5}\coth^{-1}\sqrt{5}+\ln\frac{32768}{3125}}{4}$
$h=\frac{1}{10}$	$-\sqrt{5}\coth^{-1}\left(\frac{3}{\sqrt{5}}\right)$	$\frac{1}{2}\ln\frac{3+\sqrt{5}}{2}$	$\frac{15\ln 2-5\ln 5+\sqrt{5}\ln(9-4\sqrt{5})}{4}$
$h=\frac{3}{5}$	$-\sqrt{5}\coth^{-1}\left(\frac{3}{\sqrt{5}}\right)$	$\frac{1}{2}\ln\frac{3+\sqrt{5}}{2}$	$\frac{15\ln 2-5\ln 5+\sqrt{5}\ln(9-4\sqrt{5})}{4}$
$h=\frac{3}{2}$	0	0	$\frac{-2\sqrt{5}\coth^{-1}\sqrt{5}+\ln\frac{32768}{3125}}{4}$
$h=\frac{3}{80}$	$\frac{(-5+\sqrt{5})\ln(3-\sqrt{5})-(5+\sqrt{5})\ln(3+\sqrt{5})}{2}$	$\frac{1}{2}\ln(3+\sqrt{5})$	$\frac{-5\ln 5+\sqrt{5}\ln(9-4\sqrt{5})}{4}$
$h=\frac{7}{16}$	$-5\ln 2$	$\frac{\ln 2}{2}$	$\frac{-2\sqrt{5}\coth^{-1}\sqrt{5}-5\ln 5}{4}$

Table 3.2: Entanglement entropies for the tri-critical Ising model.

3.5 Remarks on entanglement entropies for Liouville theory

In [84, 85, 90] topological interfaces for the Liouville CFT (see [91, 92] for reviews with references to the original literature) were constructed following the procedure which was used for RCFTs. There are two types of defects which are both of the form

$$I = \int_{Q/2+iP} d\alpha\; D(P)\mathcal{P}^{\alpha} \tag{3.5.1}$$

where we integrate P over the positive real line, i.e. $P \in (0,\infty)$, and one has $Q = b + 1/b$, which determines the central charge as $C = 1+6Q^2$. Here $\mathcal{P}$ is a projector on the continuum of primary states labeled by P and their descendants

$$\mathcal{P}^{\alpha} = \sum_{M,N} |\alpha, M\rangle \otimes |\overline{\alpha, N}\rangle\langle\alpha, M| \otimes \langle\overline{\alpha, N}| \tag{3.5.2}$$

As shown in [84] one can distinguish the two types of defects by associating them with the discrete degenerate primary states labeled by two positive integers

$$D_{m,n}(P) = \frac{\sinh(\frac{2\pi mP}{b})\sinh(2\pi nbP)}{\sinh(\frac{2\pi P}{b})\sinh(2\pi bP)} \tag{3.5.3}$$

and a non-degenerate primary state labeled by a continuous real parameter s

$$D_s(P) = \frac{\cos(4\pi Ps)}{2\sinh(2\pi bP)\sinh(\frac{2\pi P}{b})} \tag{3.5.4}$$

We can now calculate the K-sheeted partition function (3.2.1) with the interface (3.5.1) inserted. Using the fact that the projectors satisfy

$$\mathcal{P}^\alpha \mathcal{P}^\beta = \delta(\alpha - \beta)\,\mathcal{P}^\alpha \tag{3.5.5}$$

and the fact that the interface operator I satisfies (3.1.4) we arrive at

$$Z(K) = \int_{Q/2+iP} dP \left(D(P)\right)^{2K} \chi_P(q^{2K})\chi_P(\bar{q}^{2K}) \tag{3.5.6}$$

where $\chi_P(q)$ is the character of the non-degenerate Liouville primary field labeled by P given by

$$\chi_P(\tau) = \frac{q^{P^2}}{q^{\frac{1}{24}}\prod_{n=1}^{\infty}(1-q^n)} \tag{3.5.7}$$

with $q = e^{2\pi i\tau}$. We can use the following formula for the modular transformation of the character (3.5.7)

$$\chi_P\big(-\tfrac{1}{\tau}\big) = \sqrt{2}\int_{-\infty}^{\infty} dP'\chi_{P'}(\tau)\, e^{4\pi iPP'} \tag{3.5.8}$$

With the identification (3.2.2) and $t = 2\pi^2/\log(L/\epsilon)$ as before, the modular transformed K-sheeted partition function becomes

$$Z(K) = 2\int_0^\infty dP\,\big(D(P)\big)^{2K}\int_{-\infty}^\infty dP' e^{4\pi i PP'}\chi_{P'}\big(i\tfrac{\pi}{Kt}\big)\int_{-\infty}^\infty d\bar{P}' e^{4\pi i P\bar{P}'}\chi_{\bar{P}'}\big(i\tfrac{\pi}{Kt}\big) \tag{3.5.9}$$

In the limit $t \to 0$ we can replace the full character $\chi_P(q)$ by its leading term $q^{P^2-\frac{1}{24}}$ and perform the gaussian integrals over P' and $\bar{P}'$ which produce the same result. Hence we arrive at

$$Z(K) = \frac{Kt}{4\pi}\, e^{\frac{\pi^2}{6Kt}}\int_0^\infty dP\,\big(D(P)\big)^{2K} e^{-4P^2Kt} + \cdots \tag{3.5.10}$$

where the dots denote terms which vanish as t goes to zero. We would now like to use this expression to calculate the entanglement entropy using the replica formula (1.2.5). Note that for the case where D is labeled by a continuous parameter s and given by (3.5.4) $\big(D(P)\big)^{2K}$ in the integral (3.5.10) vanishes for large P. It is therefore legitimate to drop the exponent e^{-4P^2Kt} in the integral and the non vanishing terms in entanglement entropy for this case are given by

$$\mathcal{S}_s = \frac{1}{6}\log\frac{L}{\epsilon} + (1-\partial_K)\Big(\log\frac{Kt}{4\pi}\int_0^\infty dP\,\big(D_s(P)\big)^{2K}\Big)\Big|_{K=1} \tag{3.5.11}$$

We notice two curious features of this result. First, the logarithmically divergent term is multiplied by $\frac{1}{6}$ which is what one would expect for a $c = 1$ CFT, whereas the central charge of the Liouville theory is given by $C_L = 1 + 6Q^2$. A possible explanation for this behavior lies in the fact that for the interface labelled by (3.5.4) only the continuous primaries with conformal dimension $\Delta = Q^2/4 + P^2$ appear. Hence the vacuum with $\Delta = 0$ is excluded and the factor of $1/3$ in front of (3.5.11) is most likely associated with a shifted effective central charge.

Second, apart from finite terms as $t \to 0$ we also obtain an additonal divergent term of

the form $\log(\log \frac{L}{\epsilon})$ from the second term (3.5.11). The significance and interpretation of this term is not clear at this point and a more careful treatment of the cutoff might be necessary. For the interfaces labeled by discrete integers m, n defined in (3.5.3), D_{mn} diverges for large P and the full integral has to be evaluated first in order to obtain the entanglement entropy.

3.6 Discussion

In this chapter we have discussed entanglement entropies in the presence of topological defects in two geometric settings, namely when the interface is located at the boundary of the entangling interval $\mathcal{A}$ and when it is in the center of the entangling interval. For topological defects in RCFTs the logarithmic part of the entanglement entropy is always universal (this is not the case for general conformal interfaces) and the constant term can be expressed in a compact form in terms of the modular matrix S. Note that the entanglement entropies have a similar form in terms of the modular matrix S as the left/right entanglement entropy for a related BCFT, but the physical relation of the left/right entanglement entropy to the others is not clear at the moment.

There are several directions in which our results can be generalized. We have limited ourselves to RCFTs with diagonal partition functions. The construction of [77] also includes non-diagonal theories and it would be interesting to understand the entanglement entropy for this case. We also only considered CFTs which are rational with respect to the Virasoso algebra, it would also be very interesting to repeat the analysis for RCFTs with respect to extended chiral algebras.

Since the large m limit of minimal models is conjectured to approach a non-rational $c = 1$ CFT which is different from a free boson [93] it would be interesting to study the continuation of the minimal model entanglement entropy. It would also be interesting to understand the entanglement entropy for Liouville theory better. Apart from the calculations sketched in section 3.5 one might also consider semiclassical limits where $b \to 0$ and analyze the role of topological defects in classical Liouville theory following [85, 94].

Chapter 4

Entanglement Entropy at CFT Junctions

A natural generalization of an interface $\mathcal{I}$ connecting two CFTs is a junction $\mathcal{J}$ connecting N CFTs along a common line. If we consider an entangling region containing one of the CFTs, say CFT_i, then the entanglement entropy has the same generic form as (1.2.14); that is,

$$\mathcal{S}_i = \frac{c}{3} f_{N,i}(\mathcal{J}) \log \frac{L}{\epsilon} + \tilde{C}_{N,i}(\mathcal{J}) \tag{4.0.1}$$

For junctions between non-relativistic theories, it was shown in [95] that the universal term of (4.0.1) is related to the universal term of (1.2.14) via

$$f_{N,i}(\mathcal{J}) = f\big(\sqrt{\mathcal{T}_i}\big) \tag{4.0.2}$$

where $\mathcal{T}_i$ is the total transmission coefficient from the i-th theory to the other theories in the junction, however this has not been shown to hold in the conformal setting. In this chapter we will show that this relationship holds for arbitrary junctions between CFTs which are constructed from free conformal bosons and fermions.

This chapter is organized as follows: in section 4.1 we review the folding trick (see section

1.1) which turns the problem of constructing conformal junctions into one of constructing boundary states. We review the construction of bosonic as well as fermionic boundary states, determine the normalization using the Cardy condition, and discuss reflection and transmission coefficients for conformal junctions. In section 4.2 we calculate the entanglement entropy of bosonic and fermionic N-junctions, generalizing the methods of [21,22] (see section 1.2.1). In section 4.3 we construct boundary states corresponding to specific 3-junctions and discuss various features and limits. In section 4.4 we summarize the main results of the chapter and discuss possible extensions. Details on the special functions we use in this chapter, in addition to details involving Gaussian integrals and circular determinants we calculate, are relegated to appendices at the end of the chapter.

4.1 CFT construction of junctions

For junctions connecting $N > 2$ free boson CFTs, we proceed with the same folding methods shown in figure 1.1 applied repeatedly, as illustrated in figure 4.1. Specifically, the bosonic N-junction is folded into the N-times tensor product CFT with boundary states $|\mathrm{B}\rangle\rangle$ determined by the boundary condition

$$\left(a^i_n - S_{ij}\,\bar{a}^j_{-n}\right)|\mathrm{B}\rangle\rangle = 0 \tag{4.1.1}$$

where now S is an element of $O(N)$[1]. As before, (4.1.1) is solved by a coherent state of the form

$$|S\rangle\rangle = g\prod_{n=1}^{\infty}\exp\left(\frac{1}{n}\,S_{ij}\,a^i_{-n}\bar{a}^j_{-n}\right)\sum_{(\mathbf{a}_0,\bar{\mathbf{a}}_0)\in\Lambda} e^{i\delta_{\mathbf{a}_0,\bar{\mathbf{a}}_0}}\bigotimes_{i=1}^{N}|n_i,w_i\rangle \tag{4.1.2}$$

where Λ is an N-dimensional sublattice of the full $2N$-dimensional lattice of unconstrained eigenvalues of the a^i_0 and $\bar{a}^i_0$. Not every element of $O(N)$ will be compatible with the zero mode structure, i.e. satisfy the $n = 0$ case of (4.1.1) for the quantized eigenvalues (A.1.10), and thus the bosonic boundary states for fixed radii correspond to a countable subset of

[1]This is seen either by the easily generalized replacement in (1.1.8) or by requiring continuity of the stress tensor at the location of the junction [96].

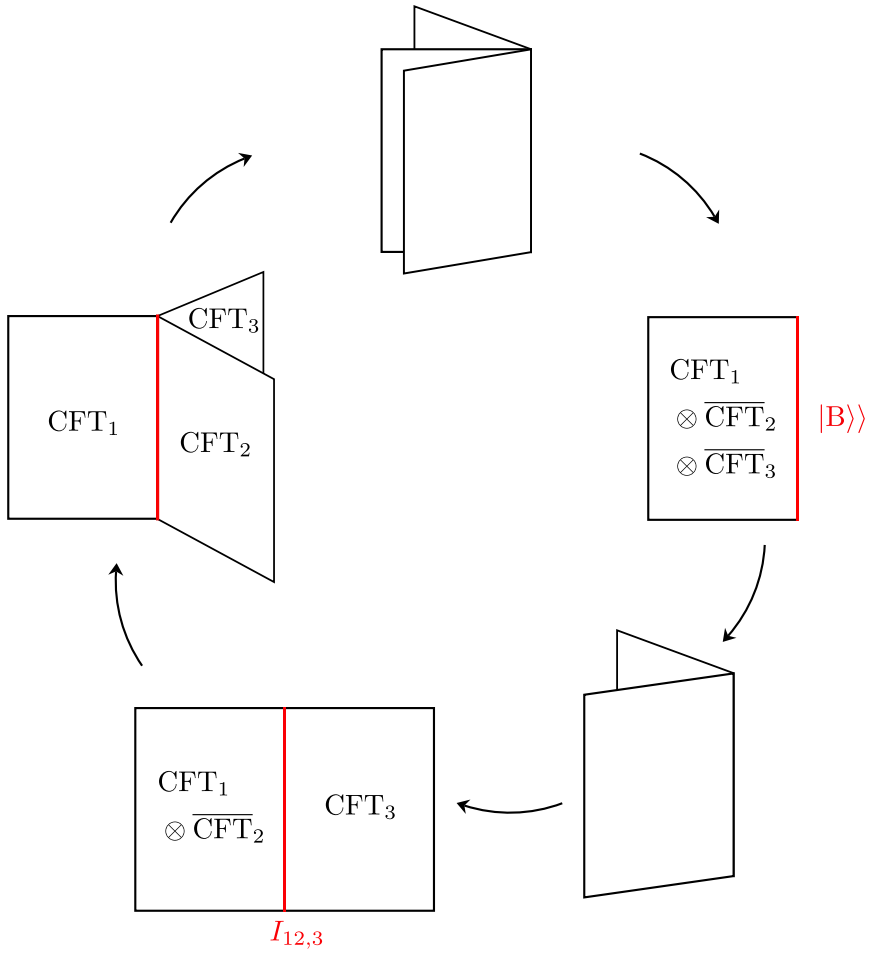

Figure 4.1: Illustrating the unfolded, folded, and partially folded pictures for a 3-junction. As before, the folded picture is used to characterize the boundary states. However, for the entanglement entropy calculations we will only unfold one CFT and work with interface operators in this partially folded picture.

$O(N)$. For $N = 2$ the restrictions (1.1.14) and (1.1.20) specify the allowed subset of $O(2)$, and in section 4.3 we find the allowed subset of $O(3)$ for $N = 3$. Lastly, the phases $\delta_{\mathbf{a}_0,\bar{\mathbf{a}}_0}$ are related to the position and dual Wilson line moduli of the D-brane, but as they will vanish from all our calculations we will not characterize them further.

We now fix the normalization through Cardy's condition for this general bosonic D-brane. Cardy's condition enforces the consistency between the open and closed string channels; that is, it requires the annulus amplitude to have a modular interpretation as a partition function on the cylinder. We will use this condition to fix the value of the normalization factor in

(4.1.2). Let $q = e^{-2\pi t}$ for some $t > 0$. The annulus amplitude is then

$$\langle\langle S|q^{\sum_{i=1}^{N}(L_0^i+\bar{L}_0^i-1/12)}|S\rangle\rangle \tag{4.1.3}$$

The quadratic operator exponentials in the boundary state complicate attempts at direct calculation; instead we linearize the exponential by means of Gaussian integrals of the form

$$e^{\mathbf{A}\cdot\mathbf{B}} = \int \frac{d^N\mathbf{Z}\, d^N\bar{\mathbf{Z}}}{\pi^N}\; e^{-\mathbf{z}\cdot\bar{\mathbf{z}}-\mathbf{z}\cdot\mathbf{A}-\bar{\mathbf{z}}\cdot\mathbf{B}} \tag{4.1.4}$$

where $\mathbf{A}$ and $\mathbf{B}$ are N-dimensional vectors whose entries are all mutually commuting operators. Linearizing each of the exponentials in (4.1.3) with (4.1.4) in a complementary fashion we obtain the expression

$$\begin{aligned}\langle\langle S|q^{\sum_{i=1}^{N}(L_0^i+\bar{L}_0^i-1/12)}|S\rangle\rangle &= g^2\,\langle\Omega|q^{\sum_{i=1}^{N}(L_0^i+\bar{L}_0^i)}|\Omega\rangle \\ &\times q^{-N/12}\prod_{n,m=1}^{\infty}\int \frac{d^N\mathbf{Z}_n d^N\bar{\mathbf{Z}}_n d^N\mathbf{W}_m d^N\bar{\mathbf{W}}_m}{\pi^{2N}}\; e^{-\mathbf{z}_n\cdot\bar{\mathbf{z}}_n-\mathbf{w}_m\cdot\bar{\mathbf{w}}_m} \\ &\times \langle 0|e^{-q^m\mathbf{w}_m\cdot S^{\mathrm{T}}\mathbf{a}_m-\frac{1}{m}q^m\bar{\mathbf{w}}_m\cdot\bar{\mathbf{a}}_m}e^{-\frac{1}{n}\mathbf{z}_n\cdot\mathbf{a}_{-n}-\bar{\mathbf{z}}_n\cdot S\bar{\mathbf{a}}_{-n}}|0\rangle\end{aligned} \tag{4.1.5}$$

where $|\Omega\rangle$ is the lattice-summed zero mode in (4.1.2) and we have used the identities (A.1.13). The form of (4.1.5) is such that the zero mode contribution, the first line of (4.1.5), is isolated from the remaining oscillator contribution. The zero mode contribution is a lattice theta function (see appendix 4.A.1)

$$g^2\,\langle\Omega|q^{\sum_{i=1}^{N}(L_0^i+\bar{L}_0^i)}|\Omega\rangle = g^2\,\Theta_\Lambda(2it) \tag{4.1.6}$$

where the dependence on the phases in $|\Omega\rangle$ have vanished. For the oscillator integrals, we

commute the two linear operator exponentials in the third line of (4.1.5) to obtain

$$q^{-N/12}\prod_{n=1}^{\infty}\int\frac{d^N\mathbf{z}_n d^N\bar{\mathbf{z}}_n d^N\mathbf{w}_n d^N\bar{\mathbf{w}}_n}{\pi^{2N}}\;e^{-\mathbf{z}_n\cdot\bar{\mathbf{z}}_n-\mathbf{w}_n\cdot\bar{\mathbf{w}}_n+q^n\mathbf{z}_n\cdot S\mathbf{w}_n+q^n\bar{\mathbf{z}}_n\cdot S\bar{\mathbf{w}}_n} \tag{4.1.7}$$

$$=q^{-N/12}\prod_{n=1}^{\infty}\int\frac{d^N\mathbf{w}_n d^N\bar{\mathbf{w}}_n}{\pi^{N}}\;e^{-(1-q^{2n})\,\mathbf{w}_n\cdot\bar{\mathbf{w}}_n}=\Big[q^{1/12}\prod_{n=1}^{\infty}\big(1-q^{2n}\big)\Big]^{-N} \tag{4.1.8}$$

where the dependence on S is removed after the $\mathbf{z}_n$, $\bar{\mathbf{z}}_n$ integration due to the fact that $S^{\mathrm{T}}S=1_N$ as S is an element of $O(N)$. Comparing this result to (4.A.21) we find that the annulus amplitude can be written in closed form as

$$\langle\langle S|q^{\sum_{i=1}^{N}(L_0^i+\bar{L}_0^i-1/12)}|S\rangle\rangle=g^2\,\Theta_\Lambda(2it)\,[\eta(2it)]^{-N} \tag{4.1.9}$$

Performing S-transformations on the above we have the equivalent expression

$$\langle\langle S|q^{\sum_{i=1}^{N}(L_0^i+\bar{L}_0^i-1/12)}|S\rangle\rangle=\frac{g^2}{\mathrm{vol}(\Lambda)}\,\Theta_{\Lambda^*}(i/2t)\,[\eta(i/2t)]^{-N} \tag{4.1.10}$$

In order for (4.1.10) to correspond to a cylinder partition function with a properly normalized vacuum we must have that the constant term as $t\to 0$ in (4.1.10) is unity. Thus, Cardy's condition fixes

$$g=\sqrt{\mathrm{vol}(\Lambda)} \tag{4.1.11}$$

In section 1.1 the various fermionic boundary states for $N=2$ were shown; here we give their straightforward generalization to arbitrary N for the Neveu-Schwarz sector

$$|S\rangle\rangle_{\mathrm{NS}}=\prod_{n\in\mathbb{N}-\frac{1}{2}}\exp\left(iS_{ij}\psi^i_{-n}\bar{\psi}^j_{-n}\right)\bigotimes_{i=1}^{N}|0\rangle \tag{4.1.12}$$

– which will be the focus of the fermionic calculations in this chapter – and for the Ramond

sector

$$|S\rangle\rangle_{\mathrm{R}} = \sqrt{\frac{2}{\det\left(1-\mathcal{F}\right)}} \prod_{n=1}^{\infty} \exp\left(iS_{ij}\psi^i_{-n}\bar{\psi}^j_{-n}\right) \exp\left(\frac{1}{2}\,\mathcal{F}_{ij}\gamma^i_{-\epsilon_i}\gamma^j_{-\epsilon_j}\right) \bigotimes_{i=1}^{N} |\epsilon_i\rangle \tag{4.1.13}$$

where

$$\gamma^i_{\pm} = \frac{1}{\sqrt{2}}\left(\psi^i_0 \pm i\bar{\psi}^i_0\right) \tag{4.1.14}$$

and $\mathcal{F}$ is an anti-symmetric matrix given by

$$S' = \left(1_N + \mathcal{F}\right)^{-1}\left(1_N - \mathcal{F}\right) \iff \mathcal{F} = \left(1_N - S'\right)\left(1_N + S'\right)^{-1} \tag{4.1.15}$$

The state in (4.1.13) is only well-defined as long as S' is in the connected component of $O(N)$. Thus we take the matrix S' to be the pure rotation part of S, i.e. we write S as an elementary reflection composed with a continuous rotation S'. The reflection content of S is then represented in the ground state through the choice of signs in the ϵ_i. If S is a pure rotation then $\epsilon_i = +1$ for all i, whereas if S includes a reflection then $\epsilon_i = -1$ for all i excepting the two indices corresponding to the plane of reflection. These considerations ensure that (4.1.13) satisfies the zero mode boundary condition

$$\left(\psi^i_0 + iS_{ij}\bar{\psi}^j_0\right)|S\rangle\rangle_{\mathrm{R}} = 0 \iff \left(\gamma^i_{\epsilon_i} + \mathcal{F}_{ij}\gamma^j_{-\epsilon_j}\right)|S\rangle\rangle_{\mathrm{R}} = 0 \tag{4.1.16}$$

while maintaining a finite normalization.

4.1.1 Reflection and transmission for junctions

In [21] and [22] it was shown that the physical quantity determining the universal term in the entanglement entropy for both the bosonic and fermionic interfaces is the transmission coefficient of the interface. This continues to be the case for $N > 2$; however, the reflection and transmission coefficients given in section 1.1 – as they were formulated by [23] – will

not suffice to describe junctions even in the partially folded picture. Here we review their generalization to conformal junctions, developed in [97].

The reflection and transmission coefficients for CFT N-junctions are related to the $N \times N$ matrix

$$R_{ij} = \frac{\langle 0|L_2^i \bar{L}_2^j|\mathrm{B}\rangle\rangle}{\langle 0|\mathrm{B}\rangle\rangle} \tag{4.1.17}$$

where $|\mathrm{B}\rangle\rangle$ is the boundary state corresponding to the junction. The average reflection and transmission coefficients of [23] (i.e. (1.1.4)) are written in terms of this matrix as

$$\mathcal{R}^{\mathrm{avg}} = \frac{2}{c_1 + c_2}\left(R_{11} + R_{22}\right) \quad \text{and} \quad \mathcal{T}^{\mathrm{avg}} = \frac{2}{c_1 + c_2}\left(R_{12} + R_{21}\right) \tag{4.1.18}$$

which are enough to characterize transport processes for $N = 2$ since in this case R is a symmetric matrix. For $N \geq 2$ these coefficients are generalized to

$$\mathcal{R}_i = \frac{2}{c_i} R_{ii} \quad \text{and} \quad \mathcal{T}_{ij} = \frac{2}{c_i} R_{ij} \tag{4.1.19}$$

where $\mathcal{R}_i$ is the reflection coefficient for CFT_i and $\mathcal{T}_{ij}$ is the transmission coefficient for transport from CFT_i to CFT_j. It should be noted for $N = 2$ that (4.1.19) is related to (4.1.18) by

$$\mathcal{T}_{12} = \frac{c_2}{c_1}\mathcal{T}_{21} = \frac{c_1 + c_2}{2c_1}\mathcal{T}^{\mathrm{avg}} \tag{4.1.20}$$

so that for $c_1 = c_2 = c$ the three different transmissions all agree. For $N > 2$ we'll also want to consider the total transmission from CFT_i, given by the sum

$$\mathcal{T}_i = \sum_{j \neq i} \mathcal{T}_{ij} \tag{4.1.21}$$

In both the free boson and free fermion cases (4.1.2) and (4.1.12), the reflection and trans-

mission coefficients of these boundary states are given by

$$\mathcal{R}_i = S_{ii}^2 \quad \text{and} \quad \mathcal{T}_{ij} = S_{ij}^2 \implies \mathcal{T}_i = 1 - S_{ii}^2 \tag{4.1.22}$$

and thus the coefficients can be lifted from the matrix S.

It is interesting to note that a completely transmissive junction, which necessarily has $\mathcal{R}_i = 0$ for all $i = 1, \ldots, N$, has its transmission coefficients constrained to be

$$\mathcal{T}_{ij} = \delta_{jk_i} \tag{4.1.23}$$

where $k_{i+1} = k_i + 1$, the index $N + 1$ is identified with 1, and $k_i \neq i$. These correspond to twisted permutation junctions whose boundary states satisfy

$$a_n^i |S\rangle\rangle = \pm \bar{a}_{-n}^{k_i} |S\rangle\rangle \tag{4.1.24}$$

for (4.1.2) and

$$\psi_n^i |S\rangle\rangle = \pm i \bar{\psi}_{-n}^{k_i} |S\rangle\rangle \tag{4.1.25}$$

for (4.1.12) with independent sign choices for each i, of which there are $2^N(N-1)$ distinct matrices S.

4.2 Entanglement entropy at N-junctions

The starting point for the junction entanglement calculations is the same as in the interface case: with the corresponding boundary state $|\mathrm{B}\rangle\rangle$ in the folded picture (see figures 1.1 and 4.1). For interfaces the tensor product CFT is then unfolded to obtain the interface operator $I_{1,2}$ to be used in calculating the replicated partition function (1.2.20). This same basic strategy can be applied to the junction case as well by noting that it is equivalent to replacing in CFT_1 with $\bigotimes_{j \neq i} \mathrm{CFT}_j$ and CFT_2 with CFT_i in figure 1.1. This is the partially

folded picture (shown in figure 4.1 for $N = 3$) where, for the purposes of calculating the entanglement entropy of CFT_i, we only need an interface operator $I_{1\ldots N,i}$ taking states from CFT_i to the rest of the CFTs in the junction as a tensor product. Thus, the replicated partition function has essentially the same from as (1.2.20); that is

$$Z(K) = \mathrm{Tr}_{1\ldots N}\left[\left(I_{1\ldots N,i}\, q^{H_i} (I_{1\ldots N,i})^\dagger q^{H_{1\ldots N}}\right)^K\right] \tag{4.2.1}$$

where $H_{1\ldots N}$ is the Hamiltonian of $\bigotimes_{j\neq i} \mathrm{CFT}_j$.

4.2.1 Bosonic junction

We'll begin our calculations with the bosonic boundary state (4.1.2). Unfolding the i-th boson according to (1.2.15), we linearize via (4.1.4) in order to obtain explicit expressions for the interface and anti-interface operators

$$\begin{aligned} I_{1\ldots N,i} = \prod_{n=1}^{\infty} \int \frac{d^N\mathbf{z}_n\, d^N\bar{\mathbf{z}}_n}{\pi^N}\; e^{-\mathbf{z}_n\cdot\bar{\mathbf{z}}_n - \frac{1}{n}\sum_{j\neq i} z_{nj} a^j_{-n} - \sum_{j\neq i}\sum_l S_{lj}\bar{z}_{nl}\bar{a}^j_{-n}} \\ \times G_{1\ldots N,i} \prod_{n=1}^{\infty} e^{\frac{1}{n} z_{ni}\bar{a}^i_n + \sum_l S_{li}\bar{z}_{nl} a^i_n} \end{aligned} \tag{4.2.2}$$

$$\begin{aligned} (I_{1\ldots N,i})^\dagger = \prod_{n=1}^{\infty} \int \frac{d^N\mathbf{w}_n\, d^N\bar{\mathbf{w}}_n}{\pi^N}\; e^{-\mathbf{w}_n\cdot\bar{\mathbf{w}}_n + \sum_l S_{il} w_{nl}\bar{a}^i_{-n} + \frac{1}{n}\bar{w}_{ni} a^i_{-n}} \\ \times (G_{1\ldots N,i})^\dagger \prod_{n=1}^{\infty} e^{-\sum_{j\neq i}\sum_l S_{jl} w_{nl} a^j_n - \frac{1}{n}\sum_{j\neq i}\bar{w}_{nj}\bar{a}^j_n} \end{aligned} \tag{4.2.3}$$

with the ground state operator given by

$$G_{1\ldots N,i} = \sqrt{\mathrm{vol}(\Lambda)} \sum_{(\mathbf{a}_0,\bar{\mathbf{a}}_0)\in\Lambda} e^{i\delta_{\mathbf{a}_0,\bar{\mathbf{a}}_0}} \Big(\bigotimes_{j\neq i} |n_j, w_j\rangle\Big) \otimes \langle -n_i, w_i| \tag{4.2.4}$$

which are needed to compute the partition function (4.2.1). From (4.2.2) and (4.2.3) we then calculate the commutation between the various exponentials of the oscillators of the

i-th boson in the relevant partition function block

$$J = q^{-N/12} I_{1\ldots N,i}\, q^{L_0^i+\bar{L}_0^i}\, (I_{1\ldots N,i})^\dagger\, q^{\sum_{j\neq i}(L_0^j+\bar{L}_0^j)} \tag{4.2.5}$$

$$= \prod_{n=1}^{\infty} \int \frac{d^N\mathbf{z}_n\, d^N\bar{\mathbf{z}}_n\, d^N\mathbf{w}_n\, d^N\bar{\mathbf{w}}_n}{\pi^{2N}}\; e^{-\mathbf{z}_n\cdot\bar{\mathbf{z}}_n - \mathbf{w}_n\cdot\bar{\mathbf{w}}_n + q^n\sum_l (S_{il} z_{ni} w_{nl} + S_{li}\bar{z}_{nl}\bar{w}_{ni})}\, \mathcal{O}_L G' \mathcal{O}_R \tag{4.2.6}$$

where the remaining oscillators are contained in

$$\mathcal{O}_L = \prod_{n=1}^{\infty} \exp\Big[-\frac{1}{n}\sum_{j\neq i} z_{nj} a^j_{-n} - \sum_{j\neq i}\sum_l S_{lj}\bar{z}_{nl}\bar{a}^j_{-n}\Big] \tag{4.2.7}$$

$$\mathcal{O}_R = \prod_{n=1}^{\infty} \exp\Big[-q^n\Big(\sum_{j\neq i}\sum_l S_{jl} w_{nl} a^j_n + \frac{1}{n}\sum_{j\neq i}\bar{w}_{nj}\bar{a}^j_n\Big)\Big] \tag{4.2.8}$$

and the zero mode information is encoded in the operator

$$G' = \mathrm{vol}(\Lambda)\, q^{-N/12} \sum_{(\mathbf{a}_0,\bar{\mathbf{a}}_0)\in\Lambda} q^{|\mathbf{a}_0|^2+|\bar{\mathbf{a}}_0|^2} \Big(\bigotimes_{j\neq i} |n_j, w_j\rangle\Big) \otimes \Big(\bigotimes_{j\neq i} \langle n_j, w_j|\Big) \tag{4.2.9}$$

Notice that in the above that the phases $\delta_{\mathbf{a}_0,\bar{\mathbf{a}}_0}$ originally present in (4.2.4) have vanished from the calculation. Also, the additional factors of q^n in (4.2.8) and the weighting of the lattice sum in (4.2.9) result from the identity (A.1.13) and the application of the propagators on the vacuum states in (4.2.4).

Using the expression (4.2.6) for the block (4.2.5), we can now write the K-sheeted partition function (4.2.1) in terms of this block

$$Z(K) = \mathrm{Tr}_{1\ldots N}\left(J^K\right) \tag{4.2.10}$$

$$= \prod_{n=1}^{\infty} \int \prod_{k=1}^{K} \frac{d^N\mathbf{z}_n^{(k)} d^N\bar{\mathbf{z}}_n^{(k)} d^N\mathbf{w}_n^{(k)} d^N\bar{\mathbf{w}}_n^{(k)}}{\pi^{2N}}\; e^{-\mathbf{z}_n^{(k)}\cdot\bar{\mathbf{z}}_n^{(k)} - \mathbf{w}_n^{(k)}\cdot\bar{\mathbf{w}}_n^{(k)} + q^n\sum_l \left(S_{il} z_{ni}^{(k)} w_{nl}^{(k)} + S_{li}\bar{z}_{nl}^{(k)}\bar{w}_{ni}^{(k)}\right)}$$

$$\times\, \mathrm{Tr}_{1\ldots N}\left(G'\mathcal{O}_R^{(1)}\mathcal{O}_L^{(2)} G' \mathcal{O}_R^{(2)} \cdots \mathcal{O}_L^{(K)} G' \mathcal{O}_R^{(K)} \mathcal{O}_L^{(1)}\right) \tag{4.2.11}$$

$$= \mathrm{vol}(\Lambda)^K q^{-NK/12}\, \Theta_\Lambda(2iKt) \prod_{n=1}^{\infty} P_n \tag{4.2.12}$$

where, denoting $(K+1) \equiv (1)$, the Gaussian integrals remaining after the commutations of all the oscillators in the products $\mathcal{O}_R^{(k)}\mathcal{O}_L^{(k+1)}$ between ground state operators in (4.2.11) are given by

$$P_n = \prod_{k=1}^{K} \int \frac{d^N\mathbf{z}_n^{(k)} d^N\bar{\mathbf{z}}_n^{(k)} d^N\mathbf{w}_n^{(k)} d^N\bar{\mathbf{w}}_n^{(k)}}{\pi^{2N}} \; e^{-\mathbf{z}_n^{(k)}\cdot\bar{\mathbf{z}}_n^{(k)} - \mathbf{w}_n^{(k)}\cdot\bar{\mathbf{w}}_n^{(k)} + q^n \sum_l \left(S_{il} z_{ni}^{(k)} w_{nl}^{(k)} + S_{li} \bar{z}_{nl}^{(k)} \bar{w}_{ni}^{(k)} \right)}$$
$$\times \, e^{q^n \sum_{j\neq i} \sum_l \left(S_{jl} z_{nj}^{(k+1)} w_{nl}^{(k)} + S_{lj} \bar{z}_{nl}^{(k+1)} \bar{w}_{nj}^{(k)} \right)} \tag{4.2.13}$$

The lattice theta function and the other factors multiplying the Gaussian integrals in (4.2.12) result from the product of the K operators G' inside the trace in (4.2.11). At this point we could perform the Gaussian integrals in (4.2.13) altogether by way of a determinant, but for the sake of simplifying the calculation we first perform each of the K one-dimensional complex Gaussian integrals in the variables z_{ni}, $\bar{z}_{ni}$ and w_{ni}, $\bar{w}_{ni}$. After performing these integrals (see appendix 4.B.1) we have a reduced expression for the Gaussian integrals

$$P_n = D_n^K \prod_{k=1}^{K} \int \frac{d^{N-1}\mathbf{z}_n^{(k)} d^{N-1}\bar{\mathbf{z}}_n^{(k)} d^{N-1}\mathbf{w}_n^{(k)} d^{N-1}\bar{\mathbf{w}}_n^{(k)}}{\pi^{2N-2}} \; e^{-\mathbf{z}_n^{(k)}\cdot\bar{\mathbf{z}}_n^{(k)} - \mathbf{w}_n^{(k)}\cdot\bar{\mathbf{w}}_n^{(k)} + \sum_{j,l\neq i} A_{jl}^{(k)}} \tag{4.2.14}$$

where

$$A_{jl}^{(k)} = q^n \left(S_{jl} + q^{2n} D_n S_{ii} S_{ji} S_{il} \right) \left(z_{nj}^{(k+1)} w_{nl}^{(k)} + \bar{z}_{nj}^{(k+1)} \bar{w}_{nl}^{(k)} \right)$$
$$+ q^{2n} D_n \left(S_{ji} S_{li} z_{nj}^{(k+1)} \bar{z}_{nl}^{(k)} + S_{ij} S_{il} w_{nj}^{(k+1)} \bar{w}_{nl}^{(k)} \right) \tag{4.2.15}$$

and $D_n = (1 - q^{2n} S_{ii}^2)^{-1}$. Now we switch to the evaluation of the Gaussian integrals through a determinant, which we do by writing (4.2.14) as a $4(N-1)K$-dimensional real Gaussian integral

$$P_n = D_n^K \int \frac{d^{4(N-1)K}\mathbf{v}}{\pi^{2(N-1)K}} \, e^{-\mathbf{v}\cdot M_K \mathbf{v}} \tag{4.2.16}$$

Ordering the real variables according to

$$\mathbf{v} = \Big(\mathrm{Re}\, z_{n1}^{(1)},\, \mathrm{Im}\, z_{n1}^{(1)}, \ldots,\, \mathrm{Re}\, z_{nN}^{(1)}, \mathrm{Im}\, z_{nN}^{(1)},\, \mathrm{Re}\, w_{n1}^{(1)},\, \mathrm{Im}\, w_{n1}^{(1)}, \ldots,\, \mathrm{Re}\, z_{n1}^{(2)},\, \mathrm{Im}\, z_{n1}^{(2)},\, \ldots\Big)$$

we find the matrix exponent has the block circulant form

$$M_K = \begin{pmatrix} 1_{4N-4} & C^{\mathrm{T}} & 0 & \cdots & 0 & C \\ C & 1_{4N-4} & C^{\mathrm{T}} & \cdots & 0 & 0 \\ 0 & C & 1_{4N-4} & \cdots & 0 & 0 \\ \vdots & \vdots & \vdots & \ddots & \vdots & \vdots \\ 0 & 0 & 0 & \cdots & 1_{4N-4} & C^{\mathrm{T}} \\ C^{\mathrm{T}} & 0 & 0 & \cdots & C & 1_{4N-4} \end{pmatrix} \tag{4.2.17}$$

with off-diagonal blocks themselves in 2×2 block form

$$C = \frac{1}{2} \begin{pmatrix} X \otimes (1_2 + \sigma^2) & 2Y \otimes \sigma^3 \\ 0 & Z \otimes (1_2 + \sigma^2) \end{pmatrix} \tag{4.2.18}$$

and the constituent $(N-1) \times (N-1)$ matrices defined in terms of q and S as

$$X_{jl} = -q^{2n} D_n S_{ji} S_{li}\,, \quad Y_{jl} = -q^n \left(S_{jl} + q^{2n} D_n S_{ii} S_{ji} S_{il}\right), \quad Z_{jl} = -q^{2n} D_n S_{ij} S_{il} \tag{4.2.19}$$

The Gaussian integral (4.2.16) is then evaluated to give

$$\begin{aligned} P_n &= D_n^K \left(\det\, M_K\right)^{-1/2} \\ &= \prod_{k=1}^{K} \left(1 - q^{2n}\right)^{N-2} \left[1 - 2\left(S_{ii}^2 + \left(1 - S_{ii}^2\right)\cos(2\pi k/K)\right) q^{2n} + q^{4n}\right] \end{aligned} \tag{4.2.20}$$

where the determinant is calculated in appendix 4.C. Comparing the above to (4.A.19) and

employing the identity

$$\prod_{k=1}^{K-1} \sin\frac{\pi k}{K} = \frac{K}{2^{K-1}} \tag{4.2.21}$$

we can immediately write down the K-sheeted partition function in terms of modular functions

$$Z(K) = \mathrm{vol}(\Lambda)^K K\, \mathcal{T}_i^{(K-1)/2}\, \Theta_\Lambda(2iKt)\, [\eta\,(2it)]^{-K(N-3)-3} \prod_{k=1}^{K-1} \theta_1^{-1}(\nu_k|2it) \tag{4.2.22}$$

with

$$\sin\pi\nu_k = \sqrt{\mathcal{T}_i}\, \sin\frac{\pi k}{K} \tag{4.2.23}$$

This partition function matches the $N = 2$ case (1.2.21), and the oscillator part remains the same for all N. Performing an S-transformation on (4.2.22) yields

$$Z(K) = K^{-(N-2)/2} \left(\mathcal{T}_i\, \mathrm{vol}(\Lambda)^2\right)^{(K-1)/2} (2t)^{(K-1)(N-2)/2}\, e^{\pi[K(N-3)+3]/24t} e^{\varphi(K)/t} + \cdots \tag{4.2.24}$$

where

$$\varphi(K) = \frac{\pi}{2} \sum_{k=1}^{K-1} \left(\nu_k - \frac{1}{2}\right)^2 \tag{4.2.25}$$

and the dots indicate terms that go to zero as $t \to 0$, corresponding to the removal of the cutoffs. Performing the analytic continuation (reviewed in appendix 4.A.3) and calculating the derivatives in (1.2.5), the entanglement entropy is

$$\mathcal{S}_i = \frac{1}{2}\, \sigma\big(\sqrt{\mathcal{T}_i}\big) \log\frac{L}{\epsilon} + \frac{1}{2}\,(N-2)\,[1 - \log(2t)] - \frac{1}{2}\log\left(\mathcal{T}_i\, \mathrm{vol}(\Lambda)^2\right) \tag{4.2.26}$$

The universal term in the above has the same functional form regardless of the value of N, following exactly the behavior described in (4.0.2). Also independent of N, the constant term retains the same dependence on the physical quantities of the junction. The only explicit dependence on the number of theories in the junction comes in the form of a new term that vanishes when $N = 2$, which contains a subleading $\log(\log(L/\epsilon))$ term, the appearance of

such a term in related contexts has been remarked previously in the literature [34,98,99]. Its presence precisely corresponds to the cases where the central charge differs between the inside and outside of the entangling region in the partially folded picture, and thus not covered in the scope of (1.2.10). However, as this term does not depend on any of the parameters of the junction it will vanish from all differences in entanglement entropy between different junctions, and thus can be considered unphysical.

4.2.2 Fermionic NS junction

If we try to extend to the general N-junction the direct methods used to obtain the fermionic interface entanglement entropy outlined in section 1.2.1, we'll need to expand the exponential in the boundary state (4.1.12), unfold the i-th fermion, and organize the non-vanishing terms into a $4(N-1)\times 4$ matrix representation of $(I_{1\cdots N,i})_n$. If we then consider the reciprocal entanglement entropy for simplicity, we'll need to calculate the 4×4 matrix representation of the partition function block and find its eigenvalues. It is not clear how these matrix computations can be done for arbitrary N. Therefore we will employ the fermionic version of the linearization methods utilized in the bosonic calculation.

We begin with the fermionic analog of (4.1.4), the complex Grassmann Gaussian integral

$$e^{\mathbf{A}\cdot\mathbf{B}} = \int d^N\eta\, d^N\bar{\eta}\; e^{\boldsymbol{\eta}\cdot\bar{\boldsymbol{\eta}}+\mathbf{A}\cdot\boldsymbol{\eta}+\bar{\boldsymbol{\eta}}\cdot\mathbf{B}} \tag{4.2.27}$$

where $\mathbf{A}$ and $\mathbf{B}$ are now N-dimensional vectors of anti-commuting operators, which are taken to be Grassmann-valued, and the measure is defined to be

$$d^N\eta\, d^N\bar{\eta} = d\eta_N\cdots d\eta_1\, d\bar{\eta}_N\cdots d\bar{\eta}_1 = (-1)^N d\eta_1\, d\bar{\eta}_1\cdots d\eta_N\, d\bar{\eta}_N \tag{4.2.28}$$

Note that the ordering of the pairs $d\eta_j\, d\bar{\eta}_j$ in the above can be changed without the introduction of additional minus signs. Using (4.2.27) we can linearize the Neveu-Schwarz boundary state (4.1.12) and unfold the i-th fermion via (1.2.24) to obtain explicit interface

and anti-interface operators

$$I_{1\ldots N,i} = \prod_{n\in\mathbb{N}-\frac{1}{2}} \int d^N\eta_n\, d^N\bar{\eta}_n\, e^{\boldsymbol{\eta}_n\cdot\bar{\boldsymbol{\eta}}_n+\sum_{j\neq i}\psi^j_{-n}\eta_{nj}+i\sum_{j\neq i}\sum_l S_{lj}\bar{\eta}_{nl}\bar{\psi}^j_{-n}}\Big(\bigotimes_{j\neq i}|0\rangle\Big)$$
$$\otimes\langle 0|\prod_{n\in\mathbb{N}-\frac{1}{2}} e^{-i\bar{\psi}^i_n\eta_{ni}-\sum_l S_{li}\bar{\eta}_{nl}\psi^i_n} \tag{4.2.29}$$

$$(I_{1\ldots N,i})^\dagger = \prod_{n\in\mathbb{N}-\frac{1}{2}} \int d^N\chi_n\, d^N\bar{\chi}_n\, e^{\boldsymbol{\chi}_n\cdot\bar{\boldsymbol{\chi}}_n+\sum_l S_{il}\bar{\psi}^i_{-n}\chi_{nl}+i\bar{\chi}_{ni}\psi^i_{-n}}|0\rangle$$
$$\otimes\Big(\bigotimes_{j\neq i}\langle 0|\Big)\prod_{n\in\mathbb{N}-\frac{1}{2}} e^{i\sum_{j\neq i}\sum_l S_{jl}\psi^j_n\chi_{nl}+\sum_{j\neq i}\bar{\chi}_{nj}\bar{\psi}^j_n} \tag{4.2.30}$$

With these expressions we can calculate the commutations between the various products of Grassmann variables and Grassmann-valued operators appearing in (4.2.1) in terms of the operator anti-commutators, e.g. for $\{\alpha,\beta\}=\{\beta,\theta\}=\{\alpha,\phi\}=0$ it follows that

$$[\alpha\theta,\beta\phi] = -\alpha\beta\{\theta,\phi\} \tag{4.2.31}$$

The NS partition function block is then

$$J = q^{-N/24} I_{1\ldots N,i}\, q^{L^i_0+\bar{L}^i_0}\,(I_{1\ldots N,i})^\dagger\, q^{\sum_{j\neq i}(L^j_0+\bar{L}^j_0)} \tag{4.2.32}$$

which we can calculate using relations like (4.2.31) and the identities (A.2.12). Performing the commutator calculations between the exponentials of the oscillators of the i-th fermion, in a similar manner to those behind (4.2.6), we obtain

$$J = \prod_{n\in\mathbb{N}-\frac{1}{2}} \int d^N\eta_n\, d^N\bar{\eta}_n\, d^N\chi_n\, d^N\bar{\chi}_n\; e^{\boldsymbol{\eta}_n\cdot\bar{\boldsymbol{\eta}}_n+\boldsymbol{\chi}_n\cdot\bar{\boldsymbol{\chi}}_n}\, e^{iq^n\sum_j(S_{ij}\eta_{ni}\chi_{nj}+S_{ji}\bar{\eta}_{nj}\bar{\chi}_{ni})}\,\mathcal{O}_L G'\mathcal{O}_R \tag{4.2.33}$$

where the remaining oscillators are contained in

$$\mathcal{O}_L = \prod_{n\in\mathbb{N}-\frac{1}{2}} \exp\Big[\sum_{j\neq i}\psi^j_{-n}\eta_{nj} + i\sum_l\sum_{j\neq i} S_{lj}\bar{\eta}_{nl}\bar{\psi}^j_{-n}\Big] \tag{4.2.34}$$

$$\mathcal{O}_R = \prod_{n\in\mathbb{N}-\frac{1}{2}} \exp\Big[q^n\Big(\sum_{j\neq i}\bar{\chi}_{nj}\bar{\psi}^j_n + i\sum_l\sum_{j\neq i} S_{jl}\psi^j_n\chi_{nl}\Big)\Big] \tag{4.2.35}$$

with ground state operator

$$G' = q^{-N/24}\Big(\bigotimes_{j\neq i}|0\rangle\Big)\otimes\Big(\bigotimes_{j\neq i}\langle 0|\Big) \tag{4.2.36}$$

We can now write the K-sheeted partition function (4.2.1) in terms of the block (4.2.33) as

$$\begin{aligned} Z(K) &= \mathrm{Tr}_{1\ldots N}\left(J^K\right) && (4.2.37)\\ &= \prod_{n\in\mathbb{N}-\frac{1}{2}}\int\prod_{k=1}^{K} d^N\eta^{(k)}_n d^N\bar{\eta}^{(k)}_n d^N\chi^{(k)}_n d^N\bar{\chi}^{(k)}_n\, e^{\boldsymbol{\eta}^{(k)}_n\cdot\bar{\boldsymbol{\eta}}^{(k)}_n+\boldsymbol{\chi}^{(k)}_n\cdot\bar{\boldsymbol{\chi}}^{(k)}_n+iq^n\sum_j\left(S_{ij}\eta^{(k)}_{ni}\chi^{(k)}_{nj}+S_{ji}\bar{\eta}^{(k)}_{nj}\bar{\chi}^{(k)}_{ni}\right)} \\ &\qquad\times\mathrm{Tr}_{1\ldots N}\left(G'\mathcal{O}^{(1)}_R\mathcal{O}^{(2)}_L G'\mathcal{O}^{(2)}_R\cdots\mathcal{O}^{(K)}_L G'\mathcal{O}^{(K)}_R\mathcal{O}^{(1)}_L\right) && (4.2.38)\\ &= q^{-NK/24}\prod_{n\in\mathbb{N}-\frac{1}{2}} P_n && (4.2.39)\end{aligned}$$

where, denoting $(K+1)\equiv(1)$, the Gaussian integrals remaining after the commutations of all the oscillators in the products $\mathcal{O}^{(k)}_R\mathcal{O}^{(k+1)}_L$ between vacuum states in (4.2.38) are given by

$$\begin{aligned} P_n = \prod_{k=1}^{K}\int d^N\eta^{(k)}_n d^N\bar{\eta}^{(k)}_n d^N\chi^{(k)}_n d^N\bar{\chi}^{(k)}_n\, e^{\boldsymbol{\eta}^{(k)}_n\cdot\bar{\boldsymbol{\eta}}^{(k)}_n+\boldsymbol{\chi}^{(k)}_n\cdot\bar{\boldsymbol{\chi}}^{(k)}_n+iq^n\sum_j\left(S_{ij}\eta^{(k)}_{ni}\chi^{(k)}_{nj}+S_{ji}\bar{\eta}^{(k)}_{nj}\bar{\chi}^{(k)}_{ni}\right)} \\ \times e^{iq^n\sum_l\sum_{j\neq i}\left(S_{jl}\eta^{(k+1)}_{nj}\chi^{(k)}_{nl}+S_{lj}\bar{\eta}^{(k+1)}_{nl}\bar{\chi}^{(k)}_{nj}\right)} \end{aligned} \tag{4.2.40}$$

At this point we could perform the integrals in (4.2.40) altogether by way of a determinant, but for the sake of simplifying the calculation we first perform each of the K one-dimensional complex Grassmann Gaussian integrals in the variables η_{ni}, $\bar{\eta}_{ni}$ and χ_{ni}, $\bar{\chi}_{ni}$. After performing

these integrals (see appendix 4.B.2) we have a reduced expression for the Gaussian integrals

$$P_n = D_n^{-K} \prod_{k=1}^{K} \int d^{N-1}\eta_n^{(k)} d^{N-1}\bar{\eta}_n^{(k)} d^{N-1}\chi_n^{(k)} d^{N-1}\bar{\chi}_n^{(k)}\, e^{\boldsymbol{\eta}_n^{(k)}\cdot\bar{\boldsymbol{\eta}}_n^{(k)} + \boldsymbol{\chi}_n^{(k)}\cdot\bar{\boldsymbol{\chi}}_n^{(k)} + \sum_{j,l\neq i} A_{jl}^{(k)}} \tag{4.2.41}$$

where

$$\begin{aligned} A_{jl}^{(k)} = {} & iq^n \left(S_{jl} - q^{2n} D_n S_{ii} S_{ji} S_{il}\right) \left(\eta_{nj}^{(k+1)} \chi_{nl}^{(k)} + \bar{\eta}_{nj}^{(k+1)} \bar{\chi}_{nl}^{(k)}\right) \\ & + q^{2n} D_n \left(S_{ji} S_{li} \eta_{nj}^{(k+1)} \bar{\eta}_{nl}^{(k)} + S_{ij} S_{il} \chi_{nj}^{(k+1)} \bar{\chi}_{nl}^{(k)}\right) \end{aligned} \tag{4.2.42}$$

and $D_n = (1 + q^{2n} S_{ii}^2)^{-1}$. Now we switch to the evaluation of the Gaussian integrals through a determinant, which we do by writing (4.2.41) as a $4(N-1)K$-dimensional real Grassmann Gaussian integral

$$P_n = D_n^{-K}\, (-1)^{(N-1)K} \int d^{4(N-1)K}\theta\, e^{\frac{1}{2}\boldsymbol{\theta}\cdot M_K \boldsymbol{\theta}} \tag{4.2.43}$$

Ordering the real Grassmann variables according to

$$\boldsymbol{\theta} = \left(\mathrm{Re}\,\eta_{n1}^{(1)},\, \mathrm{Im}\,\eta_{n1}^{(1)}, \ldots,\, \mathrm{Re}\,\eta_{nN}^{(1)}, \mathrm{Im}\,\eta_{nN}^{(1)},\, \mathrm{Re}\,\chi_{n1}^{(1)},\, \mathrm{Im}\,\chi_{n1}^{(1)}, \ldots,\, \mathrm{Re}\,\eta_{n1}^{(2)},\, \mathrm{Im}\,\eta_{n1}^{(2)},\, \ldots\right)$$

we find the matrix exponent has the block circulant form

$$M_K = \begin{pmatrix} 1_{2N-2}\otimes\sigma^2 & -C^{\mathrm{T}} & 0 & \cdots & 0 & C \\ C & 1_{2N-2}\otimes\sigma^2 & -C^{\mathrm{T}} & \cdots & 0 & 0 \\ 0 & C & 1_{2N-2}\otimes\sigma^2 & \cdots & 0 & 0 \\ \vdots & \vdots & \vdots & \ddots & \vdots & \vdots \\ 0 & 0 & 0 & \cdots & 1_{2N-2}\otimes\sigma^2 & -C^{\mathrm{T}} \\ -C^{\mathrm{T}} & 0 & 0 & \cdots & C & 1_{2N-2}\otimes\sigma^2 \end{pmatrix} \tag{4.2.44}$$

with off-diagonal blocks themselves in 2×2 block form

$$C = \frac{1}{2} \begin{pmatrix} X \otimes (1_2 + \sigma^2) & 2Y \otimes \sigma^3 \\ 0 & Z \otimes (1_2 + \sigma^2) \end{pmatrix} \tag{4.2.45}$$

where the matrices X, Y, and Z are the same as the bosonic case (4.2.19) only with the replacement $q^n \to -iq^n$. The Gaussian integral (4.2.43) is then evaluated to give

$$\begin{aligned} P_n &= D_n^{-K} \, (-1)^{(N-1)K} \, (\det \, M_K)^{1/2} \\ &= \prod_{k=1}^{K} \left(1 + q^{2n}\right)^{N-2} \left[1 + 2 \left(S_{ii}^2 + \left(1 - S_{ii}^2\right) \cos(2\pi k/K)\right) q^{2n} + q^{4n}\right] \end{aligned} \tag{4.2.46}$$

where the determinant is calculated in appendix 4.C. With this final expression for the integrals, we are able to write the replicated NS partition function in terms of modular functions and make an S-transformation

$$Z(K) = \left[\eta\left(2it\right)\right]^{-NK/2} \left[\theta_3(2it)\right]^{K(N-2)/2+1} \prod_{k=1}^{K-1} \theta_3(\nu_k|2it) \tag{4.2.47}$$

$$= e^{\pi NK/48t} e^{-\vartheta(K)/t} + \cdots \tag{4.2.48}$$

where ν_k is given by (4.2.23), the exponent $\vartheta(K)$ is

$$\vartheta(K) = \frac{\pi}{2} \sum_{k=1}^{K-1} \nu_k^2 \tag{4.2.49}$$

and the dots indicate terms which vanish as $t \to 0$. The entanglement entropy is then

$$\mathcal{S}_i = \frac{1}{2} \left[\frac{1}{2}\sqrt{\mathcal{T}_i} - \sigma\left(\sqrt{\mathcal{T}_i}\right)\right] \log \frac{L}{\epsilon} \tag{4.2.50}$$

after analytically continuing (4.2.49) – see the review in appendix 4.A.3 for details – and taking the derivatives in (1.2.5). As in the bosonic case, the entanglement entropy (4.2.50)

shows the same N-independent behavior described in (4.0.2).

4.2.3 BPS junction

Until this point we have been considering interfaces and junctions that preserve conformal symmetry, i.e. satisfy (1.1.2) in the unfolded or partially folded picture. Since we have been working with free conformal bosons and fermions we could further consider interfaces and junctions that also preserve supersymmetry.

Whereas the conformal condition (1.1.2) enforces continuity of the stress tensor across the interface, if we further require continuity of the supercurrent the interface operator must satisfy

$$\left(G^1_n - i\eta^1 \bar{G}^1_{-n}\right) I_{1,2} = I_{1,2} \left(G^2_n - i\eta^2 \bar{G}^2_{-n}\right) \tag{4.2.51}$$

with supercurrent modes

$$G^i_n = \sum_{m=-\infty}^{\infty} a^i_{-m} \psi^i_{n+m}\,, \quad \bar{G}^i_n = \sum_{m=-\infty}^{\infty} \bar{a}^i_{-m} \bar{\psi}^i_{n+m} \tag{4.2.52}$$

The constants $\eta^1 = \pm 1$ and $\eta^2 = \pm 1$ determine the type of supersymmetry in CFT_1 and CFT_2, respectively, and do not need to be equal. The generalization to a partially folded N-junction is

$$\sum_{j \neq i} \left(G^j_n - i\eta^j \bar{G}^j_{-n}\right) I_{1\cdots N,i} = I_{1\cdots N,i} \left(G^i_n - i\eta^i \bar{G}^i_{-n}\right) \tag{4.2.53}$$

If $\eta^j = 1$ for all $j = 1, \ldots, N$ then the operator produced by unfolding the supersymmetric boundary state

$$|S\rangle\rangle_{\mathrm{super}} = |S\rangle\rangle_{\mathrm{bos}} \otimes |S\rangle\rangle_{\mathrm{NS}} \tag{4.2.54}$$

will satisfy (4.2.53). Furthermore, if we redefine $\bar{\psi}^j \to \eta^j \bar{\psi}^j$ then the η^j are absorbed into the interface operator through $S_{ij} \to S'_{ij} = \eta^j S_{ij}$. Introducing these factors does not change the entropy calculations, as S' is still an element of $O(N)$ and ${S'_{ii}}^2 = S^2_{ii}$ regardless of the values of the η^j. Thus for the purposes of calculating the entanglement entropy we proceed

as though the supersymmetric boundary state (4.2.54) unfolds simply into a supersymmetry-preserving interface operator no matter the types of supersymmetry present in the individual CFTs. The replicated partition function is then the product

$$Z_{\text{super}}(K) = Z_{\text{bos}}(K) Z_{\text{NS}}(K) \tag{4.2.55}$$

and through the logarithm the entanglement entropy is the sum

$$\mathcal{S}_{\text{super}} = \mathcal{S}_{\text{bos}} + \mathcal{S}_{\text{NS}} = \frac{1}{4}\sqrt{\mathcal{T}_i}\,\log\frac{L}{\epsilon} + \frac{1}{2}\,(N-2)\,[1-\log(2t)] - \frac{1}{2}\log\left(\mathcal{T}_i\,\text{vol}(\Lambda)^2\right) \tag{4.2.56}$$

This simplification of the oscillator contribution to the universal term of the entanglement entropy is precisely the same as in [22] for $N = 2$.

4.3 Specific 3-junction geometries

We now focus on constructing the explicit boundary states describing bosonic 3-junctions using similar methods to those used to construct (1.1.15) and (1.1.18). We will also relate the quantities relevant to the entanglement entropy – the total transmission $\mathcal{T}_i$ and unit cell volume $\text{vol}(\Lambda)$ – to the geometry of the corresponding D-branes describing the junctions in the folded picture.

4.3.1 Boundary state construction

Following the procedure outlined in [20], we begin with the boundary state

$$|k_2\text{D2}/k_1\text{D0}, 0, 0\rangle\rangle = |k_2\text{D2}/k_1\text{D0}\rangle\rangle \otimes |\text{D0}\rangle\rangle \tag{4.3.1}$$

corresponding to k_2 D2-branes in the $\varphi^1\varphi^2$-plane bound to k_1 D0-branes, which we rotate to an arbitrary orientation in the compactification lattice. Through translation we can specify

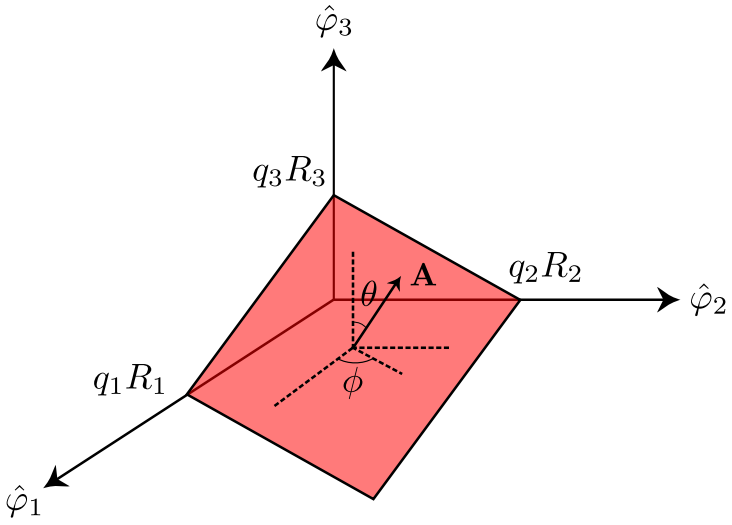

Figure 4.2: A D2-brane wrapping the bosonic 3-torus continued into the compactification lattice so as to show the axis intercepts $q_i R_i \, \hat{\varphi}_i$; see figure 4.3 for the unit cell wrapping for a specific case. The polar and azimuthal angles that specify the rotation that takes the D2-brane in the $\varphi^1\varphi^2$-plane into this pictured D2-brane are also shown.

an arbitrary orientation by the axis intercepts $q_1 R_1 \, \hat{\varphi}_1$, $q_2 R_2 \, \hat{\varphi}_2$, and $q_3 R_3 \, \hat{\varphi}_3$. Such a plane will have an area vector equal to

$$\mathbf{A} = q_2 q_3 R_2 R_3 \, \hat{\varphi}_1 + q_1 q_3 R_1 R_3 \, \hat{\varphi}_2 + q_1 q_2 R_1 R_2 \, \hat{\varphi}_3 \tag{4.3.2}$$

and thus the rotation transformation needed will be $\mathcal{R}(\theta, \phi) = \mathcal{R}_3(\phi)\mathcal{R}_2(\theta)$ where

$$\tan\theta = \frac{q_1 q_2 R_1 R_2}{\sqrt{(q_2 q_3 R_2 R_3)^2 + (q_1 q_3 R_1 R_3)^2}}, \quad \tan\phi = \frac{q_1 R_1}{q_2 R_2} \tag{4.3.3}$$

in order to obtain the rotated D-brane state $|k_2\text{D2}/k_1\text{D0}, \theta(q_1, q_2, q_3), \phi(q_1, q_2)\rangle\rangle$, see figure 4.2. To do this we will transform the boundary conditions

$$\left[g_{ij}\left(a^j_n + \bar{a}^j_{-n}\right) + b_{ij}\left(a^j_n - \bar{a}^j_{-n}\right) + \delta_{i3}\delta_{3j}\left(a^j_n - \bar{a}^j_{-n}\right)\right] |k_2\text{D2}/k_1\text{D0}, 0, 0\rangle\rangle = 0 \tag{4.3.4}$$

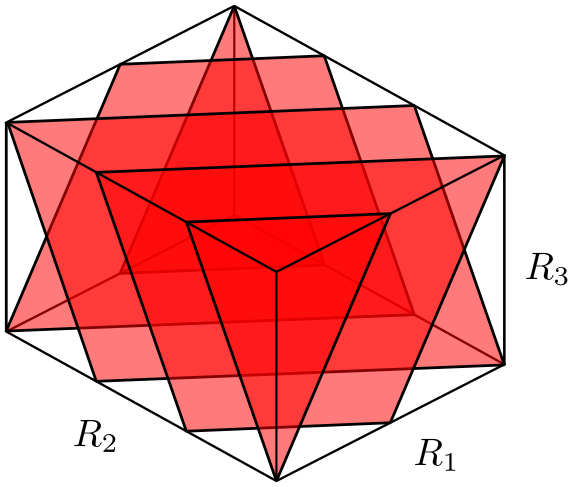

Figure 4.3: A D2-brane wrapping the bosonic 3-torus shown in the unit cell of the compactification lattice. The above corresponds to the parameters $q_1 = 3$, $q_2 = 2$, and $q_3 = 6$.

where $n \geq 0$ and

$$g = \begin{pmatrix} 1 & 0 & 0 \\ 0 & 1 & 0 \\ 0 & 0 & 0 \end{pmatrix}, \quad b = \frac{k_1 \alpha'}{k_2 R_1 R_2} \begin{pmatrix} 0 & -1 & 0 \\ 1 & 0 & 0 \\ 0 & 0 & 0 \end{pmatrix} \tag{4.3.5}$$

The metric g and $(E_{33})_{ij} \equiv \delta_{i3}\delta_{3j}$ will simply transform by similarity; however, the magnetic field will undergo an angle-dependent scaling in addition to the rotation in order for the boundary state to correspond to a bound state between k_2 D2-branes and k_1 D0-branes at all angles. Explicitly, the transformation of the magnetic field is determined through two conditions: (1) the magnetic field is oriented along the $-\hat{\mathbf{A}}$ direction; that is, perpendicular to the D2-branes

$$b_{ij}(\theta, \phi) = \beta(\theta, \phi)\, \varepsilon_{ijk} \mathcal{R}^{k3}(\theta, \phi) \tag{4.3.6}$$

and (2) the Dirac quantization condition is met at all angles

$$k_2 \int_{\mathrm{D2}} F = -k_1 \alpha' \quad \text{with} \quad F = \frac{1}{2}\, b_{ij}\, d\varphi^i \wedge d\varphi^j \tag{4.3.7}$$

Enforcing these conditions gives

$$b_{ij}(\theta,\phi) = \frac{-k_1\alpha'\varepsilon_{ijk}\mathcal{R}^{k3}(\theta,\phi)}{k_2(q_1q_2R_1R_2\cos\theta + q_3R_3\sin\theta\,(q_1R_1\sin\phi + q_2R_2\cos\phi))} \tag{4.3.8}$$

The exponent of the rotated state is then found from the boundary conditions

$$\left(M_{ij}a_n^j + \bar{M}_{ij}\bar{a}_{-n}^j\right)|S\rangle\rangle = 0 \implies S = M^{-1}\bar{M} \tag{4.3.9}$$

so that after transforming (4.3.4) we have from (4.3.9) that

$$S(\theta,\phi) = (1_3 + b(\theta,\phi))^{-1}\left[b(\theta,\phi) + \mathcal{R}(\theta,\phi)\,(E_{33} - g)\,\mathcal{R}^{\mathrm{T}}(\theta,\phi)\right] \tag{4.3.10}$$

where b is given by (4.3.8). It is important to note that S in (4.3.10) is a (special) orthogonal matrix.

The next step in our construction will be to find all zero modes that are consistent with (4.3.10). These admissible zero modes

$$\bigotimes_{i=1}^{3}|n_i, w_i\rangle \tag{4.3.11}$$

are determined by the $n = 0$ rotated version of (4.3.4), which upon acting on (4.3.11) reduce to

$$\begin{aligned}\frac{q_1R_1}{k_2A^2}\Big(q_3R_3^2\big(k_1w_3 + k_2q_3\,(q_1n_1 - q_2n_2)\,\big) - q_2R_2^2\big(k_1w_2 + k_2q_2\,(q_3n_3 - q_1n_1)\,\big)\Big)\\ + \frac{q_2q_3V^2}{R_1A^2\alpha'}\,(q_2q_3w_1 + q_1q_3w_2 + q_1q_2w_3) = 0\end{aligned} \tag{4.3.12}$$

and the other two cyclic permutations of the indices, where V is the volume of the 3-torus. The first line of (4.3.12) is the contribution to the boundary conditions of the D2-branes with magnetic flux, and the second line is the contribution due to zero winding in the direction

perpendicular to the D2-branes. Isolating the dependence on the radii we arrive at the winding constraint

$$q_2 q_3 w_1 + q_1 q_3 w_2 + q_1 q_2 w_3 = 0 \tag{4.3.13}$$

and three additional constraint equations given by

$$k_1 w_1 + k_2 q_1 \left(q_2 n_2 - q_3 n_3\right) = 0 \tag{4.3.14}$$

and the other two cyclic permutations of the indices. As long as $k_1 \neq 0$ and $k_2 \neq 0$, (4.3.13) is satisfied by any set of winding numbers that satisfy (4.3.14). The most general solution to (4.3.14) is given by

$$n_1(\mathbf{m}, \gamma) = k_1 m_1 + q_2 q_3 \gamma \,, \quad w_1(\mathbf{m}) = k_2 q_1 \left(q_3 m_3 - q_2 m_2\right) \tag{4.3.15}$$

and the other two cyclic permutations of the indices. Since there are four undetermined integers (m_1, m_2, m_3, and γ) appearing in (4.3.15), this general solution does not specify a basis for Λ but rather a generating set. Noticing that

$$w_i(m_1, m_2, m_3) = w_i(m_1 + q_2 q_3 \delta, m_2 + q_1 q_3 \delta, m_3 + q_1 q_2 \delta) \tag{4.3.16}$$

$$n_i(m_1, m_2, m_3, \gamma) = n_i(m_1 + q_2 q_3 \delta, m_2 + q_1 q_3 \delta, m_3 + q_1 q_2 \delta, \gamma - k_1 \delta) \tag{4.3.17}$$

for some integer δ, we see that choices of γ modulo k_1 correspond to distinct translations of the sublattice generated by summation over $\mathbf{m} \in \mathbb{Z}_3$. Thus, the lattice-sum zero mode in (4.1.2) is parametrized as

$$\sum_{\gamma=0}^{k_1-1} \sum_{\mathbf{m}\in\mathbb{Z}_3} e^{i\delta_{\mathbf{m},\gamma}} \bigotimes_{i=1}^{3} |n_i(\mathbf{m}, \gamma), w_i(\mathbf{m})\rangle \tag{4.3.18}$$

with $n_i(\mathbf{m}, \gamma)$ and $w_i(\mathbf{m})$ given by the corresponding permutation of (4.3.15). Applying the

result (4.A.15), we find

$$\mathrm{vol}(\Lambda) = \frac{k_2^2 A^2 + k_1^2 \alpha'^2}{\alpha'^2 V \sqrt{(2/\alpha')^3}} \tag{4.3.19}$$

It is known [38] that the g-factor, $g_{\mathrm{B}} = \langle 0|S\rangle\rangle$, for a pure D$p$-brane in the bosonic N-torus is of the form

$$g_{\mathrm{D}p}^2 = \frac{V_p^2}{\alpha'^{\,p} V_{T^N} \sqrt{(2/\alpha')^N}} \tag{4.3.20}$$

which gives the suggestive form

$$\mathrm{vol}(\Lambda) = k_2^2 g_{\mathrm{D2}}^2 + k_1^2 g_{\mathrm{D0}}^2 \tag{4.3.21}$$

If any of q_1, q_2, q_3, k_1, or k_2 are zero then the constraints of (4.3.14) are relaxed and (4.3.13) needs to be considered as well, so that (4.3.15) no longer represents all admissible zero modes. However, vol(Λ) remains of the same form as (4.3.19) in each case. For example, if $q_1 = 0$ ($q_2 = q_3 = 1$) then

$$\bigotimes_{i=1}^{3} |n_i, w_i\rangle = |m_1, 0\rangle \otimes |k_1 m_2, -k_2 m_3\rangle \otimes |k_1 m_3, k_2 m_2\rangle \tag{4.3.22}$$

which corresponds precisely to the factorizable state $|\mathrm{D0}\rangle\rangle \otimes |k_2\mathrm{D2}/k_1\mathrm{D0}\rangle\rangle$ describing k_2 D2-branes bound to k_1 D0-branes in the $\varphi^2\varphi^3$-plane. The special case $k_1 = 0$ and $k_2 = 1$ corresponds to a rotated pure D2-brane, with the associated boundary conditions solved by

$$\bigotimes_{i=1}^{3} |n_i, w_i\rangle = |q_2 q_3 m_1, -q_1 m_2\rangle \otimes |q_1 q_3 m_1, -q_2 m_3\rangle \otimes |q_1 q_2 m_1, q_3(m_2 + m_3)\rangle \tag{4.3.23}$$

Lastly, the case $k_2 = 0$ and $k_1 = 1$ corresponds to a pure D0-brane where the boundary state is $|\mathrm{D0}\rangle\rangle \otimes |\mathrm{D0}\rangle\rangle \otimes |\mathrm{D0}\rangle\rangle$.

The other class of boundary states, the D1/D3 system, are T-dual to those of the D2/D0 system. Performing a T-duality transformation on all of the three bosons maps the boundary state of k_2 D2-branes with area vector $\mathbf{A}$ given in (4.3.2) bound to k_1 D0-branes onto the

boundary state of k_2 D1-branes with length vector

$$\boldsymbol{\ell} = q_2 q_3 R_1\, \hat{\varphi}_1 + q_1 q_3 R_2\, \hat{\varphi}_2 + q_1 q_2 R_3\, \hat{\varphi}_3 \tag{4.3.24}$$

bound to k_1 D3-branes. Applying the T-duality transformation rules (A.1.12), the matrix exponent of this second class of boundary states is found from (4.3.10) to be

$$S'(\theta', \phi') = -\left(1_3 + b'(\theta', \phi')\right)^{-1} \left[b(\theta', \phi') + \mathcal{R}(\theta', \phi')\,(E_{33} - g)\,\mathcal{R}^{\mathrm{T}}(\theta', \phi')\right] \tag{4.3.25}$$

with a magnetic field

$$b'_{ij}(\theta', \phi') = \frac{-k_1 V \varepsilon_{ijk} \mathcal{R}^{k3}(\theta', \phi')}{k_2 \alpha' (q_1 q_2 R_3 \cos\theta' + q_3 \sin\theta' \,(q_1 R_2 \sin\phi' + q_2 R_1 \cos\phi'))} \tag{4.3.26}$$

and angles

$$\tan\theta' = \frac{q_1 q_2 R_3}{\sqrt{(q_2 q_3 R_1)^2 + (q_1 q_3 R_2)^2}}\,, \quad \tan\phi' = \frac{q_1 R_2}{q_2 R_1} \tag{4.3.27}$$

The admissible zero modes for all cases considered before for the D2/D0 system are given by (4.3.15), (4.3.22), and (4.3.23) with momenta and windings exchanged for each of the bosons. Taking $R_i \to \alpha'/R_i$ for all $i = 1, 2, 3$ in (4.3.19), the volume of the unit cell of Λ' is

$$\mathrm{vol}(\Lambda') = \frac{k_1^2 V^2 + k_2^2 \ell^2 \alpha'^2}{\alpha'^3 V \sqrt{(2/\alpha')^3}} = k_1^2 g_{\mathrm{D3}}^2 + k_2^2 g_{\mathrm{D1}}^2 \tag{4.3.28}$$

Lastly, there are some boundary states of the D2/D0 system that are not covered by the construction above; namely those where the D2-branes coincide with exactly one of the φ^i-axes. For these we rotate the boundary state corresponding to k_2 D2-branes in the $\varphi^1\varphi^2$-plane bound to k_1 D0-branes about the φ^1-axis, and all other D2/D0 bound states can be found by suitable permutations of the boson indices. For a rotation angle

$$\tan\xi = \frac{p_3 R_3}{p_2 R_2} \tag{4.3.29}$$

the D2-branes will have a corresponding area vector

$$\mathbf{A} = -p_3 R_1 R_3 \, \hat{\varphi}_2 + p_2 R_1 R_2 \, \hat{\varphi}_3 \tag{4.3.30}$$

with a matrix exponent

$$S(\xi) = (1_3 + b(\xi))^{-1} \left[b(\xi) + \mathcal{R}_1(\xi) \, (E_{33} - g) \, \mathcal{R}_1^{\mathrm{T}}(\xi) \right] \tag{4.3.31}$$

where the magnetic field is given by

$$b_{ij}(\xi) = \frac{-k_1 \alpha' \varepsilon_{ijk} \mathcal{R}_1^{k3}(\xi)}{k_2 R_1 (p_2 R_2 \cos\xi + p_3 R_3 \sin\xi)} \tag{4.3.32}$$

The admissible zero modes for this boundary state are

$$\bigotimes_{i=1}^{3} |n_i, w_i\rangle = |k_1 m_1, k_2 (p_2 m_2 + p_3 m_3)\rangle \otimes |-k_1 m_2, k_2 p_2 m_1\rangle \otimes |-k_1 m_3, k_2 p_3 m_1\rangle \tag{4.3.33}$$

producing a normalization factor of the same form as (4.3.19) for the area vector (4.3.30). Following again the transformation rules in (A.1.12), the dual D1/D3 bound state has a length vector

$$\boldsymbol{\ell} = -p_3 R_2 \, \hat{\varphi}_2 + p_2 R_3 \, \hat{\varphi}_3 \tag{4.3.34}$$

for the D1-branes, which is a rotation about the φ^1-axis of the bound state with D1-branes along the φ^3-axis by an angle

$$\tan\xi' = \frac{p_3 R_2}{p_2 R_3} \tag{4.3.35}$$

The matrix exponent is then determined from (4.3.31) to be

$$S'(\xi') = -\left(1_3 + b'(\xi')\right)^{-1} \left[b'(\xi') + \mathcal{R}_1(\xi') \, (E_{33} - g) \, \mathcal{R}_1^{\mathrm{T}}(\xi') \right] \tag{4.3.36}$$

where the magnetic field is given by

$$b'_{ij}(\xi') = \frac{-k_1 V \varepsilon_{ijk} \mathcal{R}_1^{k3}(\xi')}{k_2 \alpha' (p_2 R_3 \cos\xi' + p_3 R_2 \sin\xi')} \tag{4.3.37}$$

The admissible zero modes are (4.3.33) with the momenta and windings exchanged for each of the bosons, producing a normalization factor of the same form as (4.3.28) for the length vector (4.3.34).

4.3.2 Transmission and entanglement entropy

With the normalization factors (4.3.19) and (4.3.28) the only other physical quantity remaining in the entanglement entropy (4.2.26) is the total transmission $\mathcal{T}_i$ of the i-th boson. From the matrix exponents (4.3.10) and (4.3.36), the transmission coefficients of the D2/D0 system are expressed in terms of the area vector of the D2-branes as

$$\mathcal{T}_i = \frac{4k_2^2(A^2 - A_i^2)(k_2^2 A_i^2 + k_1^2 \alpha'^2)}{(k_2^2 A^2 + k_1^2 \alpha'^2)^2} \tag{4.3.38}$$

where $A_i = \mathbf{A} \cdot \hat{\varphi}_i$ is the area of each of the D2-branes projected onto the plane with normal $\hat{\varphi}_i$. For the D1/D3 system the transmission coefficients obtained from (4.3.38) by T-duality are expressed in terms of the length vector of the D1-branes as

$$\mathcal{T}_i = \frac{4k_2^2 \alpha'^2 \left(\ell^2 - \ell_i^2\right) \left(k_1^2 V^2 + k_2^2 \ell_i^2 \alpha'^2\right)}{\left(k_1^2 V^2 + k_2^2 \ell^2 \alpha'^2\right)^2} \tag{4.3.39}$$

where $\ell_i = \boldsymbol{\ell} \cdot \hat{\varphi}_i$ is the projected length of each of the D1-branes along $\hat{\varphi}_i$. At this point we have found all boundary states describing bosonic 3-junctions and their physical quantities relevant to the entanglement entropy.

From the form of (4.3.38) and (4.3.39) the i-th boson is seen to decouple either in the case of a pure D0-brane or D3-brane, or when the area or length vector aligns with the φ^i-axis. Furthermore, we see that perfectly transmissive junctions (with respect to CFT_i) are those

where

$$\frac{A_i^2}{A^2} = \frac{1}{2} - \frac{1}{2}\left(\frac{k_1\alpha'}{k_2 A}\right)^2 \qquad \text{or} \qquad \frac{\ell_i^2}{\ell^2} = \frac{1}{2} - \frac{1}{2}\left(\frac{k_1 V}{k_2 \ell \alpha'}\right)^2 \tag{4.3.40}$$

These conditions cannot be met for general real radii R_i and coupling α'; solutions are only possible when ratios of these real numbers are rational. The conditions simplify in the purely geometric cases ($k_1 = 0$), which are met by D1-branes and D2-branes whose length and area vectors lie on any of the right angle cones about each of the φ^i-axes. From the form of (4.3.40) we see that a completely transmissive junction ($\mathcal{T}_i = 1$ for $i = 1, 2, 3$) can only occur when $k_1 \neq 0$, $k_2 \neq 0$, and the quantities

$$\frac{k_1\alpha'}{k_2 R_i R_j} \qquad \text{or} \qquad \frac{k_1 R_i R_j}{k_2 \alpha'} \tag{4.3.41}$$

are all integers. The volume of the unit cell reduces to

$$\text{vol}(\Lambda) = \frac{k_1^2}{V}\sqrt{2\alpha'^3} \qquad \text{or} \qquad \text{vol}(\Lambda') = k_1^2 V \sqrt{\frac{2}{\alpha'^3}} \tag{4.3.42}$$

in these cases. This result is interesting, as the only the number of D-branes present in the bound state enter into the entanglement entropy of the completely transmissive junctions.

Finally when any of the boundary states align entirely with a single plane, the entanglement entropy reduces to the $N = 2$ results with an additional constant term corresponding to the perpendicular factor of the decoupled boson. For example, for (4.3.34) with $k_1 = 0$ and $k_2 = 1$ we have

$$\mathcal{T}_3 = \sin^2 2\xi' \qquad \text{and} \qquad \mathcal{T}_3 \,\text{vol}(\Lambda')^2 = p_2^2 p_3^2 \,\frac{\alpha'}{2R_1^2} \tag{4.3.43}$$

which differs from (1.2.23) only in the additional constant boundary entropy of the Dirichlet boundary condition along the $\hat{\varphi}_1$ direction.

4.4 Discussion

The main new results are the generalization of the $N = 2$ interface entanglement entropy of [21] and [22] to the case of $N \geq 2$ junctions, both for free boson (4.2.26) and fermion (4.2.50) CFTs. An interesting property of the result is that the both the logarithmically divergent term as well as the constant term only depend on the total transmission coefficient $\mathcal{T}_i$ from the i-th CFT (over which we trace in the entanglement entropy) and the zero mode lattice constant $\mathrm{vol}(\Lambda)$, and thus constitutes the simplest possible generalization of the $N = 2$ results. There is an additional term which is regulator dependent, independent of the parameters of the junction, and absent in the $N = 2$ case.

The most natural extension of these results would be the calculation of the entanglement entropy of CFTs $A \subset \{1, \ldots, N\}$ due to CFTs $B = \bar{A}$. We would expect the entanglement entropy result to change only by

$$\mathcal{T}_i \longrightarrow \mathcal{T}_A = \sum_{i \in A} \sum_{j \in B} \mathcal{T}_{ij} \tag{4.4.1}$$

Most of the calculations of section 4.2 would generalize straightforwardly up to (4.2.13) and (4.2.40), however we would not be able to perform the intermediate Gaussian integrals. Instead, we would need to immediately pass the calculation to the determinant of a block circulant matrix whose larger blocks would have more complicated structure.

It would also be interesting to verify that the Ramond junctions produce the same entanglement entropy as the Neveu-Schwarz junctions, as [22] showed explicitly for $N = 2$. In addition to the modification of the moding, the form of (4.2.39) would include an additional factor containing Grassmann Gaussian integrals relating to the linearization of the additional quadratic exponent in (4.1.13). Owing to the somewhat different anti-commutation relations between the operators in this additional exponent, these Gaussian integrals have a more complicated structure than those handled in this chapter. Due to modular invariance,

the K-sheeted partition function is expected to be

$$Z(K) \sim [\eta(2it)]^{-NK/2}[\theta_2(2it)]^{K(N-2)/2+1} \prod_{k=1}^{K-1} \theta_2(\nu_k|2it) \tag{4.4.2}$$

which would indeed produce the same entanglement entropy as (4.2.50). One could also consider interfaces carrying Ramond charge after performing fermion parity projections under the total ${\mathbb{Z}_2}^N$ symmetry, as was done in [22] for $N = 2$, although it is not clear how easily this could be done for arbitrary N.

It may be possible to define a fusion product of junctions, e.g. an N-junction and an N'-junction fusing in M common CFTs into $(N + N' - 2M)$-junctions connecting the remaining CFTs. It might also be interesting to consider if the left/right entanglement entropy calculations of [82, 83, 100] can be extended to D-brane boundary states corresponding to N-junctions.

In section 4.1 we have characterized the completely transmissive N-junctions as those enforcing twisted permutation gluing conditions. In rational CFTs we could generalize the twisted partition functions of [77] to study "topological" junction operators and their entanglement entropy as in chapter 3.

One could also proceed with the type IIB supergravity solutions in [96] and calculate the asymmetric 3-junction entanglement entropy holographically as in chapter 2. It would be interesting to see if the remarkable holographic agreement in the BPS case between the supergravity calculation and the toy model CFT (i.e. interfaces and junctions of single $c = 3/2$ CFTs without reference to the symmetric orbifold) continues to hold for $N = 3$. Exploring the case $N = 4$ would be more difficult, as there exist D-brane states there that cannot be constructed using successive rotations and T-duality transformations of the elevated $N = 3$ D-brane states. Also, the explicit supergravity solutions for $N \geq 4$ have not been found.

4.A Special functions

4.A.1 Theta functions and S-transformations

The fundamental theta function we use, sometimes called a lattice theta function, is

$$\Theta_\Lambda(\tau) = \sum_{\boldsymbol{\lambda}\in\Lambda} e^{\pi i\tau|\boldsymbol{\lambda}|^2} \tag{4.A.1}$$

Poisson resummation yields the S-transformation

$$\Theta_{\Lambda^*}(-1/\tau) = (-i\tau)^{d/2}\,\mathrm{vol}(\Lambda)\,\Theta_\Lambda(\tau) \tag{4.A.2}$$

where Λ^* is the lattice dual to Λ, $\mathrm{vol}(\Lambda)$ is the volume of the unit cell, and d is the dimension of the lattice. When a basis of Λ is known; that is, when we have a set of d linearly independent vectors $\{\boldsymbol{\epsilon}_1,\ldots,\boldsymbol{\epsilon}_d\}$, $\boldsymbol{\epsilon}_i\in\mathbb{R}^N$, such that

$$\Lambda = \left\{ \sum_{i=1}^{d} m^i\boldsymbol{\epsilon}_i \,\middle|\, \mathbf{m}\in\mathbb{Z}_d \right\} \tag{4.A.3}$$

then $\mathrm{vol}(\Lambda)$ and the basis of Λ^* can be computed directly. Let B be the $N\times d$ matrix whose columns are the basis vectors $\boldsymbol{\epsilon}_i$. In terms of this matrix, the volume of the unit cell is

$$\mathrm{vol}(\Lambda) = \sqrt{\det\left(B^{\mathrm{T}}B\right)} \tag{4.A.4}$$

and the dual basis is taken from the columns of

$$B^* = B\left(B^{\mathrm{T}}B\right)^{-1} \tag{4.A.5}$$

As in section 4.3, sometimes only a set of generators of Λ is known; that is, when we have a set of $D > d$ real vectors $\{\boldsymbol{\epsilon}_1, \cdots, \boldsymbol{\epsilon}_d, \boldsymbol{\delta}_1, \cdots, \boldsymbol{\delta}_{D-d}\}$ such that

$$\Lambda = \left\{ \sum_{i=1}^{d} m^i \boldsymbol{\epsilon}_i + \sum_{j=1}^{D-d} \gamma^j \boldsymbol{\delta}_j \;\middle|\; \mathbf{m} \in \mathbb{Z}_d,\, \boldsymbol{\gamma} \in \Gamma \right\} \tag{4.A.6}$$

where the $\boldsymbol{\epsilon}_i$ are linearly independent and Γ is a finite subset of $\mathbb{Z}_{D-d}$ (containing the origin). Additionally we require that Γ is chosen such that each point in Λ has a unique representation in terms of linear combinations of the above form. This amounts to describing the lattice in terms of a superposition of a finite number of distinct translations of a d-dimensional sublattice with a known basis.

In either case the lattice theta function can be expressed in terms of more conventional theta functions. The multi-dimensional theta functions with characteristics (see [101] for a wide range of properties) are given by

$$\Theta_d \begin{bmatrix} \boldsymbol{\alpha} \\ \boldsymbol{\beta} \end{bmatrix} (\mathbf{z}|\Omega) = \sum_{\mathbf{n} \in \mathbb{Z}_d} e^{2\pi i \left[\frac{1}{2} (\mathbf{n}+\boldsymbol{\alpha}) \cdot \Omega (\mathbf{n}+\boldsymbol{\alpha}) + (\mathbf{n}+\boldsymbol{\alpha}) \cdot (\mathbf{z}+\boldsymbol{\beta}) \right]} \tag{4.A.7}$$

where Ω is a $d \times d$ matrix. Using Poisson resummation, the action of an S-transformation is given by

$$\Theta_d \begin{bmatrix} -\boldsymbol{\beta} \\ \boldsymbol{\alpha} \end{bmatrix} (\Omega^{-1}\mathbf{z}| - \Omega^{-1}) = \sqrt{\det(-i\Omega)}\, e^{-2\pi i \boldsymbol{\alpha} \cdot \boldsymbol{\beta} + \pi i \mathbf{z} \cdot \Omega^{-1} \mathbf{z}}\, \Theta_d \begin{bmatrix} \boldsymbol{\alpha} \\ \boldsymbol{\beta} \end{bmatrix} (\mathbf{z}|\Omega) \tag{4.A.8}$$

For zero characteristics

$$\Theta_d(\mathbf{z}|\Omega) \equiv \Theta_d \begin{bmatrix} \mathbf{0} \\ \mathbf{0} \end{bmatrix} (\mathbf{z}|\Omega)$$

the S-transformation is reduced to

$$\Theta_d(\Omega^{-1}\mathbf{z}| - \Omega^{-1}) = \sqrt{\det(-i\Omega)}\, e^{\pi i \mathbf{z} \cdot \Omega^{-1} \mathbf{z}}\, \Theta_d(\mathbf{z}|\Omega) \tag{4.A.9}$$

The zero characteristic theta functions are related to those with nonzero characteristics through

$$\Theta_d \begin{bmatrix} \boldsymbol{\alpha} \\ \boldsymbol{\beta} \end{bmatrix} (\mathbf{z}|\Omega) = e^{\pi i(\boldsymbol{\alpha}\cdot\Omega\boldsymbol{\alpha}+2\boldsymbol{\alpha}\cdot(\mathbf{z}+\boldsymbol{\beta}))}\, \Theta_d(\mathbf{z}+\Omega\boldsymbol{\alpha}+\boldsymbol{\beta}|\Omega) \tag{4.A.10}$$

When a basis is known, the lattice theta function can be simply written as

$$\Theta_\Lambda(\tau) = \Theta_d(\tau B^{\mathrm{T}} B) \tag{4.A.11}$$

where by standard convention we omit the first argument when $\mathbf{z} = \mathbf{0}$. For the case of a given generating set we instead have

$$\Theta_\Lambda(\tau) = \sum_{\boldsymbol{\gamma}\in\Gamma} \Theta_d \begin{bmatrix} e^{\pi i/3} \left(B_0^{\mathrm{T}} B_0\right)^{-1} B_0^{\mathrm{T}} B_\delta \boldsymbol{\gamma} \\ \mathbf{0} \end{bmatrix} (\tau e^{-\pi i/3} B_0^{\mathrm{T}} B_\delta \boldsymbol{\gamma} | \tau B_0^{\mathrm{T}} B_0) \tag{4.A.12}$$

where B_0 is the basis matrix for the lattice Λ_0 generated by the set $\{\boldsymbol{\epsilon}_i\}$ alone and B_δ is the matrix whose columns are the excess generating vectors $\boldsymbol{\delta}_j$. Setting $\tau = i\varepsilon$ for $\varepsilon \ll 1$ we perform S-transformations to obtain

$$\begin{aligned} \Theta_\Lambda(i\varepsilon) &= \frac{\varepsilon^{-d/2}}{\mathrm{vol}(\Lambda_0)} \sum_{\boldsymbol{\gamma}\in\Gamma} e^{\varepsilon\pi\boldsymbol{\gamma}\cdot B_\delta^{\mathrm{T}} B_\delta \boldsymbol{\gamma}} \qquad (4.A.13) \\ &\qquad \times \Theta_d \begin{bmatrix} \mathbf{0} \\ e^{\pi i/3} \left(B_0^{\mathrm{T}} B_0\right)^{-1} B_0^{\mathrm{T}} B_\delta \boldsymbol{\gamma} \end{bmatrix} \left(e^{-\pi i/3} \left(B_0^{\mathrm{T}} B_0\right)^{-1} B_0^{\mathrm{T}} B_\delta \boldsymbol{\gamma} \,\middle|\, \frac{i}{\varepsilon} \left(B_0^{\mathrm{T}} B_0\right)^{-1} \right) \\ &= \frac{|\Gamma|}{\mathrm{vol}(\Lambda_0)}\, \varepsilon^{-d/2} \Big(1 + O[\varepsilon]\Big)\Big(1 + O[e^{-\mu/\varepsilon}]\Big) \qquad (4.A.14) \end{aligned}$$

where μ is a positive number independent of ε. Comparing this to the leading order behavior of (4.A.2) for $\tau = i\varepsilon$ we obtain

$$\mathrm{vol}(\Lambda) = \frac{\mathrm{vol}(\Lambda_0)}{|\Gamma|} \tag{4.A.15}$$

From this relationship we can determine the volume of the unit cell of Λ from a set of

generators.

Lastly, some special consideration is warranted for one-dimensional theta functions. For the case $d = 1$ we use a lowercase theta, replace the matrix argument Ω with a complex variable τ, and define $q = e^{2\pi i\tau}$ for notational simplicity

$$\theta[\alpha,\beta](z|\tau) \equiv \Theta_1 \begin{bmatrix} \alpha \\ \beta \end{bmatrix} (z|\tau) \tag{4.A.16}$$

The one-dimensional theta functions can be written in the form of an infinite product

$$\theta[\alpha,\beta](z|\tau) = e^{2\pi i\alpha(z+\beta)} q^{\alpha^2/2} \prod_{n=1}^{\infty} (1-q^n) \left(1 + q^{n+\alpha-\frac{1}{2}} e^{2\pi i(z+\beta)}\right) \left(1 + q^{n-\alpha-\frac{1}{2}} e^{-2\pi i(z+\beta)}\right) \tag{4.A.17}$$

such that the usual Jacobi theta functions

$$\begin{aligned} &\theta_1(z|\tau) = -\theta[\tfrac{1}{2},\tfrac{1}{2}](z|\tau)\,, \quad \theta_2(z|\tau) = \theta[\tfrac{1}{2},0](z|\tau)\,, \\ &\theta_3(z|\tau) = \theta[0,0](z|\tau)\,, \quad \theta_4(z|\tau) = \theta[0,\tfrac{1}{2}](z|\tau) \end{aligned} \tag{4.A.18}$$

have sum and product forms

$$\begin{aligned} \theta_1(z|\tau) &= -i \sum_{n\in\mathbb{Z}+\frac{1}{2}} (-1)^{n-\frac{1}{2}} q^{n^2/2} e^{2\pi inz} = 2\sin(\pi z)\, q^{1/8} \prod_{n=1}^{\infty} (1-q^n) \left(1 - 2q^n\cos(2\pi z) + q^{2n}\right) \\ \theta_2(z|\tau) &= \sum_{n\in\mathbb{Z}+\frac{1}{2}} q^{n^2/2} e^{2\pi inz} = 2\cos(\pi z)\, q^{1/8} \prod_{n=1}^{\infty} (1-q^n) \left(1 + 2q^n\cos(2\pi z) + q^{2n}\right) \\ \theta_3(z|\tau) &= \sum_{n=-\infty}^{\infty} q^{n^2/2} e^{2\pi inz} = \prod_{n=1}^{\infty} (1-q^n) \prod_{n\in\mathbb{N}-\frac{1}{2}} \left(1 + 2q^n\cos(2\pi z) + q^{2n}\right) \\ \theta_4(z|\tau) &= \sum_{n=-\infty}^{\infty} (-1)^n q^{n^2/2} e^{2\pi inz} = \prod_{n=1}^{\infty} (1-q^n) \prod_{n\in\mathbb{N}-\frac{1}{2}} \left(1 - 2q^n\cos(2\pi z) + q^{2n}\right) \end{aligned} \tag{4.A.19}$$

and S-transformations given by

$$\begin{aligned}
\theta_1(\tfrac{z}{\tau}|-\tfrac{1}{\tau}) &= i\sqrt{-i\tau}\, e^{\pi i z^2/\tau}\, \theta_1(z|\tau) \\
\theta_2(\tfrac{z}{\tau}|-\tfrac{1}{\tau}) &= \sqrt{-i\tau}\, e^{\pi i z^2/\tau}\, \theta_4(z|\tau) \\
\theta_3(\tfrac{z}{\tau}|-\tfrac{1}{\tau}) &= \sqrt{-i\tau}\, e^{\pi i z^2/\tau}\, \theta_3(z|\tau) \\
\theta_4(\tfrac{z}{\tau}|-\tfrac{1}{\tau}) &= \sqrt{-i\tau}\, e^{\pi i z^2/\tau}\, \theta_2(z|\tau)
\end{aligned} \tag{4.A.20}$$

4.A.2 Dedekind eta and related functions

The Dedekind eta function is

$$\eta(\tau) = q^{\frac{1}{24}} \prod_{n=1}^{\infty} (1-q^n) = \sum_{n=-\infty}^{\infty} (-1)^n q^{(6n-1)^2/24} \tag{4.A.21}$$

and has the modular transformations

$$\eta(\tau+1) = e^{\frac{i\pi}{12}}\, \eta(\tau) \tag{4.A.22}$$

$$\eta(-\tfrac{1}{\tau}) = \sqrt{-i\tau}\, \eta(\tau) \tag{4.A.23}$$

Two related functions

$$\prod_{n=1}^{\infty} (1+q^n) \quad \text{and} \quad \prod_{n\in\mathbb{N}-\frac{1}{2}} (1+q^n) \tag{4.A.24}$$

can be written in terms of the Dedekind eta and other Jacobi theta functions as

$$\prod_{n=1}^{\infty} (1+q^n) = q^{-\frac{1}{24}} \sqrt{\frac{\theta_2(\tau)}{\eta(\tau)}} \tag{4.A.25}$$

$$\prod_{n\in\mathbb{N}-\frac{1}{2}} (1+q^n) = q^{\frac{1}{48}} \sqrt{\frac{\theta_3(\tau)}{\eta(\tau)}} \tag{4.A.26}$$

4.A.3 Bernoulli polynomials and dilogarithms

The Bernoulli polynomials are explicitly given by

$$b_m(x) = \sum_{n=0}^{m} \frac{1}{n+1} \sum_{k=0}^{n} (-1)^k \binom{n}{k} (x+k)^m \tag{4.A.27}$$

These polynomials are generated by the function

$$\frac{te^{xt}}{e^t - 1} = \sum_{m=0}^{\infty} b_m(x) \frac{t^m}{m!} \quad \text{for } |t| < 2\pi \tag{4.A.28}$$

and satisfy the derivative property

$$b'_m(x) = m b_{m-1}(x) \tag{4.A.29}$$

for $m \geq 1$, and thus the Bernoulli polynomials form an Appell sequence. The values of these polynomials at zero are called the Bernoulli numbers $b_n = b_n(0)$. The first two Bernoulli numbers are

$$b_0 = b_0(1) = 1 \tag{4.A.30}$$

$$b_1 = -b_1(1) = -\tfrac{1}{2} \tag{4.A.31}$$

For $n > 1$ we have the following relations

$$b_{2n} = b_{2n}(1) = 4n\,(-1)^n \int_0^{\infty} \frac{t^{2n-1}\,dt}{1 - e^{2\pi t}} \tag{4.A.32}$$

$$b_{2n+1} = b_{2n+1}(1) = 0 \tag{4.A.33}$$

Combined with these expressions for the Bernoulli polynomials and numbers, the sum identity

$$\sum_{k=1}^{K-1} k^m = \frac{b_{m+1}(K) - b_{m+1}}{m+1} \tag{4.A.34}$$

can be used to analytically continue functions of the form

$$F(K) = \sum_{k=1}^{K-1} f\left(\frac{k}{K}\right) \tag{4.A.35}$$

where $f(x)$ is analytic at $x = 0$ and whose series expansion converges everywhere on the interval $[0, 1]$. If $f(x)$ has these properties we can write

$$\begin{aligned} F(K) &= \sum_{m=0}^{\infty} \frac{f^{(m)}(0)}{m!\, K^m} \sum_{k=1}^{K-1} k^m \\ &= \sum_{m=0}^{\infty} \frac{f^{(m)}(0)}{(m+1)!\, K^m} \left[b_{m+1}(K) - b_{m+1}\right] \end{aligned} \tag{4.A.36}$$

so that in the last line of the above $F(K)$ is now explicitly an analytic function of K (except at $K = 0$ if $f(x)$ is a nonlinear function). More so than $F(K)$ we are interested in

$$F'(K) = -\sum_{m=1}^{\infty} \frac{m f^{(m)}(0)}{(m+1)!\, K^{m+1}} \left[b_{m+1}(K) - b_{m+1}\right] + \sum_{m=0}^{\infty} \frac{f^{(m)}(0)}{m!\, K^m}\, b_m(K) \tag{4.A.37}$$

and

$$\begin{aligned} F(1) - F'(1) &= f(0) - \sum_{m=0}^{\infty} \frac{f^{(m)}(0)}{m!}\, b_m(1) \\ &= -\frac{1}{2}\, f'(0) - 2 \sum_{m=1}^{\infty} \frac{f^{(2m)}(0)}{(2m-1)!}\, (-1)^m \int_0^{\infty} \frac{t^{2m-1}\, dt}{1 - e^{2\pi t}} \\ &= -\frac{1}{2}\, f'(0) - i \int_0^{\infty} \frac{f'(it) - f'(-it)}{1 - e^{2\pi t}}\, dt \end{aligned} \tag{4.A.38}$$

In [21] and [22] (4.A.38) was calculated for

$$f_{\rm bos}(x) = \frac{1}{2\pi}\arccos^2(s\sin\pi x) \qquad \text{and} \qquad f_{\rm ferm}(x) = \frac{1}{2\pi}\arcsin^2(s\sin\pi x) \tag{4.A.39}$$

Explicitly, if we define $\Delta(s) \equiv F(1) - F'(1)$ for the s-dependent $f(x)$ in (4.A.39), then we arrive at the integrals

$$\begin{aligned}\Delta_{\rm bos}(s) &= \frac{\pi}{4}\,s - s\int_0^\infty dt\,\frac{\sinh^{-1}(s\sinh\pi t)\cosh\pi t(\coth\pi t - 1)}{\sqrt{1+s^2\sinh^2\pi t}} \\ &= \frac{\pi}{4}\,s - \frac{1}{\pi}\int_0^\infty dz\,\frac{\sqrt{s^2+z^2}-z}{z\sqrt{1+z^2}}\sinh^{-1}z\end{aligned} \tag{4.A.40}$$

and

$$\begin{aligned}\Delta_{\rm ferm}(s) &= 2s\int_0^\infty dt\,\frac{\sinh^{-1}(s\sinh\pi t)\cosh\pi t}{\sqrt{1+s^2\sinh^2\pi t}} \\ &= \frac{2}{\pi}\int_0^\infty dz\,\frac{\sqrt{s^2+z^2}}{z\sqrt{1+z^2}}\sinh^{-1}z\end{aligned} \tag{4.A.41}$$

where the substitution $z = s\sinh\pi t$ has been applied. Upon differentiating twice with respect to s both expressions for $\Delta''(s)$ simplify to a common integral which can be evaluated in terms of elementary functions; i.e.

$$\Delta''_{\rm bos}(s) = -\frac{1}{\pi}\int_0^\infty dz\,\frac{z\sinh^{-1}z}{\sqrt{(1+z^2)(s^2+z^2)^3}} = \frac{1}{\pi}\,\frac{\log s}{1-s^2} \tag{4.A.42}$$

and $\Delta''_{\rm ferm}(s) = -\Delta''_{\rm bos}(s)$. Twice integrating the above we can write

$$\begin{aligned}\Delta_{\rm bos}(s) = \frac{1}{2\pi}\,&[(s+1)\log(s+1)\log s + (s-1)\,\mathrm{Li}_2(1-s) + (s+1)\,\mathrm{Li}_2(-s)] \\ &+ \left(\Delta'_{\rm bos}(0) - \frac{\pi}{12}\right)s + \Delta_{\rm bos}(0) + \frac{\pi}{12}\end{aligned} \tag{4.A.43}$$

where the dilogarithms appearing in the above are defined by the series

$$\mathrm{Li}_2(z) \equiv \sum_{k=1}^{\infty} \frac{z^k}{k^2} \tag{4.A.44}$$

The presence of dilogarithms in (4.A.43) is due to the matching of the integral representation

$$\mathrm{Li}_2(z) = -\int_0^z dw\, \frac{\log(1-w)}{w} \tag{4.A.45}$$

with the first integral of the right-hand side of (4.A.42); the second integral is then evaluated with the help of the identity

$$\int dz\, \mathrm{Li}_2(z) = z\, \mathrm{Li}_2(z) - z - (1-z)\log(1-z) \tag{4.A.46}$$

In (4.A.43) the integration constants have been written to be matched to the behavior of $\Delta_{\mathrm{bos}}(s)$ at $s = 0$ (the series definition (4.A.44) gives $\mathrm{Li}_2(0) = 0$, $\mathrm{Li}_2(1) = \pi^2/6$, and $\mathrm{Li}_2(-1) = -\pi^2/12$), with a similar expression for $\Delta_{\mathrm{ferm}}(s)$. Expanding (4.A.40) and (4.A.41) to first order in s, we see that

$$\Delta_{\mathrm{bos}}(0) = 0\,, \;\; \Delta'_{\mathrm{bos}}(0) = \frac{\pi}{4} \quad \text{and} \quad \Delta_{\mathrm{ferm}}(0) = 0\,, \;\; \Delta'_{\mathrm{ferm}}(0) = 0 \tag{4.A.47}$$

In the notation of section 4.2, the results are

$$\varphi(1) - \varphi'(1) = \frac{\pi}{2}\,\sigma(s) - \frac{\pi}{4} \qquad \text{and} \qquad \vartheta(1) - \vartheta'(1) = \frac{\pi}{2}\,\sigma(s) - \frac{\pi}{4}\,s \tag{4.A.48}$$

where $\sigma(s)$ is given by

$$\sigma(s) = \frac{1}{6} + \frac{s}{3} + \frac{1}{\pi^2}\left[(s+1)\log(s+1)\log s + (s-1)\,\mathrm{Li}_2(1-s) + (s+1)\,\mathrm{Li}_2(-s)\right] \tag{4.A.49}$$

The behavior of $\sigma(s)$ near $s = 0$ and $s = 1$ can be calculated straightforwardly utilizing (4.A.45), giving

$$\sigma(s) = \frac{s}{2} + \frac{1}{2\pi^2}\left(2\log s - 3\right)s^2 + O[s^4] = \frac{1}{3} - \frac{1}{4}\left(1-s\right) - \frac{1}{2\pi^2}\left(1-s\right)^2 - \frac{1}{6\pi^2}\left(1-s\right)^3 + O[(1-s)^4] \tag{4.A.50}$$

4.B Intermediate Gaussian integrals

4.B.1 Bosonic integrals

In the following we repeatedly use the one-dimensional complex Gaussian integral

$$\int_{-\infty}^{\infty} dz\, d\bar{z}\; e^{\,az\bar{z}+bz+c\bar{z}} = -\frac{1}{a}\, e^{-bc/a} \tag{4.B.1}$$

in order to integrate out all of the dependence on the i-th integration variables in (4.2.13). This will involve isolating linear factors of these variables in the exponents of (4.2.13) in order to combine them via (4.B.1). We show some of the details of this process below.

Focusing on the $z_{ni}^{(k)}$, $\bar{z}_{ni}^{(k)}$ integral for an arbitrary fixed k, the linear terms in the exponents of (4.2.13) are rewritten as

$$q^n \sum_l \left(S_{il} z_{ni}^{(k)} w_{nl}^{(k)} + S_{li} \bar{z}_{nl}^{(k)} \bar{w}_{ni}^{(k)} \right) = \left(q^n \sum_j S_{ij} w_{nj}^{(k)} \right) z_{ni}^{(k)} + \left(q^n S_{ii} \bar{w}_{ni}^{(k)} \right) \bar{z}_{ni}^{(k)} + q^n \sum_{j \neq i} S_{ji} \bar{z}_{nj}^{(k)} \bar{w}_{ni}^{(k)} \tag{4.B.2}$$

$$q^n \sum_{j \neq i} \sum_l \left(S_{jl} z_{nj}^{(k)} w_{nl}^{(k-1)} + S_{lj} \bar{z}_{nl}^{(k)} \bar{w}_{nj}^{(k-1)} \right) = q^n \sum_{j \neq i} \sum_l S_{jl} z_{nj}^{(k)} w_{nl}^{(k-1)} + \left(q^n \sum_{j \neq i} S_{ij} \bar{w}_{nj}^{(k-1)} \right) \bar{z}_{ni}^{(k)} + q^n \sum_{j,l \neq i} S_{lj} \bar{z}_{nl}^{(k)} \bar{w}_{nj}^{(k-1)} \tag{4.B.3}$$

in order to isolate the $z_{ni}^{(k)}$ and $\bar{z}_{ni}^{(k)}$ factors. Applying (4.B.1) to all the $z_{ni}^{(k)}$, $\bar{z}_{ni}^{(k)}$ integrals then yields the new exponential terms

$$\begin{aligned}\left(q^n \sum_j S_{ij} w_{nj}^{(k)}\right)\left(q^n S_{ii} \bar{w}_{ni}^{(k)} + q^n \sum_{j\neq i} S_{ij} \bar{w}_{nj}^{(k-1)}\right) \\ = q^{2n} S_{ii}^2 w_{ni}^{(k)} \bar{w}_{ni}^{(k)} + \left(q^{2n} S_{ii} \sum_{j\neq i} S_{ij} w_{nj}^{(k)}\right) \bar{w}_{ni}^{(k)} \\ + \left(q^{2n} S_{ii} \sum_{j\neq i} S_{ij} \bar{w}_{nj}^{(k-1)}\right) w_{ni}^{(k)} + q^{2n} \sum_{j,l\neq i} S_{ij} S_{jl} w_{nj}^{(k)} \bar{w}_{nl}^{(k-1)}\end{aligned} \tag{4.B.4}$$

where we have isolated the $w_{ni}^{(k)}$ and $\bar{w}_{ni}^{(k)}$ factors for the next round of integration.

Focusing now on the $w_{ni}^{(k)}$, $\bar{w}_{ni}^{(k)}$ integral for an arbitrary fixed k, the quadratic term of the exponent is now $-w_{ni}^{(k)} \bar{w}_{ni}^{(k)}/D_n$ after the z_{ni}, $\bar{z}_{ni}$ integration, where $D_n = (1 - q^{2n} S_{ii}^2)^{-1}$. The remaining linear terms in the exponent are the above linear terms above in addition to those that spectated the z_{ni}, $\bar{z}_{ni}$ integration

$$\left(q^n \sum_{j\neq i} S_{ji} \bar{z}_{nj}^{(k)}\right) \bar{w}_{ni}^{(k)} + \left(q^n \sum_{j\neq i} S_{ji} z_{nj}^{(k+1)}\right) w_{ni}^{(k)} + q^n \sum_{j,l\neq i} S_{jl} \left(z_{nj}^{(k+1)} w_{nl}^{(k)} + \bar{z}_{nj}^{(k+1)} \bar{w}_{nl}^{(k)}\right) \tag{4.B.5}$$

so that applying (4.B.1) to all the $w_{ni}^{(k)}$, $\bar{w}_{ni}^{(k)}$ integrals then yields the new terms

$$D_n \left(q^n \sum_{j\neq i} S_{ji} z_{nj}^{(k+1)} + q^{2n} S_{ii} \sum_{j\neq i} S_{ij} \bar{w}_{nj}^{(k-1)}\right)\left(q^n \sum_{j\neq i} S_{ji} \bar{z}_{nj}^{(k)} + q^{2n} S_{ii} \sum_{j\neq i} S_{ij} w_{nj}^{(k)}\right) \tag{4.B.6}$$

At this point there are no linear terms remaining that mix variables with the same value of k. Once the above terms are simplified and all indices shifted so that k and $k+1$ are the only indices that appear, we recover (4.2.14) and (4.2.15).

4.B.2 Fermionic integrals

In the following we repeatedly use the one-dimensional complex Grassmann Gaussian integral

$$-\int d\eta\, d\bar{\eta}\; e^{a\eta\bar{\eta}+\beta\eta+\bar{\eta}\gamma} = a\, e^{\beta\gamma/a} \tag{4.B.7}$$

for constant a and Grassmann-valued β and γ, in order to integrate out all of the dependence on the i-th integration variables in (4.2.40). This will involve isolating linear factors of these variables in the exponents of (4.2.40) in order to combine them via (4.B.7). We show some of the details of this process below.

Focusing on the $\eta_{ni}^{(k)}$, $\bar{\eta}_{ni}^{(k)}$ integral for an arbitrary fixed k, the linear terms in the exponents of (4.2.40) are rewritten as

$$\begin{aligned} & iq^n \sum_j \left(S_{ij}\eta_{ni}^{(k)}\chi_{nj}^{(k)} + S_{ji}\bar{\eta}_{nj}^{(k)}\bar{\chi}_{ni}^{(k)} \right) \\ &= \left(-iq^n \sum_j S_{ij}\chi_{nj}^{(k)} \right) \eta_{ni}^{(k)} + \bar{\eta}_{ni}^{(k)} \left(iq^n S_{ii}\bar{\chi}_{ni}^{(k)} \right) + iq^n \sum_{j\neq i} S_{ji}\bar{\eta}_{nj}^{(k)}\bar{\chi}_{ni}^{(k)} \end{aligned} \tag{4.B.8}$$

and

$$\begin{aligned} iq^n \sum_l \sum_{j\neq i} \left(S_{jl}\eta_{nj}^{(k)}\chi_{nl}^{(k-1)} + S_{lj}\bar{\eta}_{nl}^{(k)}\bar{\chi}_{nj}^{(k-1)} \right) &= iq^n \sum_l \sum_{j\neq i} S_{jl}\eta_{nj}^{(k)}\chi_{nl}^{(k-1)} + \bar{\eta}_{ni}^{(k)} \left(iq^n \sum_{j\neq i} S_{ij}\bar{\chi}_{nj}^{(k-1)} \right) \\ &\quad + iq^n \sum_{l\neq i} \sum_{j\neq i} S_{lj}\bar{\eta}_{nl}^{(k)}\bar{\chi}_{nj}^{(k-1)} \end{aligned} \tag{4.B.9}$$

in order to isolate the $\eta_{ni}^{(k)}$ and $\bar{\eta}_{ni}^{(k)}$ factors. Applying (4.B.7) to all the $\eta_{ni}^{(k)}$, $\bar{\eta}_{ni}^{(k)}$ integrals

then yields the new terms

$$\begin{aligned}
&\left(-iq^n \sum_j S_{ij}\chi_{nj}^{(k)}\right)\left(iq^n S_{ii}\bar{\chi}_{ni}^{(k)} + iq^n \sum_{j\neq i} S_{ij}\bar{\chi}_{nj}^{(k-1)}\right) \\
&= q^{2n}S_{ii}^2\chi_{ni}^{(k)}\bar{\chi}_{ni}^{(k)} + \bar{\chi}_{ni}^{(k)}\left(-q^{2n}S_{ii}\sum_{j\neq i} S_{ij}\chi_{nj}^{(k)}\right) + \left(-q^{2n}S_{ii}\sum_{j\neq i} S_{ij}\bar{\chi}_{nj}^{(k-1)}\right)\chi_{ni}^{(k)} \\
&\quad + q^{2n}\sum_{l\neq i}\sum_{j\neq i} S_{ij}S_{il}\chi_{nj}^{(k)}\bar{\chi}_{nl}^{(k-1)}
\end{aligned} \tag{4.B.10}$$

where we have isolated the $\chi_{ni}^{(k)}$ and $\bar{\chi}_{ni}^{(k)}$ factors for the next round of integration.

Focusing now on the $\chi_{ni}^{(k)}$, $\bar{\chi}_{ni}^{(k)}$ integral for a arbitrary fixed k, the quadratic term of the exponent is now $\chi_{ni}^{(k)}\bar{\chi}_{ni}^{(k)}/D_n$ after the η_{ni}, $\bar{\eta}_{ni}$ integration, where $D_n = (1+q^{2n}S_{ii}^2)^{-1}$. The remaining linear terms in the exponent are the linear terms above in addition to those that spectated the η_{ni}, $\bar{\eta}_{ni}$ integration

$$\bar{\chi}_{ni}^{(k)}\left(-iq^n\sum_{j\neq i} S_{ji}\bar{\eta}_{nj}^{(k)}\right) + \left(iq^n\sum_{j\neq i} S_{ji}\eta_{nj}^{(k+1)}\right)\chi_{ni}^{(k)} + iq^n\sum_{l\neq i}\sum_{j\neq i} S_{jl}\left(\eta_{nj}^{(k+1)}\chi_{nl}^{(k)} + \bar{\eta}_{nj}^{(k+1)}\bar{\chi}_{nl}^{(k)}\right) \tag{4.B.11}$$

so that applying (4.B.7) to all the $\chi_{ni}^{(k)}$, $\bar{\chi}_{ni}^{(k)}$ integrals then yields the new terms

$$D_n\left(iq^n\sum_{j\neq i} S_{ji}\eta_{nj}^{(k+1)} - q^{2n}S_{ii}\sum_{j\neq i} S_{ij}\bar{\chi}_{nj}^{(k-1)}\right)\left(-iq^n\sum_{j\neq i} S_{ji}\bar{\eta}_{nj}^{(k)} - q^{2n}S_{ii}\sum_{j\neq i} S_{ij}\chi_{nj}^{(k)}\right) \tag{4.B.12}$$

At this point there are no linear terms remaining that mix variables with the same value of k. Once the above terms are simplified and all indices shifted so that k and $k+1$ are the only indices that appear, we recover (4.2.41) and (4.2.42).

4.C Calculation of determinants

In the determinant calculations there are two special forms of (equal-sized and square) block matrices that we encounter, those of the block circulant form

$$\mathcal{M}_n = \begin{pmatrix} M_0 & M_{n-1} & M_{n-2} & \cdots & M_2 & M_1 \\ M_1 & M_0 & M_{n-1} & \cdots & M_3 & M_2 \\ M_2 & M_1 & M_0 & \cdots & M_4 & M_3 \\ \vdots & \vdots & \vdots & \ddots & \vdots & \vdots \\ M_{n-2} & M_{n-3} & M_{n-4} & \cdots & M_0 & M_{n-1} \\ M_{n-1} & M_{n-2} & M_{n-3} & \cdots & M_1 & M_0 \end{pmatrix} \tag{4.C.1}$$

and 2×2 block matrices. The determinant of the block circulant matrix was shown in [102] to be

$$\det \mathcal{M}_n = \prod_{k=1}^{n} \det \left(\sum_{j=0}^{n-1} e^{2jk\pi i/n} M_j \right) \tag{4.C.2}$$

This result is remarkable as (4.C.2) is of the same form regardless of the size of the matrices M_j, including when they reduce to scalars. In general, determinants of block matrices only exhibit similar behavior either when all block entries commute [103], or when certain blocks are invertible and commute. Consider the 2×2 block matrix

$$\begin{pmatrix} A & B \\ C & D \end{pmatrix} \tag{4.C.3}$$

with A, B, C, and D all square matrices of the same dimensions. If A is invertible, then the decomposition

$$\begin{pmatrix} A & B \\ C & D \end{pmatrix} = \begin{pmatrix} A & 0 \\ C & 1 \end{pmatrix} \begin{pmatrix} 1 & A^{-1}B \\ 0 & D - CA^{-1}B \end{pmatrix} \tag{4.C.4}$$

leads to the determinant equation

$$\det \begin{pmatrix} A & B \\ C & D \end{pmatrix} = \det A \, \det \left(D - CA^{-1}B \right) \tag{4.C.5}$$

If we also have that $[A, C] = 0$ then the determinant reduces to

$$\det \begin{pmatrix} A & B \\ C & D \end{pmatrix} = \det \left(AD - CB \right) \tag{4.C.6}$$

while if $[A, B] = 0$ the determinant becomes

$$\det \begin{pmatrix} A & B \\ C & D \end{pmatrix} = \det \left(DA - CB \right) \tag{4.C.7}$$

Similar results holds if D is invertible and $[C, D] = 0$ or $[B, D] = 0$.

4.C.1 Bosonic determinant

Beginning with the matrix defined in (4.2.17), (4.2.18), and (4.2.19) we apply (4.C.2) to obtain

$$\begin{aligned} \det M_K &= \prod_{k=1}^{K} \det \left(1_{4N-4} + e^{2\pi i k/K} C + e^{-2\pi i k/K} C^{\mathrm{T}} \right) \\ &= \prod_{k=1}^{K} \det \begin{pmatrix} 1_{2N-2} + X \otimes U_k & e^{2\pi i k/K} Y \otimes \sigma^3 \\ e^{-2\pi i k/K} Y^{\mathrm{T}} \otimes \sigma^3 & 1_{2N-2} + Z \otimes U_k \end{pmatrix} \end{aligned} \tag{4.C.8}$$

where

$$U_k = \cos(2\pi k/K)\, 1_2 + i \sin(2\pi k/K)\, \sigma^2 = \exp\left(2\pi i k \sigma^2 / K \right) \tag{4.C.9}$$

In order to analyze the structure of the 2×2 block matrices above, we calculate a few properties of the blocks (4.2.19)

$$\mathrm{Tr}\,[X] = \mathrm{Tr}\,[Z] = -q^{2n} D_n \left(1 - S_{ii}^2\right) \tag{4.C.10}$$

$$X^2 = -q^{2n} D_n \left(1 - S_{ii}^2\right) X\,, \quad Z^2 = -q^{2n} D_n \left(1 - S_{ii}^2\right) Z \tag{4.C.11}$$

$$(XY)_{jl} = (YZ)_{jl} = -q^{3n} D_n^2 S_{ii} \left(1 - q^{2n}\right) S_{ji} S_{il} \tag{4.C.12}$$

$$YY^{\mathrm{T}} = q^{2n} 1_{N-1} + D_n \left(1 - q^{4n} S_{ii}^2\right) X \tag{4.C.13}$$

$$Y^{\mathrm{T}} Y = q^{2n} 1_{N-1} + D_n \left(1 - q^{4n} S_{ii}^2\right) Z \tag{4.C.14}$$

From (4.C.11) we see that $\det X = \det Z = 0$, and hence X and Z are not invertible. However, employing the matrix logarithm, the Mercator series, and the geometric series we find

$$\begin{aligned}
\det\left(1_{2N-2} + X \otimes U_k\right) &= \exp\left(-\sum_{m=1}^{\infty} \frac{(-1)^m}{m} \mathrm{Tr}[X^m]\,\mathrm{Tr}[U_k^m]\right) \\
&= \exp\left(-\sum_{m=1}^{\infty} \frac{1}{m} \left(q^{2n} D_n (1 - S_{ii}^2)\right)^m \left(e^{2\pi i m k/K} + e^{-2\pi i m k/K}\right)\right) \\
&= 1 - 2q^{2n} D_n (1 - S_{ii}^2) \cos(2\pi k/K) + q^{4n} D_n^2 (1 - S_{ii}^2)^2 \qquad (4.C.15) \\
&= \det\left(1_{2N-2} + Z \otimes U_k\right)
\end{aligned}$$

Thus $1_{2N-2} + X \otimes U_k$ and $1_{2N-2} + Z \otimes U_k$ are both invertible. A very similar determinant calculation using (4.C.13) and (4.C.14) shows that $\det Y \neq 0$ and hence Y is invertible. At

this point we make the decomposition

$$\begin{pmatrix} 1_{2N-2} + X \otimes U_k & e^{2\pi ik/K} Y \otimes \sigma^3 \\ e^{-2\pi ik/K} Y^{\mathrm{T}} \otimes \sigma^3 & 1_{2N-2} + Z \otimes U_k \end{pmatrix} =$$
$$\begin{pmatrix} e^{2\pi ik/K} B_k & e^{2\pi ik/K} Y \otimes \sigma^3 \\ 1_{2N-2} & 1_{2N-2} + Z \otimes U_k \end{pmatrix} \begin{pmatrix} e^{2\pi ik/K} Y \otimes \sigma^3 A_k^{-1} & 0 \\ 1_{N-1} \otimes \left(1_2 - q^{2n} A_k^{-1}\right) & 1_{2N-2} \end{pmatrix}^{-1} \tag{4.C.16}$$

with matrices

$$A_k = q^{2n} 1_2 - D_n \left(1 - q^{4n} S_{ii}^2\right) U_k^{-1} \tag{4.C.17}$$

and

$$B_k = Y \otimes \sigma^3 \left(1_2 + (1 - q^{2n}) A_k^{-1}\right) + XY \otimes U_k \sigma^3 A_k^{-1} \tag{4.C.18}$$

Now using (4.C.16) and (4.C.7), the determinant can be reduced to

$$\begin{aligned} \det\, M_K &= \prod_{k=1}^{K} \det \left[B_k \left(Y^{-1} \otimes A_k \sigma^3\right) + B_k \left(Z \otimes U_k\right) \left(Y^{-1} \otimes A_k \sigma^3\right) - 1_{N-1} \otimes \sigma^3 A_k \sigma^3 \right] \\ &= \prod_{k=1}^{K} \left(1 - q^{2n}\right)^{2N-2} \det \left(1_{2N-2} + \frac{2\cos(2\pi k/K) - q^{2n} - 1}{1 - q^{2n}} X \otimes 1_2 \right) \\ &= D_n^{2K} \prod_{k=1}^{K} \left(1 - q^{2n}\right)^{2N-4} \left[1 - 2 \left(S_{ii}^2 + \left(1 - S_{ii}^2\right) \cos(2\pi k/K) \right) q^{2n} + q^{4n} \right]^2 \end{aligned} \tag{4.C.19}$$

4.C.2 Fermionic determinant

In this case the block entries (4.2.19) and their properties in (4.C.10) through (4.C.14) are modified by $q^n \to -iq^n$. We proceed in a similar manner to the previous section, where now

$$\begin{aligned}
\det M_K &= \prod_{k=1}^{K} \det\left(1_{2N-2}\otimes\sigma^2 + e^{2\pi ik/K}C - e^{-2\pi ik/K}C^{\mathrm{T}}\right) \\
&= \prod_{k=1}^{K} \det \begin{pmatrix} 1_{N-1}\otimes\sigma^2 + X\otimes U_k\sigma^2 & e^{2\pi ik/K}Y\otimes\sigma^3 \\ -e^{-2\pi ik/K}Y^{\mathrm{T}}\otimes\sigma^3 & 1_{N-1}\otimes\sigma^2 + Z\otimes U_k\sigma^2 \end{pmatrix} \\
&= (-1)^{2(N-1)K}\prod_{k=1}^{K} \det \begin{pmatrix} 1_{2N-2} + X\otimes U_k & -ie^{2\pi ik/K}Y\otimes\sigma^1 \\ ie^{-2\pi ik/K}Y^{\mathrm{T}}\otimes\sigma^1 & 1_{2N-2} + Z\otimes U_k \end{pmatrix}
\end{aligned} \tag{4.C.20}$$

with U_k as in (4.C.9). Making the decomposition

$$\begin{aligned}
&\begin{pmatrix} 1_{2N-2} + X\otimes U_k & -ie^{2\pi ik/K}Y\otimes\sigma^1 \\ ie^{-2\pi ik/K}Y^{\mathrm{T}}\otimes\sigma^1 & 1_{2N-2} + Z\otimes U_k \end{pmatrix} = \\
&\qquad \begin{pmatrix} -ie^{2\pi ik/K}B_k & -ie^{2\pi ik/K}Y\otimes\sigma^1 \\ 1_{2N-2} & 1_{2N-2} + Z\otimes U_k \end{pmatrix} \begin{pmatrix} -ie^{2\pi ik/K}Y\otimes\sigma^1 A_k^{-1} & 0 \\ 1_{N-1}\otimes\left(1_2 + q^{2n}A_k^{-1}\right) & 1_{2N-2} \end{pmatrix}^{-1}
\end{aligned} \tag{4.C.21}$$

with matrices

$$A_k = -q^{2n}1_2 - D_n\left(1 - q^{4n}S_{ii}^2\right)U_k^{-1} \tag{4.C.22}$$

and

$$B_k = Y\otimes\sigma^1\left(1_2 + (1+q^{2n})A_k^{-1}\right) + XY\otimes U_k\sigma^1 A_k^{-1} \tag{4.C.23}$$

we use (4.C.21) and (4.C.7) to reduce the determinants to

$$\begin{aligned}\det M_K &= (-1)^{2(N-1)K} \prod_{k=1}^{K} \left(1+q^{2n}\right)^{2N-2} \det\left(1_{2N-2} + \frac{2\cos(2\pi k/K)+q^{2n}-1}{1+q^{2n}}\, X \otimes 1_2\right) \\ &= D_n^{2K}\,(-1)^{2(N-1)K} \prod_{k=1}^{K} \left(1+q^{2n}\right)^{2N-4} \left[1+2\left(S_{ii}^2+\left(1-S_{ii}^2\right)\cos(2\pi k/K)\right)q^{2n}+q^{4n}\right]^2\end{aligned} \tag{4.C.24}$$

Chapter 5

Holographic Topological Interfaces

In chapter 2 when we considered holographic duals to conformal interfaces in the form of deformed geometries it is notable that for no moduli were these geometries dual to topological interfaces (both solutions select $k_1 = k_2 = 1$, leading to no nontrivial values of the parameters in which the topological conditions in the boundary CFT are satisfied). This is unsurprising, as deformations of the bulk require energy and thus one would not expect to be able to freely deform between them; a key property we expect to be a feature of the bulk theory dual to a topological interface. Thus we seek to explore holographic duals to topological interfaces along a different direction, i.e. in terms of bulk interfaces of topological CS matter theories.

When one considers co-dimension one interfaces between two theories or boundaries of a single theory, the variation of the action can pick up terms localized on the interface or boundary. In order to obtain a good variational principle it may then be necessary to add counter terms to the action which are localized on the interface or boundary. For topological field theories this can lead to the introduction of non-topological degrees of freedom, and this procedure is indeed what causes the relation of CS theory on a 3-manifold with boundary and chiral WZW theories on the boundary [59, 104]. On the other hand, as shown in [65], for Abelian CS theories it is possible to impose topological boundary conditions, where no counter terms are necessary. Since any interface between two theories can be mapped

into a boundary by the folding trick [19] this statement implies the existence of topological interfaces in CS theories [105]. The aim of this chapter is to study some implications of such CS topological interface theories in the context of the AdS/CFT correspondence and relate them to topological interfaces in the dual two-dimensional CFT.

The structure of this chapter is as follows: in section 5.1 we review the construction of topological interfaces in CS theories on general manifolds (see section 1.3.2 for a review of well-known aspects of pure CS theory and its holography). In section 5.2 we relate a topological interface in the bulk of AdS_3 to the boundary by utilizing an AdS_2 slicing of AdS_3. In order to identify conserved currents in the CFT the dual currents need to have both holomorphic and anti-holomorphic parts. To accomplish this we generalize a construction first given in [106] to show that in general it is possible to obtain a topological interface in the boundary CFT from a topological interface in the AdS_3 bulk. In section 5.3 we briefly discuss higher-dimensional generalizations of this construction. We close with a discussion of open questions in section 5.4.

5.1 Background

In this section we will review the recent construction of topological interface conditions for CS theory given in [65][1]. We will be mainly following the treatment given in [105]. We divide the total 3-manifold $\mathcal{M}$ into two parts $\mathcal{M} = \mathcal{M}_L \cup_\Sigma \mathcal{M}_R$ with joining interface Σ. The $U(1)^N$ CS action is now divided into two parts

$$S_{\text{CS}} = \frac{1}{4\pi} K^{(L)}_{IJ} \int_{\mathcal{M}_L} A^{(L)^I} \wedge dA^{(L)^J} + \frac{1}{4\pi} K^{(R)}_{IJ} \int_{\mathcal{M}_R} A^{(R)^I} \wedge dA^{(R)^J} \tag{5.1.1}$$

with in general different level matrices $K^{(L)}$ and $K^{(R)}$. If the manifold $\mathcal{M}$ has a boundary we have to add an appropriate boundary term. In this section we will focus on the topological interface matching conditions which relate the $A^{(L)}$ and $A^{(R)}$ gauge fields and postpone the

[1]For related work in the condensed matter literature see, e.g. [107–111].

discussion of the boundary terms to section 5.2.3.

A topological interface is defined such that the canonical symplectic one-form

$$\mathbf{\Theta} = \delta S_{\mathrm{CS}}|_{\text{ on shell}} = -\frac{1}{4\pi}\int_{\Sigma}\left(K^{(L)}_{IJ}A^{(L)^I}\wedge\delta A^{(L)^J} - K^{(R)}_{IJ}A^{(R)^I}\wedge\delta A^{(R)^J}\right) \tag{5.1.2}$$

vanishes on shell on a half-dimensional subspace of the phase space without the introduction of additional contributions coming from counter terms localized on Σ. These bulk boundary conditions are determined by two $N\times N$ matrices $v^{(L)}$ and $v^{(R)}$ which implement the matching condition

$$v^{(L)^{\mathrm{T}}}K^{(L)}A^{(L)}\big|_{\Sigma} = -v^{(R)^{\mathrm{T}}}K^{(R)}A^{(R)}\big|_{\Sigma} \tag{5.1.3}$$

and must respect the gluing condition

$$v^{(L)^{\mathrm{T}}}K^{(L)}v^{(L)} = v^{(R)^{\mathrm{T}}}K^{(R)}v^{(R)} \tag{5.1.4}$$

Since the above gluing condition does not have unique solutions, we additionally demand that the $v^{(L)}$ and $v^{(R)}$ satisfy a primitivity condition. This translates to the condition that the $N\times N$ minors of the $2N\times N$ matrix

$$\mathbb{P} = \begin{pmatrix} v^{(L)} \\ -v^{(R)} \end{pmatrix} \tag{5.1.5}$$

all have a greatest common divisor of 1. The theories we'll consider will be those with nonsingular level matrices, and taking the determinant of (5.1.4) shows that in such theories the matrices $v^{(L)}$ and $v^{(R)}$ are then either both singular or both nonsingular; we'll only consider interfaces where the latter is true.

As an example of matching conditions between theories with unequal level matrices,

consider the case

$$K^{(L)} = kn_L^2 \begin{pmatrix} 1 & 0 \\ 0 & -1 \end{pmatrix} \quad \text{and} \quad K^{(R)} = kn_R^2 \begin{pmatrix} 1 & 0 \\ 0 & -1 \end{pmatrix} \tag{5.1.6}$$

where $k, n_L, n_R \in \mathbb{Z}$ and we assume that n_L and n_R are relatively prime. There are two types of primitive matching condition matrices satisfying (5.1.4), either

$$v_1^{(L)} = n_R \begin{pmatrix} \eta_L & 0 \\ 0 & \eta'_L \end{pmatrix} \quad \text{and} \quad v_1^{(R)} = n_L \begin{pmatrix} \eta_R & 0 \\ 0 & \eta'_R \end{pmatrix} \tag{5.1.7}$$

or

$$v_2^{(L)} = n_R \begin{pmatrix} 0 & \eta''_L \\ \eta''_L & 0 \end{pmatrix} \quad \text{and} \quad v_2^{(R)} = n_L \begin{pmatrix} 0 & \eta''_R \\ \eta''_R & 0 \end{pmatrix} \tag{5.1.8}$$

where $\eta_L, \eta'_L, \eta''_L, \eta_R, \eta'_R, \eta''_R = \pm 1$. In terms of the matching condition

$$A^{(L)}\big|_\Sigma = -v^{(L)}[v^{(R)}]^{-1} A^{(R)}\big|_\Sigma \tag{5.1.9}$$

following from (5.1.3) and (5.1.4), we have that

$$-v_1^{(L)}[v_1^{(R)}]^{-1} = -\frac{n_R}{n_L} \begin{pmatrix} \eta_L\eta_R & 0 \\ 0 & \eta'_L\eta'_R \end{pmatrix} \quad \text{and} \quad -v_2^{(L)}[v_2^{(R)}]^{-1} = -\frac{n_R}{n_L} \begin{pmatrix} \eta''_L\eta''_R & 0 \\ 0 & \eta''_L\eta''_R \end{pmatrix} \tag{5.1.10}$$

While the diagonal level matrices of (5.1.6) do not allow for matching conditions that mix the gauge fields of different levels, in general diagonal level matrices do. For example [105], the continuous level matrix

$$K^{(L)} = K^{(R)} = k \begin{pmatrix} 1 & 0 \\ 0 & m^2 - n^2 \end{pmatrix} \tag{5.1.11}$$

with n, m relatively prime, allows for the primitive matching condition matrices

$$v^{(L)} = \begin{pmatrix} m & n \\ 0 & 1 \end{pmatrix} \quad \text{and} \quad v^{(R)} = \begin{pmatrix} -n & -m \\ 1 & 0 \end{pmatrix} \implies -v^{(L)}[v^{(R)}]^{-1} = \frac{1}{m} \begin{pmatrix} n & n^2 - m^2 \\ 1 & n \end{pmatrix} \tag{5.1.12}$$

5.2 Topological interfaces in the AdS bulk

In this section we discuss how a topological interface in the bulk CS theory can be related to topological interfaces in two-dimensional CFTs via the AdS/CFT correspondence. We will first briefly discuss an important gauge choice for our investigations in section 5.2.1, then show the holographic incompatibility of the standard choice of CS counter terms with general bulk topological interfaces in section 5.2.2. In section 5.2.3 we develop a non-standard CS counter term, and in section 5.2.4 we show that this counter term is holographically compatible with general bulk topological interfaces.

5.2.1 AdS_2 slicing

A useful coordinate system to work with is that of an AdS_2 slicing of AdS_3, which we reviewed in section 1.3.1. In the coordinate system (1.3.9) we locate the CS topological interface at $\mu = 0$ and $\mathcal{M}_{L/R}$ are given by the half-spaces $\mu < 0$ and $\mu > 0$ respectively (see figure 1.5). In this coordinate system we can impose the gauge $A^I_\mu = 0$. It then follows from the flatness of the connection that the non-vanishing components $A_{z,t}$ are independent of μ and hence the connection at the CS interface can be trivially related to the connection at the boundary component of AdS_3. Note that due to the fact that the CS action is topological there is no backreaction on the metric, which remains unchanged from (1.3.7). This is to be contrasted to the case of Janus solutions involving massless scalars [45, 48], where the metric will be deformed.

5.2.2 Simple holomorphic example

In the following we consider the boundary counter terms discussed in section 1.3.2, which lead to purely holomorphic $U(1)$ currents (1.3.30) and stress tensor (1.3.31). We utilize the AdS_2 slicing coordinates given in (1.3.9) and locate the topological interface Σ in the bulk at $\mu = 0$ with the left and right CS theories in (5.1.1) occupying $\mu < 0$ and $\mu > 0$ respectively. As discussed above, the gauge $A_\mu = 0$ allows for $A_a, a = z, t$, to be trivially continued to the AdS_3 boundary at $\mu = \pm\infty$ and compared at the location of the CFT interface at $\partial\Sigma$. Using this, the matching condition (5.1.3) at the bulk topological interface translates into the following condition for the currents

$$\left(v^{(L)}\right)^{\mathrm{T}} J_z^{(L)}\big|_{\partial\Sigma} = -\left(v^{(R)}\right)^{\mathrm{T}} J_z^{(R)}\big|_{\partial\Sigma} \tag{5.2.1}$$

We can use this matching condition to relate the holomorphic stress tensor for the left and right CFTs at the location of the interface

$$\begin{aligned}
\left(J^{(L)}\right)^{\mathrm{T}} K_{(L)}^{-1} J^{(L)} &= \left(J_z^{(R)}\right)^{\mathrm{T}} v^{(R)} \left(v^{(L)}\right)^{-1} K_{(L)}^{-1} \left((v^{(L)})^{\mathrm{T}}\right)^{-1} \left(v^{(R)}\right)^{\mathrm{T}} J_z^{(R)} \\
&= \left(J_z^{(R)}\right)^{\mathrm{T}} v^{(R)} \left((v^{(L)})^{\mathrm{T}} K_{(L)} v^{(L)}\right)^{-1} \left(v^{(R)}\right)^{\mathrm{T}} J_z^{(R)} \\
&= \left(J_z^{(R)}\right)^{\mathrm{T}} v^{(R)} \left((v^{(R)})^{\mathrm{T}} K_{(R)} v^{(R)}\right)^{-1} \left(v^{(R)}\right)^{\mathrm{T}} J_z^{(R)} \\
&= \left(J_z^{(R)}\right)^{\mathrm{T}} K_{(R)}^{-1} J_z^{(R)}
\end{aligned} \tag{5.2.2}$$

where in the last line we used the gluing condition (5.1.4) for the K matrices. It follows from the definition (1.3.31) that the holomorphic components of the stress tensor are continuous

$$T_{zz}^{(L)}\big|_{\partial\Sigma} = T_{zz}^{(R)}\big|_{\partial\Sigma} \tag{5.2.3}$$

which is the first condition in (1.1.7) a topological CFT interface must satisfy. However, in the purely holomorphic formulation discussed so far it is not possible to construct the

anti-holomorphic stress tensor and hence verify the second condition in (1.1.7).[2] Even when the level matrices decompose according to $K^{(L,R)} = k^{(L,R)} \oplus (-\tilde{k}^{(L,R)})$, where we can choose to source holomorphic currents from the gauge fields mixed by $k^{(L,R)}$ and source anti-holomorphic currents from the gauge fields mixed by $-\tilde{k}^{(L,R)}$, there are problems with the continuity of the stress tensor components. To see this, let us write

$$A^{(L,R)}\big|_{\partial\mathcal{M}_{L,R}} = \begin{pmatrix} a^{(L,R)} \\ \tilde{a}^{(L,R)} \end{pmatrix} \tag{5.2.4}$$

so that we have

$$J_z^{(L,R)} = \frac{1}{2\pi}\, k^{(L,R)} a_z^{(L,R)} \quad \text{and} \quad \tilde{J}_{\bar{z}}^{(L,R)} = \frac{1}{2\pi}\, \tilde{k}^{(L,R)} \tilde{a}_{\bar{z}}^{(L,R)} \tag{5.2.5}$$

and the stress tensor components are given by

$$T_{zz}^{(L,R)} = \frac{\pi}{2}\, J_z^{(L,R)} (k^{(L,R)})^{-1} J_z^{(L,R)} + \frac{1}{8\pi}\, \tilde{a}_z^{(L,R)} \tilde{k}^{(L,R)} \tilde{a}_z^{(L,R)} \tag{5.2.6}$$

$$T_{\bar{z}\bar{z}}^{(L,R)} = \frac{1}{8\pi}\, a_{\bar{z}}^{(L,R)} k^{(L,R)} a_{\bar{z}}^{(L,R)} + \frac{\pi}{2}\, \tilde{J}_{\bar{z}}^{(L,R)} (\tilde{k}^{(L,R)})^{-1} \tilde{J}_{\bar{z}}^{(L,R)} \tag{5.2.7}$$

One can check that (5.2.6) and (5.2.7) are separately continuous for the matching conditions (5.1.10), but not for those of (5.1.12). Generally, the stress tensor components produced by these counter terms will only be separately continuous if the matching conditions decompose according to

$$-\, v^{(L)} v^{(R)^{-1}} = \begin{pmatrix} V & 0 \\ 0 & \tilde{V} \end{pmatrix} \tag{5.2.8}$$

[2] If the interface condition is conformal and satisfies (1.1.1) the holomorphic condition (5.2.3) implies the anti-holomorphic one.

which from the matching conditions on $a^{(L,R)}$ on $\partial\Sigma$

$$v^{(L)^{\mathrm{T}}}\begin{pmatrix} 2\pi J_z^{(L)} \\ -\tilde{k}^{(L)}\tilde{a}_z^{(L)} \end{pmatrix}\Big|_{\partial\Sigma} = -v^{(R)^{\mathrm{T}}}\begin{pmatrix} 2\pi J_z^{(R)} \\ -\tilde{k}^{(R)}\tilde{a}_z^{(R)} \end{pmatrix}\Big|_{\partial\Sigma} \tag{5.2.9}$$

$$v^{(L)^{\mathrm{T}}}\begin{pmatrix} k^{(L)}a_{\bar{z}}^{(L)} \\ -2\pi\tilde{J}_{\bar{z}}^{(L)} \end{pmatrix}\Big|_{\partial\Sigma} = -v^{(R)^{\mathrm{T}}}\begin{pmatrix} k^{(R)}a_{\bar{z}}^{(R)} \\ -2\pi\tilde{J}_{\bar{z}}^{(R)} \end{pmatrix}\Big|_{\partial\Sigma} \tag{5.2.10}$$

we see is related to the possible mixing between holomorphic and anti-holomorphic boundary currents and the remaining components of the bulk fields. With counter term choices like (1.3.28) we will always have this problem owing to the fact that the holomorphic and anti-holomorphic currents are independent from each other. This is the reason why we generalize the counter terms in the next section in order to obtain a conserved current with both holomorphic and anti-holomorphic parts.

5.2.3 Pure CS counter terms and conserved currents

In [106], an interesting counter term was chosen in order for the bulk CS theory to source a boundary current whose components had a common dependence on the boundary values of the gauge fields. This boundary current was constructed such that there is no chiral anomaly as a result of the flatness of the gauge fields which source it. Specifically, the action of the theory is given by

$$S = \frac{k}{4\pi}\int_{\mathcal{M}}\left(A\wedge dA - \bar{A}\wedge d\bar{A}\right) + \frac{k}{8\pi}\int_{\partial\mathcal{M}} d^2z\left(A_zA_{\bar{z}} + \bar{A}_z\bar{A}_{\bar{z}} - 2A_{\bar{z}}\bar{A}_z\right) \tag{5.2.11}$$

where the first two terms in the counter term allow $A_{\bar{z}}$ and $\bar{A}_z$ to be fixed on the boundary and the final term is chosen to produce a conserved current; i.e. the boundary currents

$$J_z = \frac{\delta S}{\delta A_{\bar{z}}} = \frac{k}{2\pi}\left(A_z - \bar{A}_z\right)\Big|_{\partial\mathcal{M}} \quad \text{and} \quad J_{\bar{z}} = \frac{\delta S}{\delta \bar{A}_z} = -\frac{k}{2\pi}\left(A_{\bar{z}} - \bar{A}_{\bar{z}}\right)\Big|_{\partial\mathcal{M}} \tag{5.2.12}$$

can be regarded as components of a single current satisfying

$$\partial^\mu J_\mu = \frac{k}{2\pi}\left[(\partial_{\bar{z}} A_z - \partial_z A_{\bar{z}}) - \left(\partial_{\bar{z}} \bar{A}_z - \partial_z \bar{A}_{\bar{z}}\right)\right]\Big|_{\partial\mathcal{M}} = 0 \tag{5.2.13}$$

by the flatness of A and $\bar{A}$. If we want A and $\bar{A}$ to source left- and right-moving currents, respectively, then (5.2.11) is the unique counter term for which such a conserved current can be constructed; however, if we make no assumptions about which gauge fields source the left-moving and right-moving currents then larger classes of counter terms are possible.

Consider the pure CS action (1.3.24) of $2N$ gauge fields in AdS_3, with the addition of a generic quadratic counter term. Making use of the Hodge star on $\partial\mathcal{M}$, we can write such a counter term in the coordinate invariant form

$$S_{\text{CT}} = \frac{1}{8\pi}\int_{\partial\mathcal{M}} \left(X_{IJ} * A^I \wedge A^J + Y_{IJ}\, A^I \wedge A^J\right) \tag{5.2.14}$$

where here X and Y are symmetric and anti-symmetric $2N \times 2N$ matrices, respectively. The variation of the total action is then given by

$$\delta S_{\text{total}} = \frac{1}{4\pi}\int_{\partial\mathcal{M}} * \left[X_{IJ} A^I + (K_{IJ} + Y_{IJ}) * A^I\right] \wedge \delta A^J \tag{5.2.15}$$

Decomposing the term in the brackets above in terms of its self-dual and anti-self-dual parts, we see that in order to allow for a well-defined variational principle consistent with N left-moving and N right-moving boundary currents it must be the case that the matrices

$$P_\pm = X \pm Y \pm K \tag{5.2.16}$$

each be half-rank. Furthermore, the nullspaces of these matrices and their transposes determine the boundary currents and the gauge fields which source them. Specifically, the left- and right-moving boundary currents will correspond to combinations of the gauge fields

valued in the orthogonal complements to the nullspaces of $P_\pm^{\mathrm{T}}$, $\mathrm{Null}(P_\pm^{\mathrm{T}})^\perp$; and the combinations of the gauge fields sourcing them will be valued in the orthogonal complements to the nullspaces of $P_\pm$, $\mathrm{Null}(P_\pm)^\perp$. Thus, for a well-defined variational principle we must specifically have that $\mathrm{Null}(P_+) \cup \mathrm{Null}(P_-) = \mathbb{R}^{2N}$, and for it to be possible to construct N conserved currents we must have $\mathrm{Null}(P_+^{\mathrm{T}}) = \mathrm{Null}(P_-^{\mathrm{T}})$. Such matrices can be constructed from a spanning set of vectors $\{v_i^+, v_i^-\}$ and another set of linearly independent vectors $\{w_i\}$ and setting

$$P_\pm^T = \sum_{i=1}^{N} v_i^\pm w_i^{\mathrm{T}} \tag{5.2.17}$$

where the $\{v_i^\pm\}$ form bases for $\mathrm{Null}(P_\pm)^\perp$ and the $\{w_i\}$ form a basis for $\mathrm{Null}(P_\pm^{\mathrm{T}})^\perp$. Furthermore, consistency with (5.2.16) constrains the possible vectors in (5.2.17). First, if

$$X = \frac{1}{2}\left(P_+^{\mathrm{T}} + P_-^{\mathrm{T}}\right) \tag{5.2.18}$$

is to be a symmetric matrix then we must set $w_i = v_i^+ + v_i^-$. Then, writing K in spectral form as

$$K = \sum_{i=1}^{N} \left(k_i^+ u_i^+ u_i^{+\mathrm{T}} - k_i^- u_i^- u_i^{-\mathrm{T}}\right) \tag{5.2.19}$$

where $u_i^\pm$ are the unit eigenvectors corresponding to the positive and negative eigenvalues $\pm k_i^\pm$ of K, we see that

$$K = \frac{1}{2}\left[\frac{1}{2}\left(P_+^{\mathrm{T}} - P_-^{\mathrm{T}}\right) + \frac{1}{2}\left(P_+ - P_-\right)\right] = \frac{1}{2}\sum_{i=1}^{N}\left(v_i^+ v_i^{+\mathrm{T}} - v_i^- v_i^{-\mathrm{T}}\right) \tag{5.2.20}$$

determines the possible $\{v_i^\pm\}$ to be given by

$$\begin{pmatrix} v_i^{+\mathrm{T}} \\ v_i^{-\mathrm{T}} \end{pmatrix} = M \begin{pmatrix} \sqrt{2k_i^+}\, u_i^{+\mathrm{T}} \\ \sqrt{2k_i^-}\, u_i^{-\mathrm{T}} \end{pmatrix} \tag{5.2.21}$$

where M is an arbitrary $O(N,N)$ matrix acting on the $\{I\}$ coordinates in some ordering

$\{i, i+N\}$.

In terms of the solution (5.2.21), the variation (5.2.15) can be written as

$$\delta S = \int_{\partial\mathcal{M}} \left[* \left(J^i + *J^i \right) \wedge \delta A_i + * \left(J^i - *J^i \right) \wedge \delta \bar{A}_i \right] \tag{5.2.22}$$

with the fields sourcing the self-dual and anti-self-dual currents being

$$A_i = c_i \left(v_i^+ \right)_I A^I = c_i \left(MUA \right)_i \quad \text{and} \quad \bar{A}_i = -c_i \left(v_i^- \right)_I A^I = -c_i \left(MUA \right)_{i+N} \tag{5.2.23}$$

where the c_i are arbitrary proportionality constants and the matrix U is constructed row-wise as

$$U = \begin{pmatrix} \sqrt{2k_i^+}\, u_i^{+\mathrm{T}} \\ \sqrt{2k_i^-}\, u_i^{-\mathrm{T}} \end{pmatrix} \tag{5.2.24}$$

In terms of the A_i and $\bar{A}_i$, the currents are given by

$$J_i = * \frac{1}{2\pi c_i^2} \left(A_i - \bar{A}_i \right) \Big|_{\partial\mathcal{M}} \tag{5.2.25}$$

As advertised, we have that

$$d * J_i = \frac{1}{2\pi c_i^2} \left(dA_i - d\bar{A}_i \right) \Big|_{\partial\mathcal{M}} = 0 \tag{5.2.26}$$

by the flatness of the gauge fields. In terms of (5.2.23) and (5.2.25), the counter term can be written as

$$S_{\mathrm{CT}} = \int_{\partial\mathcal{M}} \left[\frac{\pi c_i^2}{2}\, J^i \wedge * J_i + \frac{1}{4\pi c_i^2}\, A^i \wedge \bar{A}_i \right] \tag{5.2.27}$$

from which we see that the stress tensor is of the Sugawara form, given by

$$T_{\mu\nu} = -\frac{\pi c_i^2}{2} \left(J_\mu^i J_{i,\nu} - \tfrac{1}{2}\, g_{\mu\nu} J_\lambda^i J_i^\lambda \right) \tag{5.2.28}$$

In flat coordinates, the non-zero components are

$$T_{zz} = -\frac{\pi c_i^2}{2}\, J_z^i J_{i,z} \quad \text{and} \quad T_{\bar{z}\bar{z}} = -\frac{\pi c_i^2}{2}\, J_{\bar{z}}^i J_{i,\bar{z}} \tag{5.2.29}$$

5.2.4 Interfaces with conserved currents

In order for an interface to preserve the stress tensor components (5.2.29), the matching conditions on the gauge fields must act as an $O(N)$ transformation on the $c^i J^i$. Specifically, if the boundary conditions on the fields are

$$A_I^{(L)} = \Lambda_I^J A_J^{(R)} \tag{5.2.30}$$

then we are concerned with the matrix $\hat{\Lambda}$ implementing the conditions on the $c_i^{-1} A_i$ and $c_i^{-1}\bar{A}_i$,

$$\begin{pmatrix} \frac{1}{c_i^{(L)}}\big(A_i^{(L)} - \bar{A}_i^{(L)}\big) \\ \frac{1}{c_i^{(L)}}\big(A_i^{(L)} + \bar{A}_i^{(L)}\big) \end{pmatrix} = \hat{\Lambda} \begin{pmatrix} \frac{1}{c_i^{(R)}}\big(A_i^{(R)} - \bar{A}_i^{(R)}\big) \\ \frac{1}{c_i^{(R)}}\big(A_i^{(R)} + \bar{A}_i^{(R)}\big) \end{pmatrix} \tag{5.2.31}$$

given by

$$\hat{\Lambda} = \frac{1}{2}\begin{pmatrix} 1 & 1 \\ 1 & -1 \end{pmatrix} M^{(L)} U^{(L)} \Lambda \big(M^{(R)} U^{(R)}\big)^{-1} \begin{pmatrix} 1 & 1 \\ 1 & -1 \end{pmatrix} \tag{5.2.32}$$

Thus, in order for the matching conditions (5.2.30) to act as

$$c_i^{(L)} J_i^{(L)} = S_i^j\, c_j^{(R)} J_j^{(R)} \tag{5.2.33}$$

for some $S \in O(N)$, the matrix $\hat{\Lambda}$ must decompose according to

$$\hat{\Lambda} = \begin{pmatrix} S & 0 \\ \hat{\Lambda}_{21} & \hat{\Lambda}_{22} \end{pmatrix} \tag{5.2.34}$$

Writing (5.1.4) in terms of Λ and utilizing the spectral decomposition of the level matrices, we see that the combination

$$M_\Lambda = U^{(L)}\Lambda\big(U^{(R)}\big)^{-1} \tag{5.2.35}$$

is always an $O(N,N)$ matrix, from which fact we determine that all solutions obeying (5.2.34) are given by

$$M^{(L)}M_\Lambda\big(M^{(R)}\big)^{-1} = \begin{pmatrix} S & 0 \\ 0 & S \end{pmatrix} \tag{5.2.36}$$

The above shows that there is always enough freedom in the choice of counter terms on the left and right theories to produce a continuous boundary stress tensor.

As an example, for $N = 1$ (5.2.36) implies that

$$M_\Lambda = \pm M^{\eta_+^{(L)}\eta_+^{(R)}}_{\eta_-^{(L)}\eta_-^{(R)}}(\lambda^{(R)} - \lambda^{(L)}) \tag{5.2.37}$$

where

$$M^{\eta_+}_{\eta_-}(\lambda) = \begin{pmatrix} \cosh\lambda & \sinh\lambda \\ \sinh\lambda & \cosh\lambda \end{pmatrix}\begin{pmatrix} \eta_+ & 0 \\ 0 & \eta_- \end{pmatrix} \tag{5.2.38}$$

is a general $O(1,1)$ element. We will consider two examples of $N = 1$ bulk interfaces, the first of which are

$$M_\Lambda = \begin{pmatrix} \eta_1 & 0 \\ 0 & \eta_2 \end{pmatrix} \tag{5.2.39}$$

for the matching conditions respecting the gluing conditions of the level matrices (5.1.6), where $\eta_1, \eta_2 = \pm 1$. In order for (5.2.37) to be obeyed, we must have $\eta_+^{(L)}\eta_+^{(R)} = \pm\eta_1$, $\eta_-^{(L)}\eta_-^{(R)} = \pm\eta_2$, and $\lambda^{(L)} = \lambda^{(R)}$. As a second example, we consider

$$M_\Lambda = \begin{pmatrix} \frac{n}{m} & \sqrt{\frac{n^2}{m^2} - 1} \\ \sqrt{\frac{n^2}{m^2} - 1} & \frac{n}{m} \end{pmatrix} \tag{5.2.40}$$

for the matching conditions respecting the level matrices (5.1.11). This time, the condition

(5.2.37) sets $\eta_+^{(L)} = \eta_-^{(L)} = \pm\eta_+^{(R)} = \pm\eta_-^{(R)}$ and $\lambda^{(R)} - \lambda^{(L)} = \operatorname{arccosh}(n/m)$.

5.3 Higher-dimensional generalizations

We can consider higher-dimensional generalizations of three-dimensional CS topological field theory. The most straightforward generalization exists in $d = 4n+3$ dimensions with $n \geq 1$, utilizing $(2n+1)$-dimensional anti-symmetric tensor fields

$$S = \frac{K_{IJ}}{4\pi} \int_{\mathcal{M}_{4n+3}} B^I \wedge dB^J \tag{5.3.1}$$

For $n = 1$ the matrix K is symmetric just as for the three-dimensional CS theory, and the theory describes the topological sector of $(2,0)$ theories on M5-branes. This topological field theory has been studied in the past, see e.g. [112–114]. Following the three-dimensional example we can consider a $(4n+2)$-dimensional interface Σ separating two AST theories with different K matrices living on $\mathcal{M}_{L,R}$ respectively[3]

$$S_{\text{int}} = \frac{K_{IJ}^{(L)}}{4\pi} \int_{\mathcal{M}_L} B^{(L)I} \wedge dB^{(L)J} + \frac{K_{IJ}^{(R)}}{4\pi} \int_{\mathcal{M}_R} B^{(R)I} \wedge dB^{(R)J} \tag{5.3.2}$$

A topological interface with a good variational principle would, as before, have a vanishing symplectic one-form

$$\boldsymbol{\Theta} = \delta S|_{\text{on shell}} = -\frac{1}{4\pi} \int_\Sigma \left(K_{IJ}^{(L)} B^{(L)I} \wedge \delta B^{(L)J} - K_{IJ}^{(R)} B^{(R)I} \wedge \delta B^{(R)J} \right) + \boldsymbol{\Theta}_{\text{CT}} \tag{5.3.3}$$

with matching conditions which restrict the AST fields to a half-dimensional Lagrangian subspace. A topological interface condition is given when no counter terms which depend on the induced metric on the interface Σ have to be added. While there are many mathematical subtleties in the exact treatment of these theories [113, 115] it seems likely that topological

[3]For theories in $d = 4n+1$ with $2n$-dimensional AST fields, the matrix K is anti-symmetric and the analysis of topological interface theories does not parallel the CS case.

interfaces can be constructed for these theories, and it would be interesting to investigate what would be the analog of the two-dimensional topological interfaces for the boundary theories when (5.3.2) is placed in AdS_{4n+3}.

5.4 Discussion

In this chapter we placed Abelian three-dimensional CS theories in AdS_3 and related the topological interfaces in this theory to topological interfaces in the boundary CFT. In order to obtain both holomorphic and anti-holomorphic currents and stress tensors, we generalized a construction which produces conserved $U(1)$ currents with both holomorphic and anti-holomorphic components in the boundary. There are many open questions which would be interesting to pursue. The relation between CS theories and rational CFTs generalizes to non-Abelian CS theories (and WZW models); does the relation of topological interfaces in bulk and boundary theories generalize to this case? The first step in answering this question involves generalizing the classification of topological interfaces in Abelian CS theories [65] to the non-Abelian case. One very important property of topological interfaces in two-dimensional CFTs is that they have a nontrivial fusion product, which can be constructed by bringing two topological interfaces close together. It would be interesting to understand what the analog of this product is on the bulk side. The higher-dimensional generalization is also very interesting, in particular whether the topological interfaces – if they can be consistently defined – have any interpretation or application in the M5-brane $(2, 0)$ theory.

Appendix A

CFT conventions

In this appendix we review the explicit CFT conventions that we use throughout the paper, specifically the free boson and free fermion theories on the cylinder and torus.

A.1 Free scalar field

For a cylinder of circumference 2π the action

$$S[\varphi] = \frac{1}{4\pi\alpha'} \int d^2x \, \partial_\mu \varphi \, \partial^\mu \varphi \tag{A.1.1}$$

describes the compact free boson field $\varphi(x,t) = \varphi(x+2\pi,t) - 2\pi w R$, where w is the integer winding number of the boson around the cylinder and R is the compactification radius. The equation of motion is satisfied by

$$\begin{aligned} \varphi(z,\bar{z}) = \varphi_0 - i\left(\frac{n\alpha'}{2R} + \frac{1}{2}\,wR\right)\ln z + i\sqrt{\frac{\alpha'}{2}}\sum_{k\neq 0}\frac{1}{k}\,a_k z^{-k} \\ - i\left(\frac{n\alpha'}{2R} - \frac{1}{2}\,wR\right)\ln \bar{z} + i\sqrt{\frac{\alpha'}{2}}\sum_{k\neq 0}\frac{1}{k}\,\bar{a}_k \bar{z}^{-k} \end{aligned} \tag{A.1.2}$$

with holomorphic and anti-holomorphic coordinates given by

$$z = e^{t+ix}\,, \quad \bar{z} = e^{t-ix} \tag{A.1.3}$$

If we define

$$a_0 = \frac{n}{R}\sqrt{\frac{\alpha'}{2}} + \frac{wR}{\sqrt{2\alpha'}}\,, \quad \bar{a}_0 = \frac{n}{R}\sqrt{\frac{\alpha'}{2}} - \frac{wR}{\sqrt{2\alpha'}} \tag{A.1.4}$$

then the mode expansion (A.1.2) is brought into the simpler holomorphic and anti-holomorphic expressions

$$i\partial\varphi(z) = \sqrt{\frac{\alpha'}{2}}\sum_{k=-\infty}^{\infty} a_k z^{-k-1}\,, \quad i\bar{\partial}\bar{\varphi}(\bar{z}) = \sqrt{\frac{\alpha'}{2}}\sum_{k=-\infty}^{\infty} \bar{a}_k \bar{z}^{-k-1} \tag{A.1.5}$$

Radial quantization on the complex plane imposes commutation relations between the bosonic operators (formerly expansion coefficients)

$$[a_n, a_m] = [\bar{a}_n, \bar{a}_m] = n\,\delta_{n+m,0}\,, \quad [a_n, \bar{a}_m] = 0 \tag{A.1.6}$$

The Hamiltonian of this boson (on the torus) is now

$$H = L_0 + \bar{L}_0 - \frac{1}{12} \tag{A.1.7}$$

with Virasoro generators given by

$$L_n = \frac{1}{2}\sum_{m=-\infty}^{\infty} :a_{n-m}a_m:\,, \quad \bar{L}_n = \frac{1}{2}\sum_{m=-\infty}^{\infty} :\bar{a}_{n-m}\bar{a}_m: \tag{A.1.8}$$

for $n \neq 0$ and

$$L_0 = \sum_{n=1}^{\infty} a_{-n}a_n + \frac{1}{2}\,a_0^2\,, \quad \bar{L}_0 = \sum_{n=1}^{\infty} \bar{a}_{-n}\bar{a}_n + \frac{1}{2}\,\bar{a}_0^2 \tag{A.1.9}$$

The ground state quantum numbers, the momentum and winding number n and w, are related to the eigenvalues of the zero mode operators by

$$\sqrt{\frac{1}{2\alpha'}}\,(a_0+\bar{a}_0)\,|n,w\rangle = \frac{n}{R}\,|n,w\rangle\,, \quad \sqrt{\frac{1}{2\alpha'}}\,(a_0-\bar{a}_0)\,|n,w\rangle = \frac{wR}{\alpha'}\,|n,w\rangle \tag{A.1.10}$$

The action of the Hamiltonian on these vacuum states is

$$H\,|n,w\rangle = \left(\frac{n^2\alpha'}{2R^2} + \frac{w^2R^2}{2\alpha'} - \frac{1}{12}\right)|n,w\rangle \tag{A.1.11}$$

With these conventions, the effects of a T-duality transformation are

$$n \longleftrightarrow w\,, \quad R \longleftrightarrow \frac{\alpha'}{R}\,, \quad a_n \longleftrightarrow a_n\,, \quad \bar{a}_n \longleftrightarrow -\bar{a}_n \tag{A.1.12}$$

Two important identities for bosonic oscillators are

$$e^{a_n}q^{L_0} = q^{L_0}e^{q^n a_n} \quad \text{and} \quad e^{\bar{a}_n}q^{\bar{L}_0} = q^{\bar{L}_0}e^{q^n\bar{a}_n} \tag{A.1.13}$$

where $n \geq 0$ and $q = e^{2\pi i\tau}$. These follow from $[a_n, L_0] = [\bar{a}_n, \bar{L}_0] = n$ and the general braiding relation

$$\mathrm{Ad}_{e^A} = e^{\mathrm{ad}_A} \implies e^{\mathrm{Ad}_{e^A}B} = \mathrm{Ad}_{e^A}e^B = e^{e^{\mathrm{ad}_A}B} \tag{A.1.14}$$

where the group and algebra adjoints are defined to be $\mathrm{Ad}_A B \equiv ABA^{-1}$ and $\mathrm{ad}_A B \equiv [A,B]$.

A.2 Free spin-$\frac{1}{2}$ field

The free Majorana fermion on the cylinder is described by the action

$$S[\psi,\bar{\psi}] = \frac{1}{2\pi\alpha'}\int d^2z\,\left(\bar{\psi}\,\partial\bar{\psi} + \psi\,\bar{\partial}\psi\right) \tag{A.2.1}$$

where ψ and $\bar{\psi}$ are the component spinors of the Majorana fermion. The equations of motion simply require $\psi(z)$ to be a holomorphic function and $\bar{\psi}(\bar{z})$ to be an anti-holomorphic function. These spinors are chosen to be either periodic $\psi(ze^{2\pi i}) = \psi(z)$ or anti-periodic $\psi(ze^{2\pi i}) = -\psi(z)$. The anti-periodic spinors are said to be in the Neveu-Schwarz sector and have the mode expansions

$$i\psi(z) = \sum_{n\in\mathbb{Z}-\frac{1}{2}} \psi_n \, z^{-n-1/2} \quad \text{and} \quad i\bar{\psi}(\bar{z}) = \sum_{n\in\mathbb{Z}-\frac{1}{2}} \bar{\psi}_n \, \bar{z}^{-n-1/2} \tag{A.2.2}$$

The periodic spinors are said to be in the Ramond sector and have the mode expansions

$$i\psi(z) = \sum_{n=-\infty}^{\infty} \psi_n \, z^{-n-1/2} \quad \text{and} \quad i\bar{\psi}(\bar{z}) = \sum_{n=-\infty}^{\infty} \bar{\psi}_n \, \bar{z}^{-n-1/2} \tag{A.2.3}$$

In either case, radial quantization on the complex plane imposes anti-commutation relations between the fermionic operators (formerly expansion coefficients)

$$\{\psi_n, \psi_m\} = \{\bar{\psi}_n, \bar{\psi}_m\} = \delta_{n+m,0}\,, \quad \{\psi_n, \bar{\psi}_m\} = 0 \tag{A.2.4}$$

The Hamiltonian of this fermion (on the torus) is now

$$H = L_0 + \bar{L}_0 - \frac{1}{24} \tag{A.2.5}$$

with Virasoro generators given by

$$L_n = \frac{1}{2}\sum_m \left(m + \tfrac{1}{2}\right) : \psi_{n-m}\psi_m :, \quad \bar{L}_n = \frac{1}{2}\sum_m \left(m + \tfrac{1}{2}\right) : \bar{\psi}_{n-m}\bar{\psi}_m : \tag{A.2.6}$$

for $n \neq 0$, where m is summed over the half-integers or integers for the Neveu-Schwarz or Ramond sectors, respectively. For the Neveu-Schwarz sector the $n = 0$ generators are

$$L_0 = \sum_{n \in \mathbb{N} - \frac{1}{2}} n \, \psi_{-n} \psi_n \,, \quad \bar{L}_0 = \sum_{n \in \mathbb{N} - \frac{1}{2}} n \, \bar{\psi}_{-n} \bar{\psi}_n \tag{A.2.7}$$

and for the Ramond sector the $n = 0$ generators are

$$L_0 = \sum_{n=1}^{\infty} n \, \psi_{-n} \psi_n + \frac{1}{16} \,, \quad \bar{L}_0 = \sum_{n=1}^{\infty} n \, \bar{\psi}_{-n} \bar{\psi}_n + \frac{1}{16} \tag{A.2.8}$$

The action of the Neveu-Schwarz Hamiltonian on the vacuum state is

$$H \, |0\rangle = -\frac{1}{24} \, |0\rangle \tag{A.2.9}$$

and the action of the Ramond Hamiltonian on the vacuum states is

$$H \, |\pm\rangle = \frac{1}{12} \, |\pm\rangle \tag{A.2.10}$$

The zero mode operators of the Ramond sector act on these vacuum states according to

$$\psi_0 |\pm\rangle = \frac{1}{\sqrt{2}} \, e^{\pm i\pi/4} |\mp\rangle \,, \quad \bar{\psi}_0 |\pm\rangle = \frac{1}{\sqrt{2}} \, e^{\mp i\pi/4} |\mp\rangle \tag{A.2.11}$$

furnishing a representation of (A.2.4) for $n = m = 0$.

The fermionic analogs of the bosonic identities (A.1.13) are

$$e^{\beta \psi_n} q^{L_0} = q^{L_0} e^{q^n \beta \psi_n} \quad \text{and} \quad e^{\beta \bar{\psi}_n} q^{\bar{L}_0} = q^{\bar{L}_0} e^{q^n \beta \bar{\psi}_n} \tag{A.2.12}$$

where $n \geq 0$ and $q = e^{2\pi i \tau}$. They can be shown through direct expansion; explicitly,

$$\begin{aligned} q^{n\psi_{-n}\psi_n} &= \sum_{m=0}^{\infty} \frac{1}{m!} \left(n \log q\right)^m \left(\psi_{-n}\psi_n\right)^m \\ &= 1 + \sum_{m=1}^{\infty} \frac{1}{m!} \left(n \log q\right)^m \psi_{-n}\psi_n = 1 + \left(q^n - 1\right) \psi_{-n}\psi_n \end{aligned} \tag{A.2.13}$$

so that

$$\begin{aligned} e^{\beta\psi_n} q^{n\psi_{-n}\psi_n} &= \left(1 + \beta\psi_n\right) \left(1 + \left(q^n - 1\right) \psi_{-n}\psi_n\right) \\ &= 1 + q^n \beta\psi_n + \left(q^n - 1\right) \psi_{-n}\psi_n = q^{n\psi_{-n}\psi_n} e^{q^n \beta\psi_n} \end{aligned} \tag{A.2.14}$$

As a final note, specific values of the coupling α' are often chosen in the literature. In [21] and [22] the authors use $\alpha' = 1/2$. In other works, e.g. [96], $\alpha' = 2$ is used.

Bibliography

[1] M. Gutperle and J. D. Miller, "Entanglement entropy at holographic interfaces," *Phys. Rev.* **D93** (2016), no. 2 026006, 1511.08955.

[2] M. Gutperle and J. D. Miller, "A note on entanglement entropy for topological interfaces in RCFTs," *JHEP* **04** (2016) 176, 1512.07241.

[3] M. Gutperle and J. D. Miller, "Entanglement entropy at CFT junctions," *Phys. Rev.* **D95** (2017), no. 10 106008, 1701.08856.

[4] M. Gutperle and J. D. Miller, "Topological interfaces in Chern-Simons theory and the AdS_3/CFT_2 correspondence," *Phys. Rev.* **D99** (2019), no. 2 026014, 1810.08713.

[5] V. Riva and J. L. Cardy, "Scale and conformal invariance in field theory: A Physical counterexample," *Phys. Lett.* **B622** (2005) 339–342, hep-th/0504197.

[6] A. A. Belavin, A. M. Polyakov, and A. B. Zamolodchikov, "Infinite Conformal Symmetry in Two-Dimensional Quantum Field Theory," *Nucl. Phys.* **B241** (1984) 333–380.

[7] V. S. Dotsenko, "Critical Behavior and Associated Conformal Algebra of the Z(3) Potts Model," *Nucl. Phys.* **B235** (1984) 54–74.

[8] P. Di Francesco, H. Saleur, and J. B. Zuber, "Modular Invariance in Nonminimal Two-dimensional Conformal Theories," *Nucl. Phys.* **B285** (1987) 454.

[9] B. Bellazzini, M. Mintchev, and P. Sorba, "Bosonization and scale invariance on quantum wires," *J. Phys.* **A40** (2007) 2485–2508, hep-th/0611090.

[10] A. Sen, "String network," *JHEP* **03** (1998) 005, hep-th/9711130.

[11] C. P. Bachas, "On the Symmetries of Classical String Theory," in *Quantum Mechanics of Fundamental Systems: The Quest for Beauty and Simplicity: Claudio Bunster Festschrift*, pp. 17–26, 2009. 0808.2777.

[12] G. Vidal, J. I. Latorre, E. Rico, and A. Kitaev, "Entanglement in quantum critical phenomena," *Phys. Rev. Lett.* **90** (2003) 227902, quant-ph/0211074.

[13] L. Bombelli, R. K. Koul, J. Lee, and R. D. Sorkin, "A Quantum Source of Entropy for Black Holes," *Phys. Rev.* **D34** (1986) 373–383.

[14] M. Srednicki, "Entropy and area," *Phys. Rev. Lett.* **71** (1993) 666–669, hep-th/9303048.

[15] S. Ryu and T. Takayanagi, "Aspects of Holographic Entanglement Entropy," *JHEP* **08** (2006) 045, hep-th/0605073.

[16] M. Van Raamsdonk, "Building up spacetime with quantum entanglement," *Gen. Rel. Grav.* **42** (2010) 2323–2329, 1005.3035. [Int. J. Mod. Phys.D19,2429(2010)].

[17] J. Maldacena and L. Susskind, "Cool horizons for entangled black holes," *Fortsch. Phys.* **61** (2013) 781–811, 1306.0533.

[18] B. Czech, L. Lamprou, S. McCandlish, and J. Sully, "Integral Geometry and Holography," *JHEP* **10** (2015) 175, 1505.05515.

[19] C. Bachas, J. de Boer, R. Dijkgraaf, and H. Ooguri, "Permeable conformal walls and holography," *JHEP* **06** (2002) 027, hep-th/0111210.

[20] C. Bachas and I. Brunner, "Fusion of conformal interfaces," *JHEP* **02** (2008) 085, 0712.0076.

[21] K. Sakai and Y. Satoh, "Entanglement through conformal interfaces," *JHEP* **12** (2008) 001, 0809.4548.

[22] E. M. Brehm and I. Brunner, "Entanglement entropy through conformal interfaces in the 2D Ising model," *JHEP* **09** (2015) 080, 1505.02647.

[23] T. Quella, I. Runkel, and G. M. T. Watts, "Reflection and transmission for conformal defects," *JHEP* **04** (2007) 095, hep-th/0611296.

[24] N. Ishibashi, "The Boundary and Crosscap States in Conformal Field Theories," *Mod. Phys. Lett.* **A4** (1989) 251.

[25] J. L. Cardy, "Boundary Conditions, Fusion Rules and the Verlinde Formula," *Nucl. Phys.* **B324** (1989) 581–596.

[26] C. Bachas, I. Brunner, and D. Roggenkamp, "A worldsheet extension of $O(d, d|\mathbb{Z})$," *JHEP* **10** (2012) 039, 1205.4647.

[27] A. Recknagel, "Permutation branes," *JHEP* **04** (2003) 041, hep-th/0208119.

[28] I. Brunner and M. R. Gaberdiel, "Matrix factorisations and permutation branes," *JHEP* **07** (2005) 012, hep-th/0503207.

[29] J. Fuchs, M. R. Gaberdiel, I. Runkel, and C. Schweigert, "Topological defects for the free boson CFT," *J. Phys.* **A40** (2007) 11403, 0705.3129.

[30] I. Brunner, N. Carqueville, and D. Plencner, "Orbifolds and topological defects," *Commun. Math. Phys.* **332** (2014) 669–712, 1307.3141.

[31] P. Di Vecchia and A. Liccardo, "D Branes in String Theory, I," *NATO Sci. Ser. C* **556** (2000) 1–60, hep-th/9912161.

[32] P. Di Vecchia and A. Liccardo, "D-branes in string theory. 2.," in *YITP Workshop on Developments in Superstring and M Theory Kyoto, Japan, October 27-29, 1999*, pp. 7–48, 1999. hep-th/9912275.

[33] P. Calabrese and J. L. Cardy, "Entanglement entropy and quantum field theory," *J. Stat. Mech.* **0406** (2004) P06002, hep-th/0405152.

[34] C. Holzhey, F. Larsen, and F. Wilczek, "Geometric and renormalized entropy in conformal field theory," *Nucl. Phys.* **B424** (1994) 443–467, hep-th/9403108.

[35] T. Azeyanagi, A. Karch, T. Takayanagi, and E. G. Thompson, "Holographic calculation of boundary entropy," *JHEP* **03** (2008) 054–054, 0712.1850.

[36] I. Affleck and A. W. W. Ludwig, "Universal noninteger 'ground state degeneracy' in critical quantum systems," *Phys. Rev. Lett.* **67** (1991) 161–164.

[37] M. Oshikawa and I. Affleck, "Boundary conformal field theory approach to the critical two-dimensional Ising model with a defect line," *Nucl. Phys.* **B495** (1997) 533–582, cond-mat/9612187.

[38] J. A. Harvey, S. Kachru, G. W. Moore, and E. Silverstein, "Tension is dimension," *JHEP* **03** (2000) 001, hep-th/9909072.

[39] J. M. Maldacena, "The Large N limit of superconformal field theories and supergravity," *Int. J. Theor. Phys.* **38** (1999) 1113–1133, hep-th/9711200. [Adv. Theor. Math. Phys.2,231(1998)].

[40] S. S. Gubser, I. R. Klebanov, and A. M. Polyakov, "Gauge theory correlators from noncritical string theory," *Phys. Lett.* **B428** (1998) 105–114, hep-th/9802109.

[41] E. Witten, "Anti-de Sitter space and holography," *Adv. Theor. Math. Phys.* **2** (1998) 253–291, hep-th/9802150.

[42] O. Aharony, S. S. Gubser, J. M. Maldacena, H. Ooguri, and Y. Oz, "Large N field theories, string theory and gravity," *Phys. Rept.* **323** (2000) 183–386, hep-th/9905111.

[43] E. D'Hoker and D. Z. Freedman, "Supersymmetric gauge theories and the AdS / CFT correspondence," in *Strings, Branes and Extra Dimensions: TASI 2001: Proceedings*, pp. 3–158, 2002. hep-th/0201253.

[44] O. DeWolfe, "TASI Lectures on Applications of Gauge/Gravity Duality," *PoS* **TASI2017** (2018) 014, 1802.08267.

[45] D. Bak, M. Gutperle, and S. Hirano, "A Dilatonic deformation of AdS_5 and its field theory dual," *JHEP* **05** (2003) 072, hep-th/0304129.

[46] E. D'Hoker, J. Estes, and M. Gutperle, "Ten-dimensional supersymmetric Janus solutions," *Nucl. Phys.* **B757** (2006) 79–116, hep-th/0603012.

[47] A. B. Clark, D. Z. Freedman, A. Karch, and M. Schnabl, "Dual of the Janus solution: An interface conformal field theory," *Phys. Rev.* **D71** (2005) 066003, hep-th/0407073.

[48] E. D'Hoker, J. Estes, and M. Gutperle, "Exact half-BPS Type IIB interface solutions. I. Local solution and supersymmetric Janus," *JHEP* **06** (2007) 021, 0705.0022.

[49] A. Karch and L. Randall, "Open and closed string interpretation of SUSY CFT's on branes with boundaries," *JHEP* **06** (2001) 063, hep-th/0105132.

[50] O. DeWolfe, D. Z. Freedman, and H. Ooguri, "Holography and defect conformal field theories," *Phys. Rev.* **D66** (2002) 025009, hep-th/0111135.

[51] O. Aharony, O. DeWolfe, D. Z. Freedman, and A. Karch, "Defect conformal field theory and locally localized gravity," *JHEP* **07** (2003) 030, hep-th/0303249.

[52] D. Bak, M. Gutperle, and S. Hirano, "Three dimensional Janus and time-dependent black holes," *JHEP* **02** (2007) 068, hep-th/0701108.

[53] M. Chiodaroli, M. Gutperle, and L.-Y. Hung, "Boundary entropy of supersymmetric Janus solutions," *JHEP* **09** (2010) 082, 1005.4433.

[54] M. Chiodaroli, M. Gutperle, and D. Krym, "Half-BPS Solutions locally asymptotic to $AdS_3 \times S^3$ and interface conformal field theories," *JHEP* **02** (2010) 066, 0910.0466.

[55] J. Kumar and A. Rajaraman, "New supergravity solutions for branes in $AdS_3 \times S^3$," *Phys. Rev.* **D67** (2003) 125005, hep-th/0212145.

[56] J. Kumar and A. Rajaraman, "Supergravity solutions for $AdS_3 \times S^3$ branes," *Phys. Rev.* **D69** (2004) 105023, hep-th/0310056.

[57] M. Chiodaroli, E. D'Hoker, and M. Gutperle, "Open Worldsheets for Holographic Interfaces," *JHEP* **03** (2010) 060, 0912.4679.

[58] M. Chiodaroli, E. D'Hoker, Y. Guo, and M. Gutperle, "Exact half-BPS string-junction solutions in six-dimensional supergravity," *JHEP* **12** (2011) 086, 1107.1722.

[59] E. Witten, "Quantum field theory and the Jones polynomial," *Communications in Mathematical Physics* **121** (Sep, 1989) 351–399.

[60] P. Kraus, "Lectures on black holes and the AdS_3/CFT_2 correspondence," *Lect. Notes Phys.* **755** (2008) 193–247, hep-th/0609074.

[61] S. Deser, R. Jackiw, and S. Templeton, "Topologically massive gauge theories," *Annals of Phys.* **140** (1982), no. 2 372.

[62] S. Gukov, E. Martinec, G. W. Moore, and A. Strominger, "Chern-Simons gauge theory and the AdS_3/CFT_2 correspondence," in *From Fields to Strings* (M. Shifman *et. al.*, eds.), vol. 2. World Scientific, Singapore.

[63] H.-C. Chang, M. Fujita, and M. Kaminski, "From Maxwell-Chern-Simons theory in AdS_3 towards hydrodynamics in $1+1$ dimensions," *JHEP* **10** (2014) 118, 1403.5263.

[64] D. M. Hofman and N. Iqbal, "Generalized global symmetries and holography," *SciPost Phys.* **4** (2018), no. 1 005, 1707.08577.

[65] A. Kapustin and N. Saulina, "Topological boundary conditions in abelian Chern-Simons theory," *Nucl. Phys.* **B845** (2011) 393–435, 1008.0654.

[66] E. Witten, "(2+1)-Dimensional Gravity as an Exactly Soluble System," *Nucl. Phys.* **B311** (1988) 46.

[67] A. Achucarro and P. K. Townsend, "A Chern-Simons Action for Three-Dimensional anti-De Sitter Supergravity Theories," *Phys. Lett.* **B180** (1986) 89.

[68] E. Bergshoeff, M. P. Blencowe, and K. S. Stelle, "Area Preserving Diffeomorphisms and Higher Spin Algebra," *Commun. Math. Phys.* **128** (1990) 213.

[69] A. Campoleoni, S. Fredenhagen, S. Pfenninger, and S. Theisen, "Asymptotic symmetries of three-dimensional gravity coupled to higher-spin fields," *JHEP* **11** (2010) 007, 1008.4744.

[70] J. Erdmenger, M. Flory, C. Hoyos, M.-N. Newrzella, and J. M. S. Wu, "Entanglement Entropy in a Holographic Kondo Model," *Fortsch. Phys.* **64** (2016) 109–130, 1511.03666.

[71] M. R. Gaberdiel and R. Gopakumar, "Higher Spins & Strings," *JHEP* **11** (2014) 044, 1406.6103.

[72] M. R. Gaberdiel and R. Gopakumar, "Stringy Symmetries and the Higher Spin Square," *J. Phys.* **A48** (2015), no. 18 185402, 1501.07236.

[73] M. Gutperle, "A note on interface solutions in higher-spin gravity," *JHEP* **07** (2013) 091, 1302.3653.

[74] M. Ammon, A. Castro, and N. Iqbal, "Wilson Lines and Entanglement Entropy in Higher Spin Gravity," *JHEP* **10** (2013) 110, 1306.4338.

[75] J. de Boer and J. I. Jottar, "Entanglement Entropy and Higher Spin Holography in AdS_3," *JHEP* **04** (2014) 089, 1306.4347.

[76] J. de Boer, A. Castro, E. Hijano, J. I. Jottar, and P. Kraus, "Higher spin entanglement and $\mathcal{W}_N$ conformal blocks," *JHEP* **07** (2015) 168, 1412.7520.

[77] V. B. Petkova and J. B. Zuber, "Generalized twisted partition functions," *Phys. Lett.* **B504** (2001) 157–164, hep-th/0011021.

[78] V. B. Petkova and J. B. Zuber, "The Many faces of Ocneanu cells," *Nucl. Phys.* **B603** (2001) 449–496, hep-th/0101151.

[79] J. Frohlich, J. Fuchs, I. Runkel, and C. Schweigert, "Kramers-Wannier duality from conformal defects," *Phys. Rev. Lett.* **93** (2004) 070601, cond-mat/0404051.

[80] J. Frohlich, J. Fuchs, I. Runkel, and C. Schweigert, "Duality and defects in rational conformal field theory," *Nucl. Phys.* **B763** (2007) 354–430, hep-th/0607247.

[81] E. M. Brehm, I. Brunner, D. Jaud, and C. Schmidt-Colinet, "Entanglement and topological interfaces," *Fortsch. Phys.* **64** (2016), no. 6-7 516–535, 1512.05945.

[82] L. A. Pando Zayas and N. Quiroz, "Left-Right Entanglement Entropy of Boundary States," *JHEP* **01** (2015) 110, 1407.7057.

[83] D. Das and S. Datta, "Universal features of left-right entanglement entropy," *Phys. Rev. Lett.* **115** (2015), no. 13 131602, 1504.02475.

[84] G. Sarkissian, "Defects and Permutation branes in the Liouville field theory," *Nucl. Phys.* **B821** (2009) 607–625, 0903.4422.

[85] H. Poghosyan and G. Sarkissian, "On classical and semiclassical properties of the Liouville theory with defects," *JHEP* **11** (2015) 005, 1505.00366.

[86] G. W. Moore and N. Seiberg, "Polynomial Equations for Rational Conformal Field Theories," *Phys. Lett.* **B212** (1988) 451–460.

[87] J. Fuchs, I. Runkel, and C. Schweigert, "TFT construction of RCFT correlators 1. Partition functions," *Nucl. Phys.* **B646** (2002) 353–497, hep-th/0204148.

[88] H. J. Schnitzer, "Left-Right Entanglement Entropy, D-Branes, and Level-rank duality," 1505.07070.

[89] P. Di Francesco, P. Mathieu, and D. Senechal, *Conformal Field Theory*. Graduate Texts in Contemporary Physics. Springer-Verlag, New York, 1997.

[90] N. Drukker, D. Gaiotto, and J. Gomis, "The Virtue of Defects in 4D Gauge Theories and 2D CFTs," *JHEP* **06** (2011) 025, 1003.1112.

[91] J. Teschner, "Liouville theory revisited," *Class. Quant. Grav.* **18** (2001) R153–R222, hep-th/0104158.

[92] Y. Nakayama, "Liouville field theory: A Decade after the revolution," *Int. J. Mod. Phys.* **A19** (2004) 2771–2930, hep-th/0402009.

[93] I. Runkel and G. M. T. Watts, "A Nonrational CFT with c = 1 as a limit of minimal models," *JHEP* **09** (2001) 006, hep-th/0107118.

[94] A. R. Aguirre, "Type-II defects in the super-Liouville theory," *J. Phys. Conf. Ser.* **474** (2013) 012001, 1312.3463.

[95] P. Calabrese, M. Mintchev, and E. Vicari, "Entanglement Entropy of Quantum Wire Junctions," *J. Phys.* **A45** (2012) 105206, 1110.5713.

[96] M. Chiodaroli, M. Gutperle, L.-Y. Hung, and D. Krym, "String Junctions and Holographic Interfaces," *Phys. Rev.* **D83** (2011) 026003, 1010.2758.

[97] T. Kimura and M. Murata, "Transport Process in Multi-Junctions of Quantum Systems," *JHEP* **07** (2015) 072, 1505.05275.

[98] W. Donnelly and A. C. Wall, "Geometric entropy and edge modes of the electromagnetic field," *Phys. Rev.* **D94** (2016), no. 10 104053, 1506.05792.

[99] B. Michel and M. Srednicki, "Entanglement Entropy and Boundary Conditions in 1+1 Dimensions," 1612.08682.

[100] L. A. Pando Zayas and N. Quiroz, "Left-Right Entanglement Entropy of Dp-branes," *JHEP* **11** (2016) 023, 1605.08666.

[101] B. Deconinck, "Multidimensional Theta Functions," in *NIST Handbook of Mathematical Functions* (F. W. J. Olver, D. W. Lozier, R. F. Boisvert, and C. W. Clark, eds.), p. 537. Cambridge University Press, 2010.

[102] G. J. Tee, "Eigenvectors of block circulant and alternating circulant matrices," *Lett. Inf. Math. Sci* **8** (2005) 123.

[103] J. R. Silvester, "Determinants of Block Matrices," *The Mathematical Gazette* **84** (2000), no. 501 460–467.

[104] S. Elitzur, G. W. Moore, A. Schwimmer, and N. Seiberg, "Remarks on the Canonical Quantization of the Chern-Simons-Witten Theory," *Nucl. Phys.* **B326** (1989) 108–134.

[105] J. R. Fliss, X. Wen, O. Parrikar, C.-T. Hsieh, B. Han, T. L. Hughes, and R. G. Leigh, "Interface Contributions to Topological Entanglement in Abelian Chern-Simons Theory," *JHEP* **09** (2017) 056, 1705.09611.

[106] V. Keranen, "Chern-Simons interactions in AdS_3 and the current conformal block," 1403.6881.

[107] F. D. M. Haldane, "Stability of Chiral Luttinger Liquids and Abelian Quantum Hall States," *Phys. Rev. Lett.* **74** (1995) 2090–2093.

[108] A. Kitaev and L. Kong, "Models for Gapped Boundaries and Domain Walls," *Comm. Math. Phys.* **313** (2012), no. 2 351, 11104.5047.

[109] J. Wang and X.-G. Wen, "Boundary Degeneracy of Topological Order," *Phys. Rev.* **B91** (2015), no. 12 125124, 1212.4863.

[110] M. Levin, "Protected Edge Modes without Symmetry," *Phys. Rev. X* **3** (2013) 021009, 1301.7355.

[111] T. Lan, J. C. Wang, and X.-G. Wen, "Gapped Domain Walls, Gapped Boundaries and Topological Degeneracy," *Phys. Rev. Lett.* **114** (2015), no. 7 076402, 1408.6514.

[112] E. P. Verlinde, "Global aspects of electric - magnetic duality," *Nucl. Phys.* **B455** (1995) 211–228, hep-th/9506011.

[113] D. Belov and G. W. Moore, "Holographic Action for the Self-Dual Field," hep-th/0605038.

[114] J. J. Heckman and L. Tizzano, "6D Fractional Quantum Hall Effect," *JHEP* **05** (2018) 120, 1708.02250.

[115] D. S. Freed and C. Teleman, "Relative quantum field theory," *Commun. Math. Phys.* **326** (2014) 459–476, 1212.1692.